LIGHT AMPLIFICATION AND LIGHT AMPLIFIERS

by:

DENİZ BALKAN

Advisor:

Prof. Dr. MUSTAFA SANTUR

Department of Electrical Engineering

School of Engineering

Robert College

Bebek, İstanbul, Turkey

December 1969

LIGHT AMPLIFICATION AND LIGHT AMPLIFIERS

by:

DENİZ BALKAN

Advisor:

Prof. Dr. MUSTAFA SANTUR

Department of Electrical Engineering

School of Engineering

Robert College

Bebek, İstanbul, Turkey

December 1969

PREFACE

This thesis is prepared in partial fullfillment of the requirements of the Robert College, School of Engineering for the degree of Master of Science in Electrical Engineering.

The author would like to express her gratitude to Prof. Dr. Mustafa Santur for suggesting the subject and for his help in the preparation of the work.

She also wishes to thank Mrs. Sevinç Toksöz for her help in the literary survey and Miss Mine Atalay for typing the manuscript.

Deniz Balkan

December, 1969

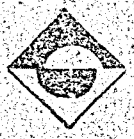

SUMMARY

Light amplification is accomplished using luminous devices which are called light amplifiers. Light outputs of these devices are much brighter than their light inputs.

This thesis is devoted to the amplification of visible light as well as to the transformation of infrared, ultraviolet radiations and X-rays into visible radiation. In case of radiation transformation, wavelength conversion is of the primary importance. Obtaining a gain is sometimes desirable.

The range of the input radiation which can be amplified by the device is determined by the spectral response of its photosensitive surface.

In this thesis light amplifiers based on four different principles are studied, emphasis being made on the Solid-state Light Amplifiers. These amplifiers can be classified as follows:

1. Solid-state Light Amplifiers (Light amplifiers using photoconductivity and electroluminescence)
2. Phosphor - Photoemitter Light Amplifiers.
3. Transmitted Secondary Electron Multiplication (TSEM) Light Amplifiers.
4. Light Amplifiers based on the Electron Bombardment Induced Conductivity (EBIC) Principle.

A solid-state light amplifier mainly consists of a sandwich of photoconductive and electroluminescent layers, with an alternating electric field applied across the combination. Applied voltage is an audio frequency

alternating voltage.

The conductivity of the photoconductive layer is increased when the light is incident upon it. This causes an increase in the voltage appearing across the electroluminescent layer so that a bright output will be obtained. Overall optical gain (of the order of 100) depends on the electroluminescent layer efficiency and the photoconductor sensitivity. Best results are obtained by photoconductive CdS powder and electroluminescent ZnS layer. This combination is suitable for applications which do not require fast response. If fast response is required CdSe photoconductor replaces CdS.

A phosphor-photoemitter light amplifier consists of a photoemitting surface and a luminescent screen parallel to each other. A very high voltage (10-20kV) applied between them provides the electric field to accelerate the emitted electrons. If the photoemitter is exposed to low-intensity light, it will emit electrons which will be accelerated by the field and strike the luminescent layer and produce a brighter image of the incident light signal. The light gain depends on the accelerating voltage, the photosurface sensitivity and the efficiency of the screen. To obtain high gain cascaded amplifiers are used.

TSEM light amplifiers use high gain dynodes which emit secondary electrons when they are bombarded with primary electrons. A TSEM tube has a photosensitive screen which emits electrons if a low intensity image is focused upon it. Accelerated electrons are multiplied by the dynodes, and focused onto the screen which provides the output image. Acceleration is provided by the voltage (30-40 kV) applied between the photosurface and

the luminescent screen.

An amplifier based on the EBIC principle mainly has a photosurface and an EBIC target. Electrons emitted out of the photosurface will strike the target and produce a video signal with the help of a scanning beam. The video signal is amplified by a video amplifier and is fed to a display unit to obtain the output image.

Each method has its own advantages and shortcomings over the others. However, all of them have useful applications in a variety of fields.

TABLE OF CONTENTS

I. SOLID STATE LIGHT AMPLIFIERS

A. INTRODUCTION

A solid state light amplifier consists of a photoconductive layer on top of an electroluminescent layer, with an alternating voltage applied across the combination.

Simpler devices have been made earlier. Mention might be made of a single-layer amplifier which uses evaporated zinc sulphide activated by manganese impurity and requires a steady applied field.

The operation of an elemental light amplifier (Fig. I-1) employing an electroluminescent panel in series with a photoconductive crystal of CdS showed initially the possibility of a panel type of light amplifier. The series combination is excited by an alternating voltage of audio frequency; e.g. 400 Hz. In the dark, the CdS crystal has very high impedance, so, a very small fraction of the applied voltage appears across the electroluminescent layer. As the incident illumination is increased, the impedance of the CdS crystal decreases giving rise to greater voltage across the phosphor layer. It was demonstrated that, with equal areas, emitted light could be many times greater than (e.g. 50 times) the incident light.

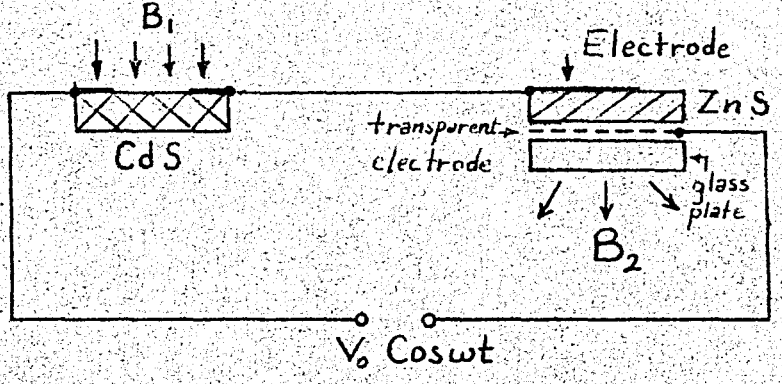

Fig.I-1. Elemental light amplifier

After the development of a photoconductive powder, large-area light-intensifying panels were produced. The principal layers of a panel light amplifier are the electroluminescent phosphor layer which produces the output image and the photoconductive layer whose resistance varies in accordance with the input radiation. Size of the panel is arbitrary and it looks like a conventional fluoroscope screen in outward appearance. Amplification occurs within the panel and it does not need any external equipment, except for a simple power supply, for operation. These devices are used for image conversion and intensification with various radiation (X-rays, ultraviolet, visible,infrared) sources.

B. AMPLIFIER DESIGN

To obtain a well-operating panel light amplifier several structures were designed and tested. The best performance was obtained by the grooved-photoconductor type amplifier.

It consists of three main layers, namely, the photoconductive layer, the current diffusing layer and the electroluminescent layer. In addition to these, an opaque layer is provided to avoid optical feedback. a.c. voltage can be applied to the panel by means of the electrodes.

Grooved-photoconductor type amplifier (Fig.I.2) uses CdS powder in bonded form as a current diffusing layer. A transparent conducting coating on a glass plate is sprayed with a thin (about 1 mil thick) phosphor layer. Then, the electroluminescent layer is covered with an opaque layer (lampblack in Araldite) of about a fraction of a mil thick. The current diffusing

layer of conducting CdS powder, bonded with Araldite, (initially about 20 mil thick) is spread on the opaque layer and machined flat to about 10 mils thickness. Then, a heavy layer of photoconductive CdS powder which is bonded in Araldite and of 20 mils thick is spread on the current-diffusing layer and machined to about 14 mils. After spraying the photoconductor surface with air-drying silver paint, fine "V" grooves are cut into the photoconductor. "V" grooves (of about 60 degrees included angle) are 15 mils deep, and the distance between centers is 25 mils. The tops of the "V" grooves are left with narrow conducting silver lines of several mils wide, and they are connected to a common terminal which acts as one electrode for the device. The bottoms of the grooves cut slightly into the conducting CdS layer. The second electrode of the device is the transparent conducting coating.

These amplifiers require machinable plastic-bonded layers of photoconductive powder which retaines full sensitivity. This is accomplished by using CN-502 Araldite which is suitably diluted with diacetone alcohol.

Due to "V" grooves, the amplifier can be illuminated efficiently. Grooved-photoconductor type amplifiers are produced up to 12 inches x 12 inches in area. They have high gain and good resolution properties and their output pictures are highly uniform.

Imperfect bonding of the photoconductive and current-diffusing layers causes small dark spots over the output picture. If narrow dark lines are observed, they are attributed to the disconnected conducting lines.

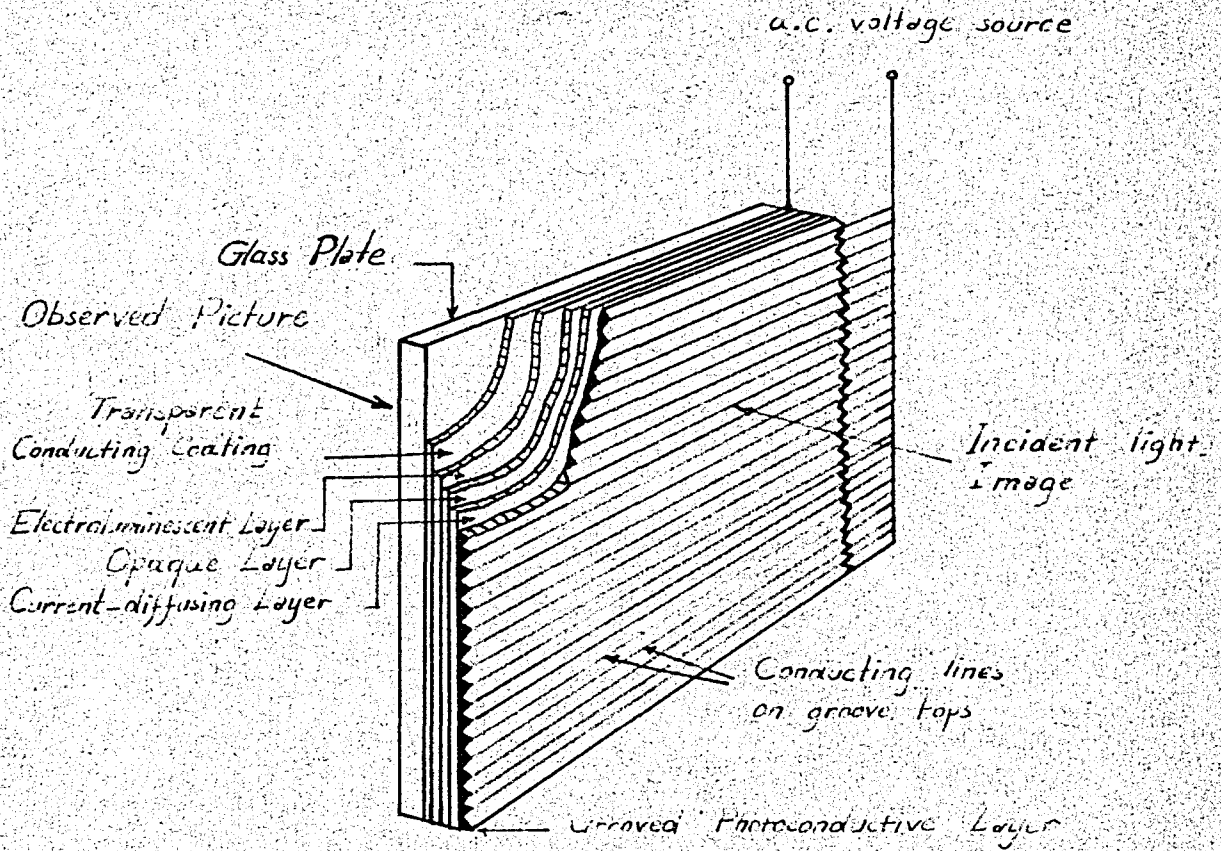

Fig. I.2 - Grooved photoconductor type amplifier

C. PRINCIPLE OF OPERATION

In the preceding section the grooved-photoconductor type panel light amplifier was described. In this section we shall discuss the operation principle. In Fig. I.3, the cross-sectional view of a simple amplifying panel is shown. To operate the amplifier, a.c. voltage should be applied across the two electrodes. In the dark, the impedance of the photoconductor is very high, so, the current flow through the electroluminescent phosphor is limited to a very low level. If radiation falls upon the photoconductor, its conductivity is increased at the illuminated portions. This causes

the flow of current to increase through the corresponding areas of the phosphor with the emission of light.

The capacitive impedance and the thickness of the photoconductive layer are higher than those of the phosphor layer. For large area panels sintered or powder (usually CdS or CdSe) photoconductors are employed. They provide low dark current and high sensitivity to the light amplifier. The photoconductor acts as a distributed valve, controlling the flow of alternating currents into the phosphor layer at each point. For the phosphor layer, ZnS activated by Cu is the most common material. Panel light amplifiers employing sensitive photoconductors and efficient phosphors can produce output light whose energy is many times greater than the energy of the incident radiation.

The opaque layer which is placed between the photoconductor and phosphor prevents output light from feeding back and exciting the photoconductor. Both of the electrodes are transparent. For this reason, the one in contact with the phosphor does not avoid viewing and the other one permits the incident radiation to penetrate to the photoconductor.

To provide good resolution, the currents, should be spread over the surface of the phosphor layer. This is accomplished by the current diffusing layer. In case of grooved structures, photoconductive grooves are spaced 25 mils on centers, so the picture details are seperated down to about this size.

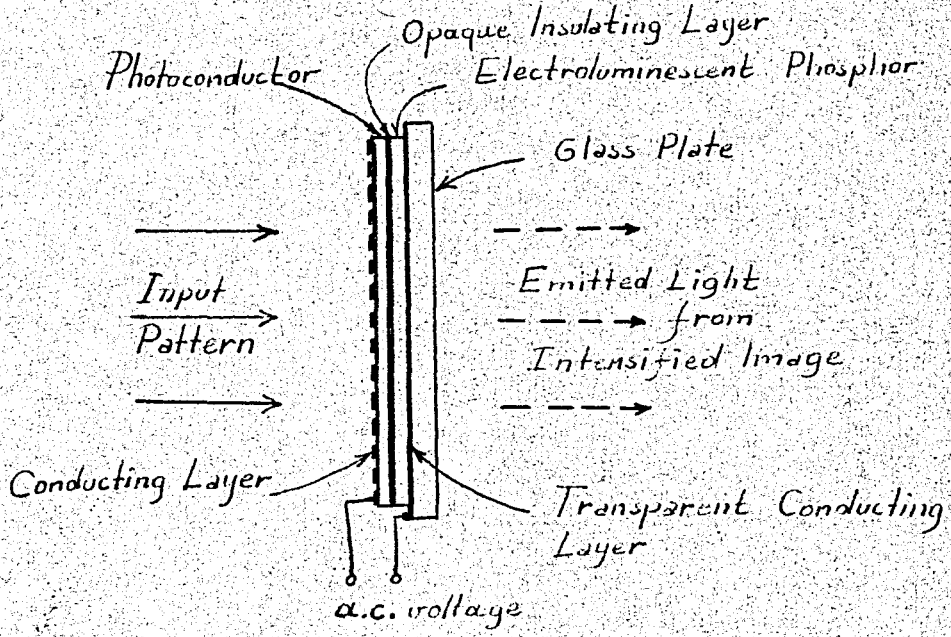

Fig. I.3 - Simple form of amplifying panel.

D. COMPONENT CHARACTERISTICS

The photoconductive layer, the current-diffusing layer and the electroluminescent layer are the three main components of a solid-state light amplifier.

a. The Photoconductive Layer:

The photoconductor is not ohmic in behavior. If a d.c. field is applied across a bonded photoconductive powder, the conductivity varies linearly with the incident light intensity. The field dependence of the conductivity is not linear. It changes as a fourth or higher power of the field, for a given light intensity. The dark current is usually small

compared to the photocurrent and varies as a high power of the applied voltage.

Under a.c. conditions, a capacitive current flows in addition to the photocurrent and the dark current. The dark current is much smaller than the capacitive current.

Fig. I.4 shows the variation of the photocurrent as a function of illumination for a bonded CdS powder. This is obtained using a standard gap of 5 mm. length and 0.5 mm. width. Bonded CdS powder was placed between the two electrodes of the gap and was illuminated with a 3.4 ft-c intensity, 40 W tungsten filament light source operated at rated voltage. 400 V d.c. is applied across the gap. We see that at low illumination levels deviation from the linearity is greater compared to the illumination levels.

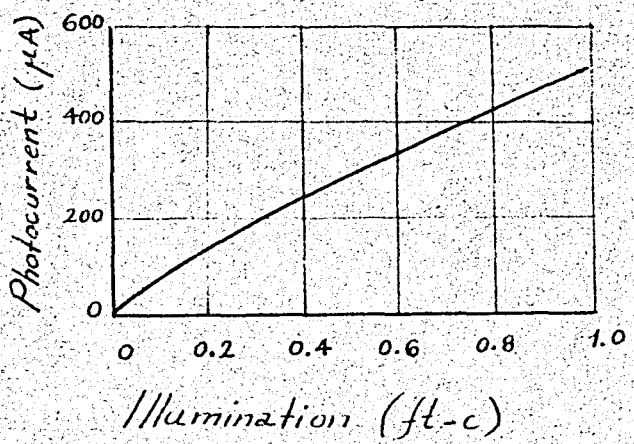

Fig. I.4 - Photocurrent as a function of Illumination

In Fig. I.5, the voltage dependence of measured d.c. photocurrents is shown. This was obtained for a photoconductive (bonded CdS powder) cell which has an electrode spacing of 20 mils, an effective area of 0.75 cm^2.

The cell was illuminated with 0,035 ft-c (2780°K Tungsten source). The value of the threshold voltage V_T can be obtained from the curve. The slope of the straight line portion gives the conductance (1/R) of the photoconductor which varies linearly with the input illumination. As the illumination level increases the maximum applicable voltage decreases.

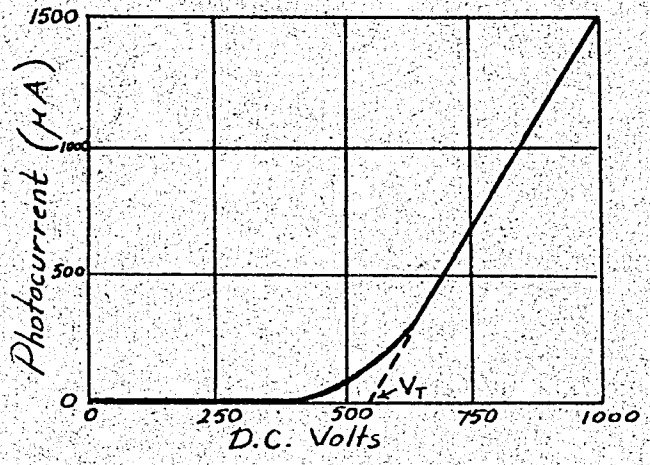

Fig. I.5 - Photocurrent as a function of applied dc. voltage.

The response characteristic given in Fig. I.6, belongs to the standard gap described above. We see that powder photoconductors have broader spectral response compared to crystals. For crystals the peak is at about 5000 Å. Using powder photoconductors we can broaden the range of radiation which can be amplified.

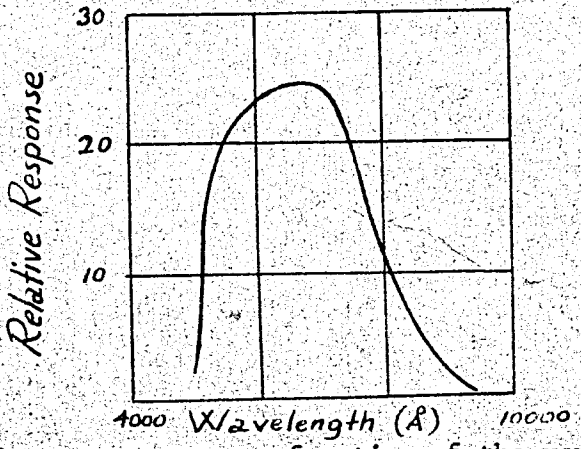

Fig. I.6 - Photoresponse as a function of the wavelength of the incident light.

The response time of the photoconductor used varies between 0.1 seconds to several seconds. Its risetime is equal to the decay time. The shortest response time is obtained at the high light levels.

b. The Current Diffusing Layer:

The current-diffusing layer is a non-photoconductive resistive layer of specially prepared CdS powder. Its conductivity is not lowered by a.c. voltage. In Fig. I.7, d.c. current versus d.c. voltage characteristic of a 1 cm^2 bonded sample of this material 10 mils thick, with electrodes on opposite surfaces is shown. The small value of the voltage drop (smaller than 30 V) through the layer is due to the small current values (below 1 mA/cm^2) required by the light amplifier. As we seen in Fig. I.7, the impedance of the layer shows a rapid increase with the decreasing voltage below 30 V. This property is useful for small - area contrast and maintaining picture resolution.

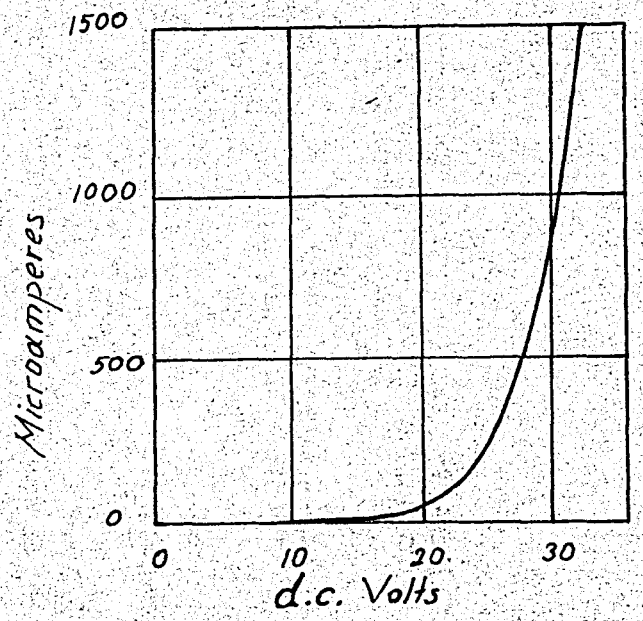

Fig. I.7 - Current vs applied voltage for current-diffusing layer

c. The Electroluminescent Layer:

The electroluminescent layer acts as a capacitor with negligible losses at the audio frequencies. For layers of 1 mil thick, the capacitance is about 200 $\mu\mu f/cm^2$. The phosphor response time, upon sudden application of voltage depends on its previous excitation and on the audio frequency used. It is in the range of 1 to 30 msec. Decay time of phosphor after the removal of voltage is very short (about 1 msec.). In Fig. I.8, a curve of measured values of electroluminescent light output as a function of applied a.c. voltage is illustrated. The frequency of the applied voltage is 400 Hz.

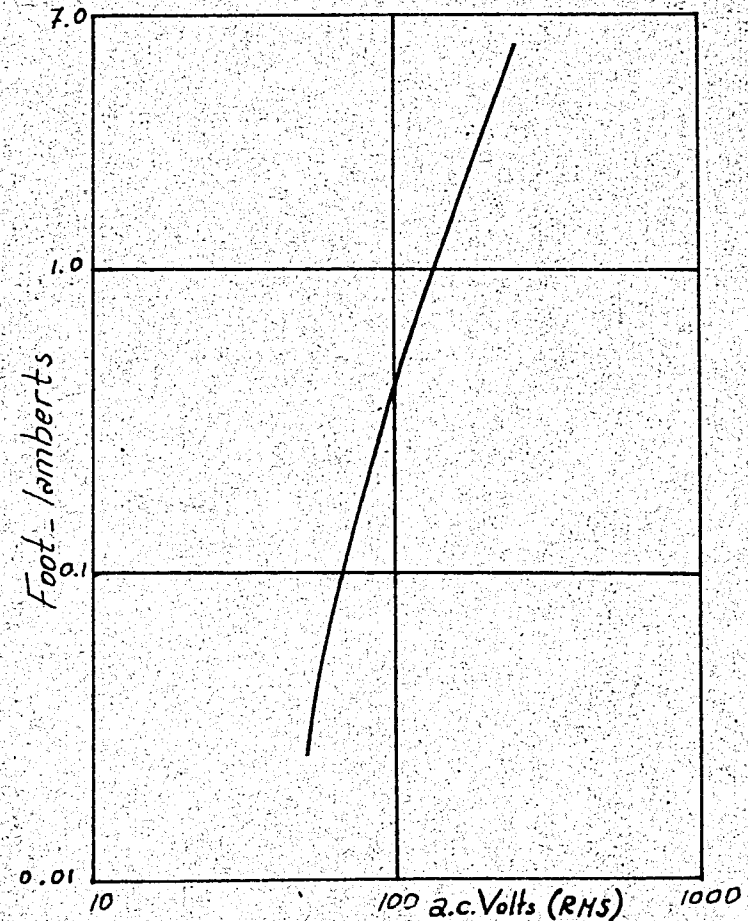

Fig. I.8 - Curve of Electroluminescent Light vs applied Voltage.

E. ANALYSIS OF THE SOLID STATE LIGHT AMPLIFIER

a. The Static Characteristic and The Gain:

The static characteristic of the amplifier is the relation between the input and the output radiations, the latter being observed after the input radiation has been incident for a long time.

Here we shall show two different methods of obtaining the static characteristic and the gain characteristic of the light amplifier. The first method gives an approximate analysis while the second one showing a more exact way of arriving at the results.

i) Approximate Analysis:

To analyze the amplifier in an approximate way we shall represent it by a simple series circuit as shown in Fig. I.9. The photoconductive layer can be represented by an ohmic resistance for convenience. Actually, it is non-ohmic in behavior. The electroluminescent layer is represented by a capacitance.

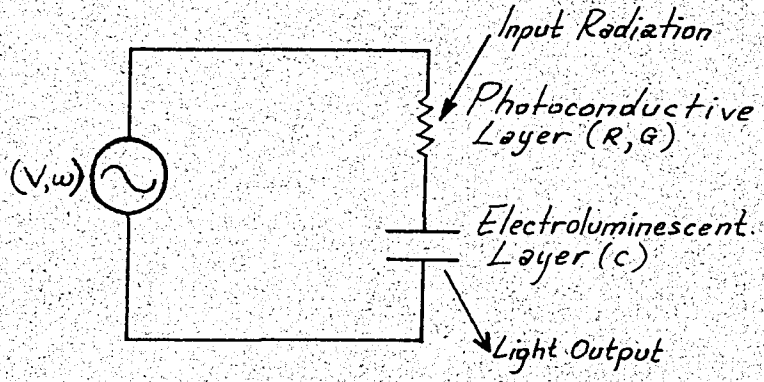

Fig. I.9—Equivalent Circuit for the Light Amplifier.

The conductance of the photoconductive layer is given by

$$G = G_o L^n \qquad \text{I-1}$$

where L is the illumination and n and G_o are constants. Equation I-1 applies after the illumination has been incident for a long time.

The output or brightness of the electroluminescent layer is represented by

$$B = B_o \omega^a V_c^m \qquad \text{I-2}$$

where B_o, a, m are constants, V_c is the voltage across the layer and $\frac{\omega}{2\pi}$ is the frequency of the applied voltage.

For convenience the output brightness of the amplifier will be represented by B_s. It is given by

$$B_s = B_m \frac{G^m}{\left[G^2 + (C\omega)^2\right]^{m/2}} \qquad \text{I-3}$$

where $B_m = B_o \omega^a V^m$, C is the capacitance of the electroluminescent layer, and G is the conductance of the photoconductor. By plotting Eq. I-3 over the various illumination regions, idealized static characteristic shown in Fig. I.10 is obtained.

It is of interest to discuss various regions of this characteristic.

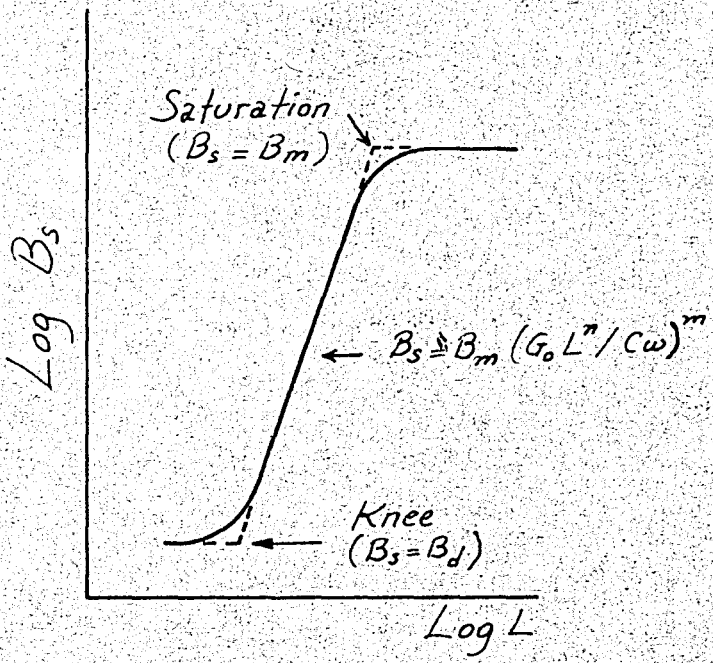

Fig. I.10 - Idealized curve for static characteristic.

Low-input Region: For low input levels, the conductance, which is caused by leakage, is usually small compared to the susceptance. In this region, Eq. I-3 can be modified as follows,

$$B_s = B_d = B_m \left(\frac{G_d}{C\omega}\right)^m \qquad \text{I-4}$$

where B_d is the background and G_d is the leakage conductance.

Intermediate Region: In this region, the conductanue is small compared to the susceptance and it is represented by Eq. I-1. By substituting Eq. I-1 into Eq. I-3 and neglecting the conductance with respect to the susceptance the following equation is obtained;

$$B_s = B_m \left(\frac{G_o L^n}{C\omega}\right)^m \qquad \text{I-5}$$

This equation gives the straight line portion of the characteristic. The characteristic has a slope of (m n) in the intermediate region.

Saturation Region: This is the high input region of the characteristic. In this region, the susceptance is much smaller than the conductance, and Eq. I-3 is reduced to the following equation.

$$B_s = B_m \qquad \text{I-6}$$

The lowest useful input, the saturation point, and the gain under static conditions are of interest.

The lowest useful input radiation is determined by the knee of the characteristic curve. The knee is the intersection point of the straight line portions of the low-input and the intermediate regions. At the knee, the conductance is given by

$$G = G_o L^n = G_d \qquad \text{I-7}$$

which defines the lowest useful input.

The saturation point, which is the intersection of the straight line portions of the intermediate and the saturation regions of the curve is given by

$$G_o L^n = C\omega \qquad \text{I-8}$$

The gain under static conditions is defined as (B/L). This quantity can be determined from Equations I-1 and I-3. By solving

$$\frac{d}{dL}\left(\frac{B_s}{L}\right) = 0$$

the condition for maximum gain,

$$G_o L^n = \left[\sqrt{mn - 1}\right] C\omega \qquad \text{I-9}$$

is obtained. It is given by

$$\text{Gain (max.)} = B_m \left(\frac{G_o}{\omega C}\right)^{\frac{1}{n}} \left[\frac{(mn-1)^{\frac{mn-1}{2n}}}{(mn)^{m/2}}\right] \qquad \text{I-10}$$

Experimental curves (Fig. I.11 and I.12) show that the maximum gain is close to the saturation point. The lowest useful input is about 0.001 foot-candles for the amplifier of these curves. This can be expected from the photocurrent and the dark current properties of the CdS photoconductor. m is about 3.5 for the zinc sulfo-selenide phosphor, n is about 0.7 for the photoconductor and (m n) is about 2.5. The steepness of the intermediate region is due to this value of (m n).

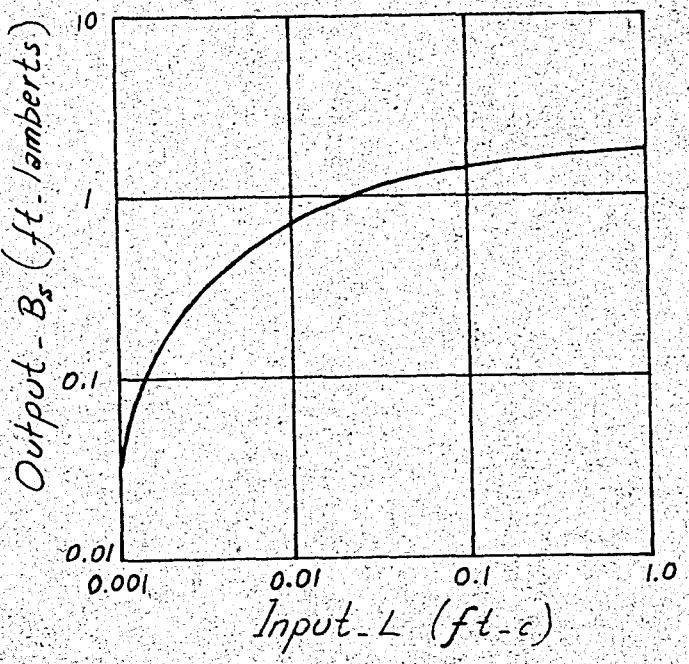

Fig. I.11 - Static characteristic (light input).

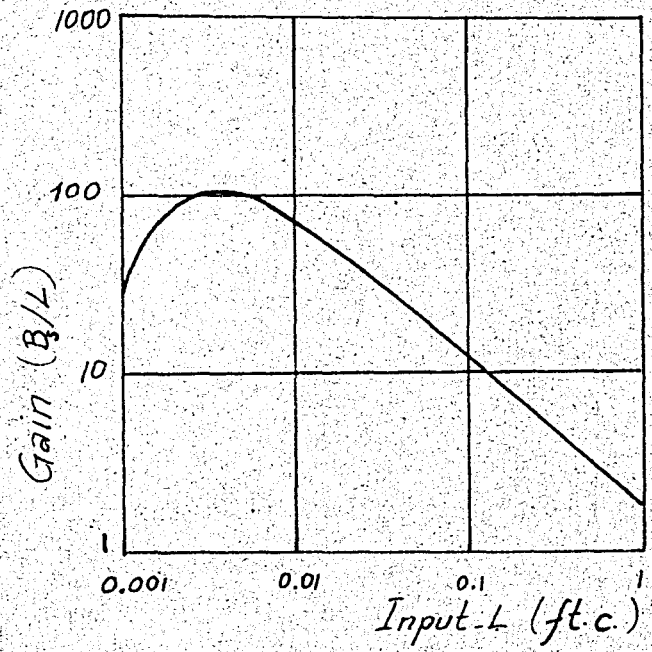

Fig. I.12 - Gain (light input).

ii) Exact Analysis:

In this section we shall present a more exact analysis of the solid state light amplifier compared to the previous one. In Fig. I.13 the equivalent electrical diagram of the complete amplifier is shown. Z_1 and Z_2 are respectively the impedances of the photoconductive and electroluminescent layers per unit area.

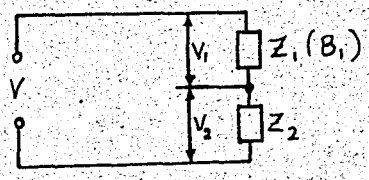

Fig. I.13 - Equivalent electrical circuit of the solid state light amplifier.

Before going into the details of the analysis we shall mention some assumptions on which the calculations are based:

a. The conductance of the photoconductive layer is a linear function of the incident light intensity. It can be shown as follows;

$$g_1 = b_1(B_o + B_1) \qquad \text{I-11}$$

where b_1 is a constant, "b_1B_o" is the dark conductance of the layer and B_1 is the incident light intensity and g_1 representing the conductance per unit area.

b. g_1 is not dependent on the operating frequency.

c. g_1 is not dependent on the operating voltage. This holds if the amplifier is operated in the linear region of the i-V characteristic.

d. The capacitance of the photoconductive layer is independent of B_1. Then, the complex admittance of the layer per unit area is given by;

$$Y_1 = g_1 + j\omega C_1 \qquad \text{I-12}$$

e. We shall calculate the characteristics of an amplifier operated with an a.c. voltage $V = V_o \cos\omega t$ applied across it. The output of the electroluminescent layer $V_2 = V_{20} \cos\omega t$ being applied across it is given by,

$$B_2 = \omega B_{2\infty} \exp(-A/V_{20}^{1/2}) \qquad \text{I-13}$$

where $B_{2\infty}$ and A are constants(Actually ω has an exponent changing between 0.5 and 1.)

The admittance of the electroluminescent layer is given by,

$$Y_2 = g_2 + j\,C_2 \qquad \text{I-14}$$

where g_2 is the conductance and C_2 is the capacitance of the layer per unit area. Y_2 is practically independent of B_2.

f. We also assume that the feedback is avoided by an opaque layer the a.c. impedance of which is negligible.

Referring to Fig. I.13, we can write the voltage across the electroluminescent layer as follows;

$$V_2 = V\,\frac{Z_2}{Z_1 + Z_2} \qquad \text{I-15}$$

where $Z_1 = (1/Y_1)$ and $Z_2 = (1/Y_2)$ are given by Equations I-12 and I-14.

If $g_2 = 0$

$$\left|\frac{V_{20}}{V_0}\right|^2 = \frac{|Z_2|^2}{|Z_1+Z_2|^2} = \frac{g_a}{g_a + p(p+2)} \qquad \text{I-16}$$

where $g_a = 1 + (g_1/\omega C_1)^2$, $p = C_2/C_1$

Combining Equations I-13 and I-16 we obtain;

$$\frac{B_2}{\omega B_{2\infty}} = \exp\left(-A V_0^{-1/2}\left[1 + \frac{p(p+2)}{g_a}\right]^{1/4}\right) \qquad \text{I-17}$$

Inserting Eq. I-11 in Eq. I-17 and putting $B_0 = 0$ we get,

$$\ln\left[\left(B_2/\omega B_{2\infty}\right)^{V_0^{1/2}/A}\right] = -\left[1 + \frac{p(p+2)}{1+\left(\frac{f_1 B_1}{\omega}\right)^2}\right]^{1/4} \qquad \text{I-18}$$

where $f_1 = (b_1/c_1)$.

Equation I-18 gives the relation between the input radiation B_1 and the output radiation B_2.

Since the electrical properties and the thickness of the electroluminescent layer is more or less prescribed, the parameters p and f_1 can be used to describe the variations of the layer. In Fig. I.14 a plot of

$$(B_2/\omega B_{2\infty})V_o^{1/2}/A \quad \text{versus} \quad f_1 B_1/\omega$$

for p = 1, p = 10 and p = 100 given on a log-log scale. We obtained the S shaped characteristics and minimum and maximum values of B_2 as we did by the previous method. B_{2min} cannot be lower than 10^{-2} lumens/m^2 and B_{2max} is determined either by the characteristic of the amplifier or by the breakdown of the electroluminescent layer. With good layers breakdown occurs at about $B_2/\omega B_{2\infty} = 10^{-1}$ per period.

In a certain range

$$B_2 = \text{Constant } B_1^{\gamma} \qquad \text{I-19}$$

may hold. In this equation γ is defined as the contrast amplification and gives the slope of the log B_2 vs log B_1 curve at intermediate regions. $\gamma > 1$ means contrast expansion, $\gamma < 1$ means contrast compression. At the inflection point of the curve γ takes its maximum value.

For low input intensities (B_1), Eq. I-18 reduces to

$$B_2 = B_{20} = \omega B_{2\infty} e^{-A(1+p)^{1/2}/V_o^{1/2}} \qquad \text{I-20}$$

so that B_{20} increases with increasing ω. For intermediate values of B_1, B_2

decreases with increasing ω. For large values of B_1 saturation occurs. In this case Eq. I-18 reduces to,

$$B_2 = B_{2s} = \omega B_{2\infty} e^{-A/V_o^{1/2}} \qquad \text{I-21}$$

so that B_{2s} increases with increasing ω. The relation,

$$B_2 = B_{20} + \text{Constant } B_1^{\gamma} \qquad \text{I-22}$$

can be satisfied almost accurately over a wide variety of regions except the saturation region. For large p values, the variation range of B_2 $(B_{20} < B_2 < B_{2s})$ increases.

In practice Eq. I-22 is valid over a wide range of input intensities and the gain can be expressed as

$$\frac{B_2}{B_1} = \text{Constant } B_1^{\gamma-1} \qquad \text{I-23}$$

The gain increases with increasing B_1 if $\gamma > 1$ and decreases with increasing B_1 if $\gamma < 1$.

We see that B_2 depends on B_1 only in the middle region.

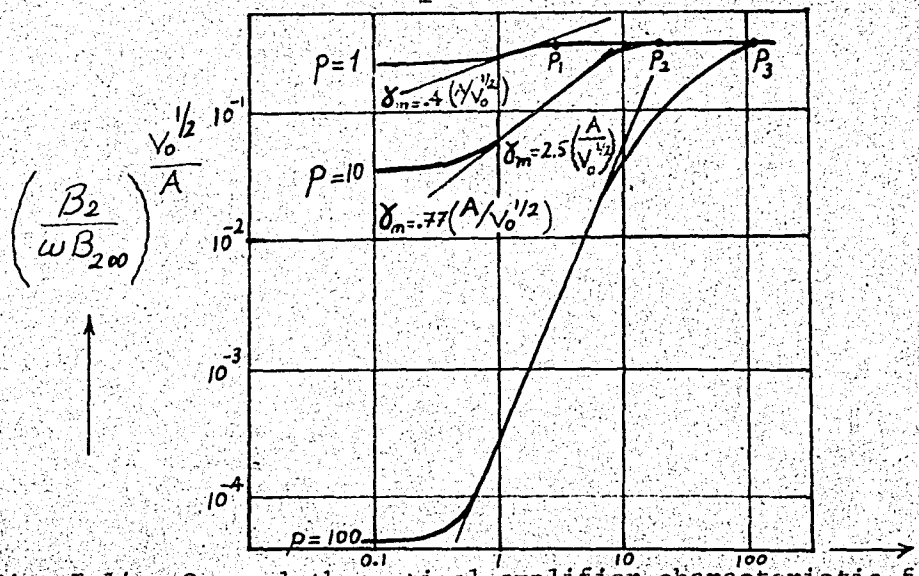

Fig. I.14 - General theoretical amplifier characteristic for various values of the capacitance ratio p. (If C_1 is changed, p and f_1 are also changed.)

b. Amplifier Parameters:

In addition to the static and the gain characteristics discussed above, it would be of interest to see the influence of various parameters on the operation of the amplifier. For this purpose, we shall take a sample CdS-ZnS combination and use the theoretical numerical values belonging to it in plotting the curves of Figures I-15, 16, 17, 18 and 19. The sample consists of a sintered CdS layer activated by Cu and Ga (with input light in the wavelength region matched to the thickness of the layer; μ = mobility of carriers $= 2 \times 10^{-3}$ m^2/V-sec), τ = Life time = 10^{-2} sec, $\bar{\varepsilon}_1$ = average relative dielectric constant of the photoconductive layer = 10, $g_o \cong 0$ and electron equivalent = q $= 10^8$ electrons/watt-sec) and a green electroluminescent layer of ZnS activated by Cu and Al suspended in urea-formaldehyde, having a thickness of 50μ ($\bar{\varepsilon}_2$ = Average relative dielectric constant of the electroluminescent layer = 5, $g_2 = 0$, $A = 60V^{1/2}$ and $B_{2\infty} = 1$ lumen/m^2, $B_{2\infty}$ has been taken as unity in plotting the curves.

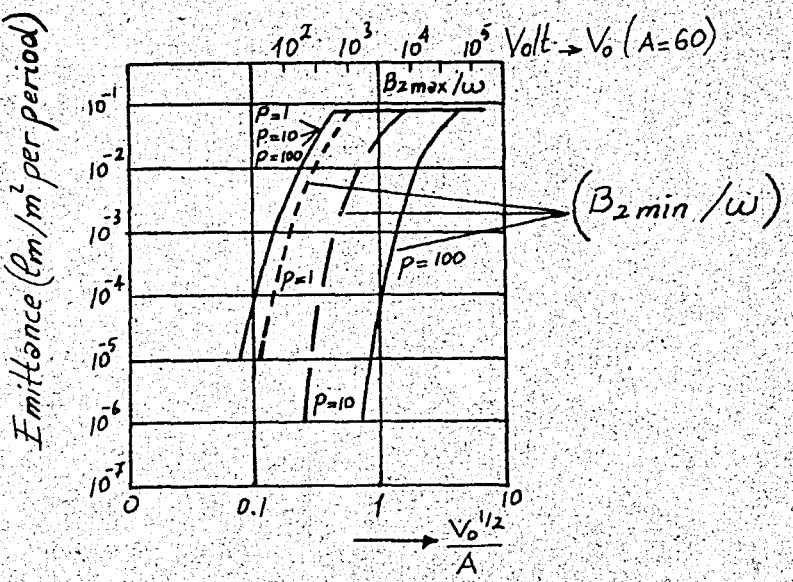

Fig. I.15 - Minimum and Maximum B_2 values (p and $\bar{\varepsilon}_1$ are parameters).

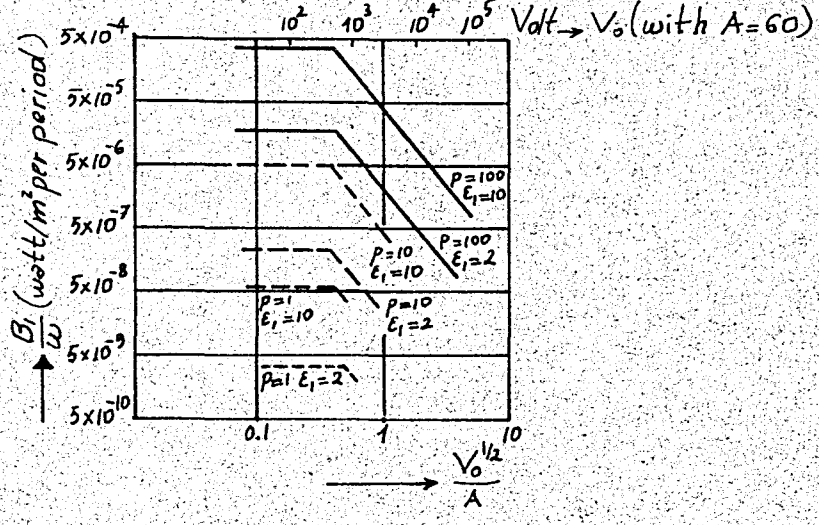

Fig. I.16 - B_1 values corresponding to maximum B_2 values (p and $\bar{\varepsilon}_1$ are parameters).

To have a high value of the output emittance the operating voltage should be as high as possible compared to the breakdown and the power dissipation of the photoconductive layer, γ and G of the amplifier. V_o = 500 V with p = 10 and 500 V $< V_o <$ 5000V with p = 100 are the favourable values.

i) The Maximum Amplification Factor (G_m):

G_m is the maximum value of the ratio of B_2 to B_1 (both in Watts/m^2). In Fig. I.17, G_m is plotted as a function of $\frac{V_o^{1/2}}{A}$. As seen in the figure G_m increases quickly as the operating voltage is increased. G_m is not influenced by ω because of the occurance of the combinations (B_1/ω) and (B_2/ω). Fig. I.17 was obtained by plotting (B_2/B_1) belonging to the points

P_1, P_2 and P_3 (see Fig. I.14). To obtain high G_m values for p = 100, high values for operating voltage should be used. For example $V_o \approx 5$ kV is a favorable value.

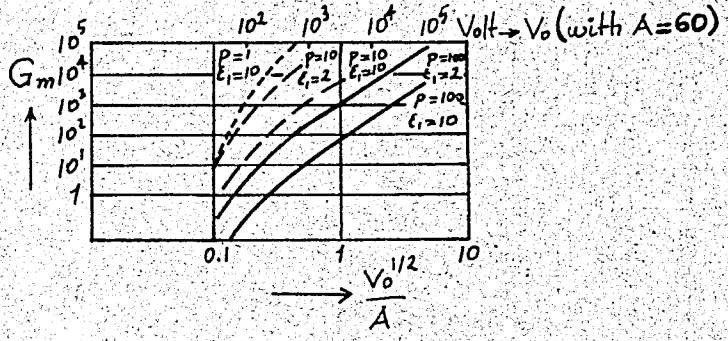

Fig. I.17 - Maximum value G_m of absolute amplification (p and $\bar{\ell}_1$ are the parameters).

ii) The Maximum Value of the Contrast Amplification (γ_m):

In Fig. I.18, γ_m is plotted as a function of $V_o^{1/2}/A$. γ_m is a decreasing function of V_o. To have the amplification as linear as possible high V_o values (also high G_m values) are required. High γ - values could be obtained by operating the amplifier with low V_o values, and high $\bar{\ell}_1$ and p values. This means low G_m, R_{B2} and high B_1 values. To obtain high values of G_m, two or more amplifiers can be operated by connecting them in series.

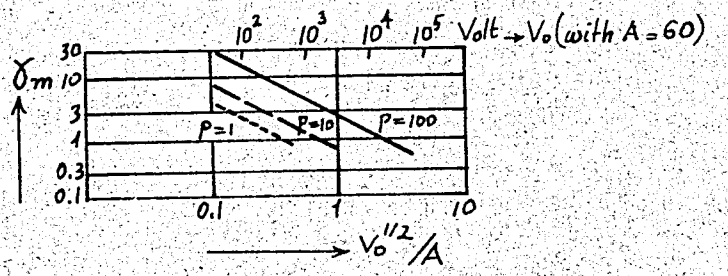

Fig. I.18 - Maximum values of contrast amplification (γ_m) (p as a parameter)

ω does not influence γ_m for the same reason we stated for G_m.

iii) Output Range (R_{B2}):

The output range is defined as the difference between B_{2max} and B_{2min} for a given frequency. For a given voltage V_o, R_{B2} shows a strong dependence on "p". Depending on the kind of application the useful range is a fraction of R_{B2}. This is due to the shape of (B_2, B_1) characteristic.

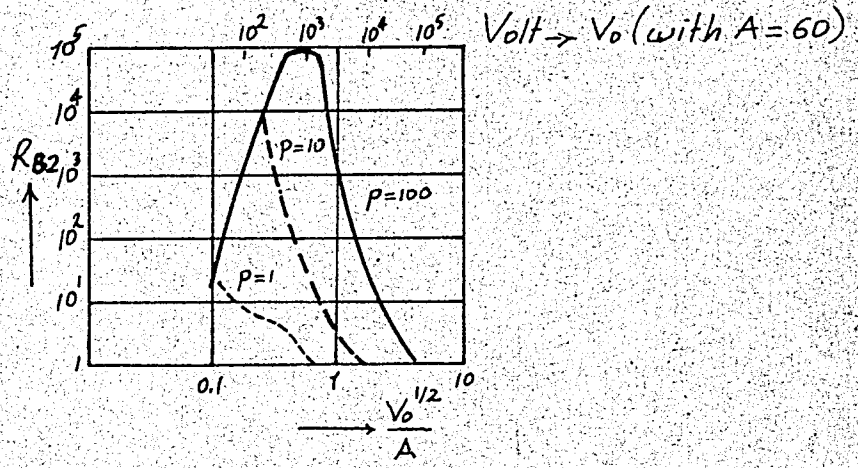

Fig. I.19 - Output range $R_{B2} = B_{2max} - B_{2min}$

X-ray and radar applications require high γ values. In choosing γ as high as possible the amplification factor and output emittance should be taken into consideration.

iv) The Operating Frequency (ω):

As we pointed out before ω does not influence γ_m and G_m, but it influences the level of amplification. In Fig. I.20, the shift of log B_2 vs log B_1 curve along a $+45^o$ slope for a change in ω is seen. The characteristic

can be linearized by a frequency modulation or by using a combination of two or more operating frequencies. The result is an envelope of the individual characteristics having a slope of 45^{o}.

To obtain high input sensitivity and high output level a series combination of two amplifiers, first one being operated at low ω and the second at high ω, is used.

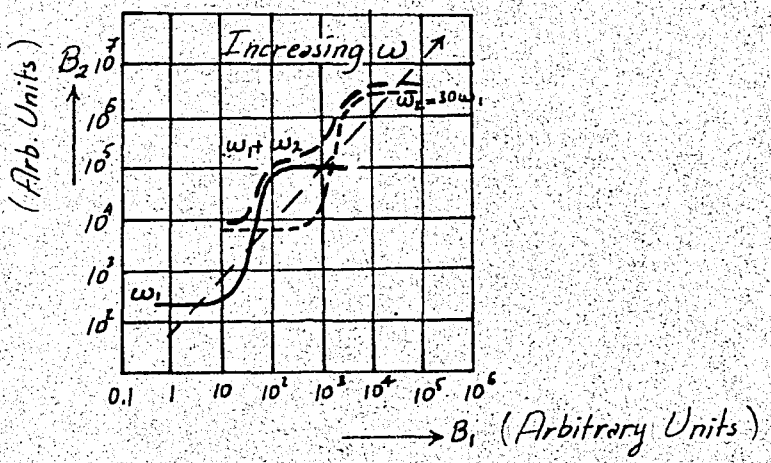

Fig. I.20 - B_2 vs B_1 on log-log scale.

Frequency changes will effect the impedance balance between the resistance and the ractance of the photoconductive layer. If the resistance of the layer becomes very small compared to its reactance when $V_2 = \frac{1}{2} V$ the relation

$$\frac{1}{R_1} = (2\pi C_2) f \qquad \text{I-24}$$

holds and shows that photoconductivity changes directly with frequency.

c. Voltage Effects:

The dark impedance of the photoconductive layer will change with a change in the applied voltage. This is due to the increase in the dark conductivity with applied voltage. This increase may be attributed to space charge limited currents. For CdS crystals, the variation of dark current as a function of V^n ($n > 1$) has been observed.

This effect is of importance if the decreased dark resistance becomes of the order of the electroluminescent reactance.

In the above analyses we assumed that the capacitance of the electroluminescent layer is constant. Actually, the increased applied voltage will cause an increase in this capacitance. The relation could be typically represented by

$$C_2 = C_o + KV_2^{1/3} \qquad \text{I-25}$$

where C_o = zero bias capacitance of electroluminescent layer.

C_2 and V_2 are the capacitance and the voltage of the electroluminescent layer. K is a constant.

Equation I-25 cannot be taken as an exact relation. The increase in the capacitance of the electroluminescent layer decreases the voltage applied to the electroluminescent layer. So, the external voltage required to achieve a given V_2 is increased beyond that of the simple capacitance model by the factor

$$\frac{V'}{V} = 1 + \frac{R_1 \omega K}{R_1 \omega C_o + 1} V_2^{1/3} \qquad \text{I-26}$$

where R_1 is the resistance of the photoconductive layer. The gain of the amplifier increases with the increasing voltage as well as the output brightness.

d. Negative Electrical Feedback:

A neutral impedance layer of an amplifier provides negative electrical feedback. The opaque insulating layer, placed between the photoconductive and the electroluminescent layers, is of this character. In Fig. I.21, the effect of this layer is represented by a third impedance Z_3. Addition of Z_3 decreases V_{20}/V_o and the slope of the log B_2 vs log B_1 curve. This is a way of correcting γ values for $\gamma > 1$. A resistive layer gives the best result for this purpose.

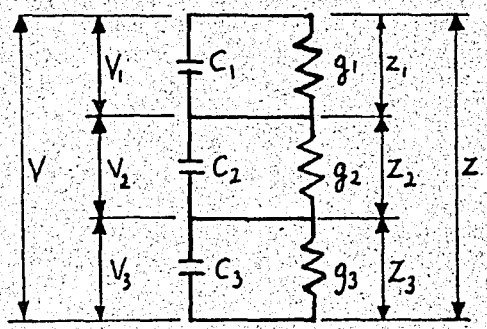

Fig. I.21 - Equivalent circuit of a three-layer amplifier.

To obtain the characteristics shown in Fig. I.23, the impedance ratio Z_2/Z can be constructed in the complex plane (Fig. I.22) and the voltage ratio $V_2/V = Z_2/Z$ can be read from it easily.

In Fig. I.22, Z_1, Z_2 and Z_3 are plotted and added vectorily. As B_1 is changed Z_1 moves along the half-circle, so it is possible to read Z_2/Z

corresponding to any input light intensity. In Fig. I.22, all admittances are expressed in units ωC_1 and all impedances in $1/\omega C_1$. By replacing V_{20} values in Eq. I-13 the amplifier characteristics of Fig. I.23 are obtained.

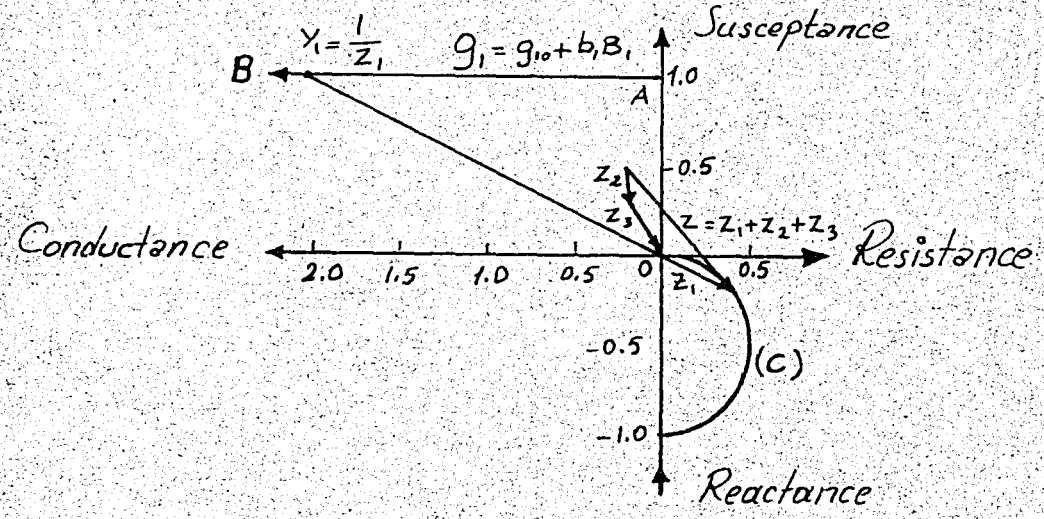

Fig. I.22 - Construction of the impedance ratio Z_2/Z in the complex plane.

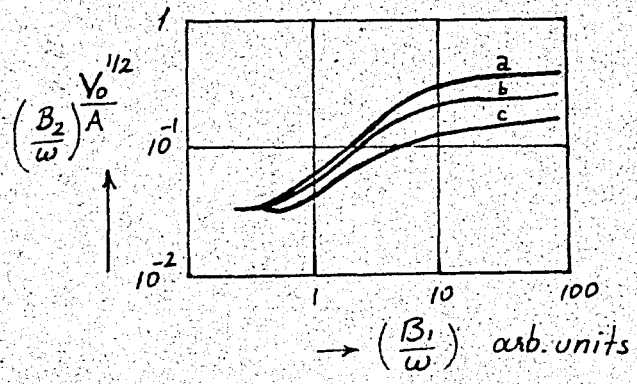

Fig. I.23 - Influence of a series impedance layer on the amplifier characteristic. ($p = 10$; $g_o = g_2 = 0$)

Curve a : $Z_3 = 0$

Curve b : $Z_3 = 1/j\omega C_2$ (Capacitive Layer)

Curve c : $Z_3 = 3/\omega C_2$ (Resistive Layer)

In addition to the linearization of the $\log B_2$ vs $\log B_1$ plot, the neutral auxiliary impedance layer reduces the amplification factor.

e. Positive Optical Feedback:

Solid-state light amplifiers employ an opaque layer to avoid optical feedback. Here we shall discuss the performance of the amplifier without an opaque layer and with an opaque mesh structure. We shall take an amplifier consisting of sintered CdS photoconductive layer (500μ) and a green electroluminescent ZnS layer (50μ) as the example. Fig. I.24-2 shows the situation without an antifeedback layer. A local radiation B_1 introduces a column of conductivity through the CdS layer and gives rise to a green emission, B_2. If there were not feedback we would obtain a bright spot. However, due to feedback a thin conducting surface is created. Conductivity in the sintered layer does not diffuse to the parts which are not irradiated, but the green light B_2, scattered in the electroluminescent layer induces the surface conductivity in a few seconds in CdS.

In case of non-transparent mesh structure (see Fig. I.24-b), there is a certain amount of feedback, but the instability is not as severe as before.

In Fig. I.25 spectral distributions of ZnS and the response of CdS are shown. The two curves overlap each other giving rise to a feedback fraction, m, which is of the order of some percent.

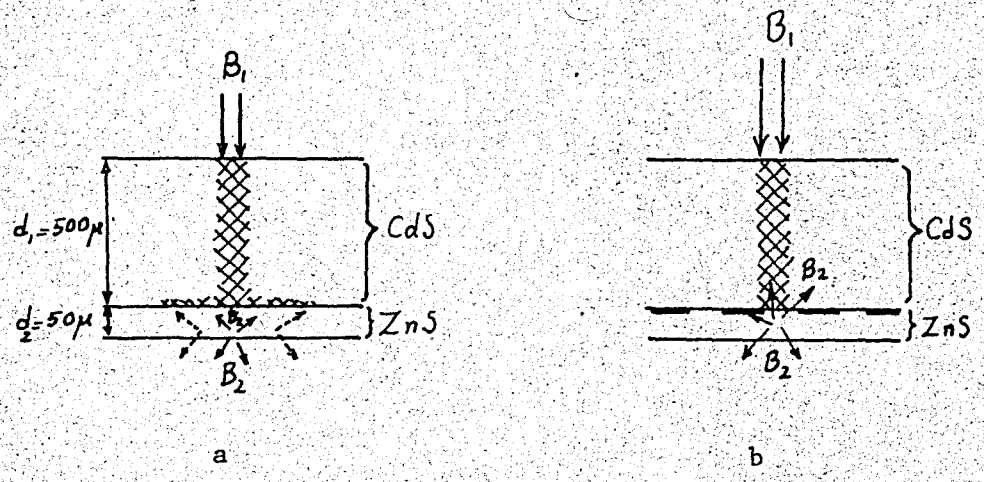

Fig. I.24 - Optical feedback; a) Without an opaque layer
b) With an absorbing mesh.

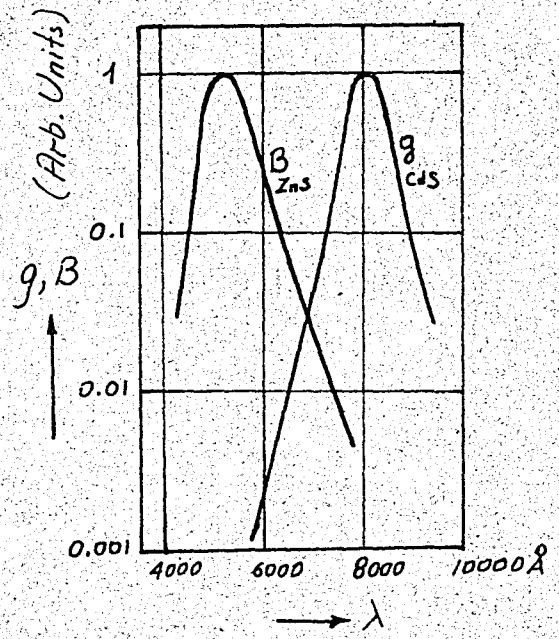

Fig. I.25 - Spectral distribution of green electroluminescent ZnS and response of photoconductivity for a CdS layer (d_1 = 500μ)

It is of interest to analyze the performance of a light amplifier with a certain amount of feedback and find the operating points of it graphically. In Fig. I.26, we have the amplificon characteristic plotted on a semi-log paper together with the feedback curve. The characteristic can be represented by

$$y = C(X) \qquad \text{I-27}$$

where $x = \frac{f_1 B_1}{\omega}$ and $y = \log\left(\frac{B_2}{\omega B_{2\infty}}\right)^{V_o^{1/2}/A}$

The feedback condition is given by;

$$B_1 = B_{10} + mB_2 \qquad \text{I-28}$$

where B_{10} = external input radiation.

mB_2 = feedback radiation,

and B_1 = Equivalent intensity of the sum of B_{10} and mB_2. m depends on three factors, namely; the overlapping in Fig. I.25, the relative response of the photoconductive layer to B_1 and B_2 and the transmission of the opaque layer. The feedback condition can be written in terms of x and y as follows;

$$y = v\left[\log (x - x_o) + \log \left(\frac{1}{m_1}\right)\right] \qquad \text{I-29}$$

where

$$v = V_o^{1/2}/A; \quad x_o = f_1 B_{10}/\omega \quad ; \quad m_1 = f_1 B_{2\infty} m$$

The operating points of the amplifier are given by the intersection points of the characteristic and feedback curves as seen in Fig. I.26. These

curves belong to the amplifier whose various characteristic properties were described by Figures I.15 to 19 and they are plotted putting $x_o = 0$, which means no external input radiation, $v = 0.67$, $m_1 = 63$, which corresponds to $m \approx 10^{-2}$ and $\bar{\varepsilon}_1 = 10$. Two of the three operating points P_1 and P_3 are stable while P_2 is unstable. The previous conditions of the amplifier will decide whether P_1 or P_3 will be the operating point. By adjusting X_o, m and V_o the relative positions of the feedback and the characteristic curves may be changed.

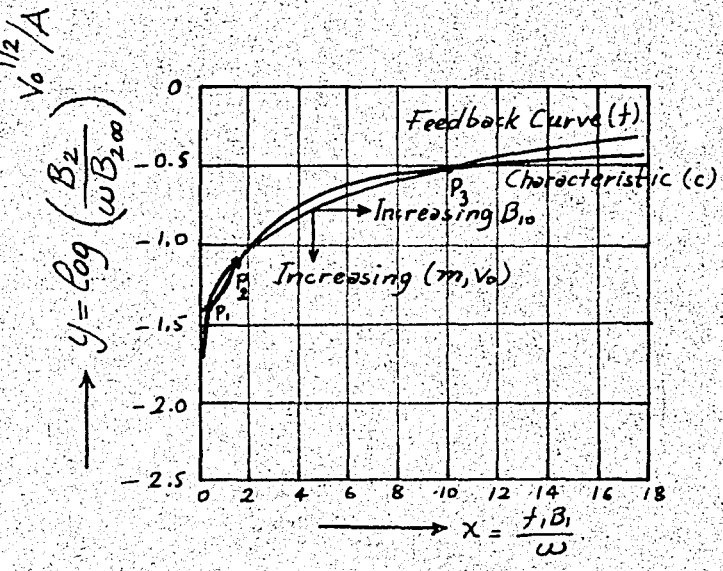

Fig. I.26 - Amplificon characteristic and feedback curve p = 10. (Variations of the feedback curve with B_{10}, m and V_o are shown by the arrows.)

For $\gamma = 1$ we can obtain a suitable relation between B_2 and B_{10} to explain the effect of optical feedback. Suppose we operate in a region at which Eq. I-22 is valid. Substituting I-28 into I-22 we obtain,

$$B_2 = B_{20} + C(B_{10} + mB_2)^{\gamma} \qquad \text{I-30}$$

where C = constant.

Putting $\gamma = 1$ in Eq. I-30,

$$B_2 = \frac{B_{20} + CB_{10}}{1 - Cm} \qquad \text{I-31}$$

is obtained. Eq. I-31 shows that the feedback is thus always positive (regenerative), and instability occurs if $mC > 1$.

f. Storage:

The storage property of the amplifier is another interesting aspect. The amplifier could be adjusted to operate at point P_1 in the absence of B_{10}. It can be triggered by a pulse of radiation, B_{10}, to point P_3 since an increase in X_o shifts the feedback curve to the right. At the end of the B_{10} pulse the amplifier shifts back to the first point, P_1, but before X_o becomes zero. The two values of X_o, which shift the operating point from P_1 to P_3 and P_3 to P_1 are not equal. The first one denoted by X_{oa} is greater than the second one, X_{oc}. The duration of the decay ofthe output is determined by the relaxation times of the amplificon layers. In Fig. I.27, storage is shown schematically. The input intensity X_o and the log of the output intensity y are plotted vs time t. τ_1 and τ_2 are storage times for the two levels of output intensity (1) and (2).

Another way of shifting the operating point from P_3 to P_1 is to decrease the value of V_o.

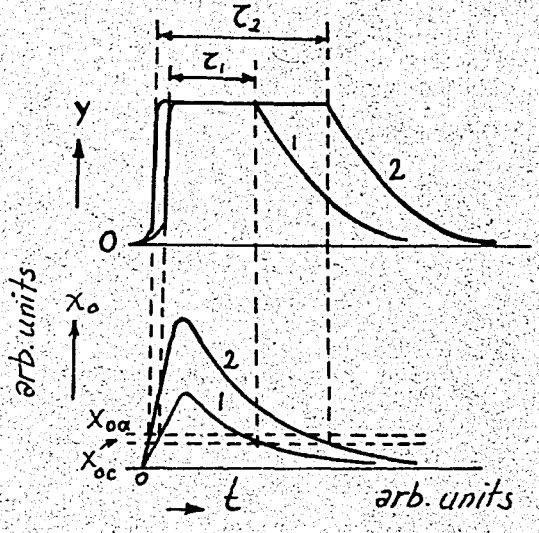

Fig. I.27 - Schematic representation of storage by triggering combined with the possibility of gradation in the output image.

g. Instantaneous Dynamic Characteristic (Approximate Analysis):

Instantaneous dynamic characteristic is obtained by applying a short pulse of input radiation to the amplifier, and observing the output immediately. This kind of operation is useful in X-ray applications. In Fig. I.28 a hypothetical curve for instantaneous dynamic characteristic is given.

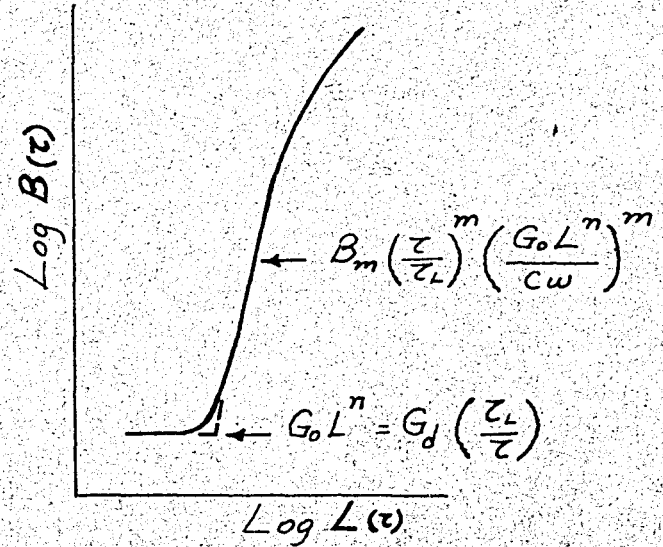

Fig. I.28 - Hypothetical curve for instantaneous dynamic characteristic.

The conductivity of the photoconductor, being approximately an exponential function of time, can be given by,

$$G = G_o L^n \left[1 - \exp\left(- \frac{\tau}{\tau_L} \right) \right] \qquad \text{I-32}$$

where τ = exposure time and τ_L is the time constant associated with illumination L. For the usual case τ is very small compared to τ_L so,

$$e^{-\frac{\tau}{\tau_L}} = 1 - \frac{\tau}{\tau_L} \quad \text{for} \quad \tau \ll \tau_L$$

substituting this into Eq. I-32, we obtain,

$$G = G_o L^n \left(\frac{\tau}{\tau_L} \right) \qquad \text{I-33}$$

Substituting Eq. I-33 in Eq. I-3 and neglecting G compared to ωC in the denominator for the intermediate region we obtain the following equation for the output brightness at time τ.

$$B(\tau) = B_m \left(\frac{\tau}{\tau_L} \right)^m \left(\frac{G_o L^n}{C\omega} \right)^m \qquad \text{I-34}$$

The minimum illumination is obtained at the knee of the curve and is given by,

$$G_o L^n = G_d \left(\frac{\tau_L}{\tau} \right) \qquad \text{I-35}$$

h. Integrated Dynamic Characteristic (Approximate Analysis):

To obtain the integrated dynamic characteristic, the output energy is considered as a function of the input energy associated with a short exposure. This is used when the output is desired to be recorded. The integrated

dynamic characteristic is plotted as $\int_0^{\tau_i} B.dt$ as a function of $L\tau$. τ_i is the time during which the output is observed. In Fig. I.29 the idealized curve of integrated dynamic characteristic is given. It is of interest to analyze the three regions of the curve.

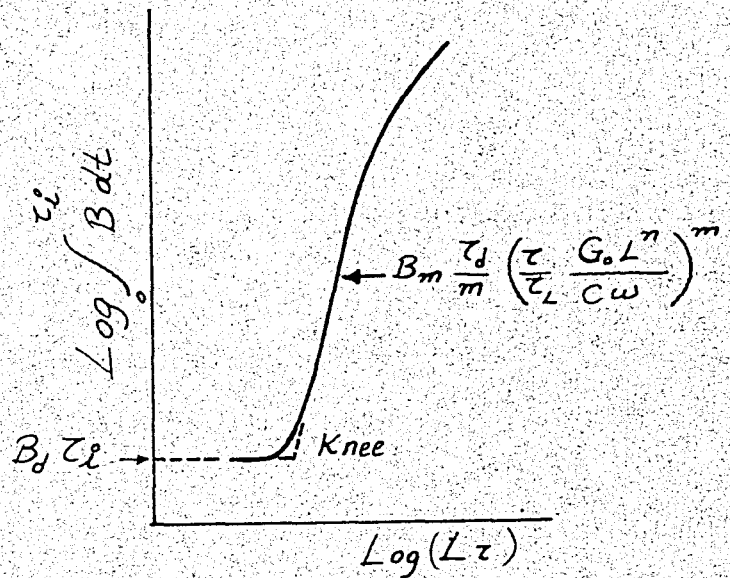

Fig. I.29 - Idealized curve of integrated dynamic characteristic.

Low-input Region: At low light levels, the output of the amplifier is equal to the background value, B_d, which is a constant. The dynamic integrated output is,

$$\int_0^{\tau_i} B.dt = B_d.\tau_i \qquad \text{I-36}$$

Intermediate Region: The conductance of the photoconductive layer rises exponentially during exposure and starts to decay with a time constant τ_d at the end of the exposure. τ_d is the characteristic of very low input level. During exposure the brightness reaches the level given by Eq. I-34 and then starts to decay as given by Eq. I-37.

$$B(t) = B(\tau)\ \exp\left[\frac{-mt}{\tau_d}\right] \qquad \text{I-37}$$

If Eq. I-37 is integrated from zero to infinity we obtain the integrated output of the amplifier. This is convenient for all practical purposes. Therefore,

$$\int_0^{\tau_i} B.dt = B_m\left(\frac{\tau_d}{m}\right)\left(\frac{\tau}{\tau_L}.\frac{G_o L^n}{\omega C}\right)^m \qquad \text{I-38}$$

is the integrated dynamic output of the amplifier for the intermediate region.

Saturated Region: This region is reached at higher input levels.

The lowest useful exposure can be determined from the intersection point of two straight-line portions of the characteristic. This point is the knee of the curve. Equating I-38 to I-36 and substituting Eq. I-4 in the equality we obtain,

$$\frac{m\tau_i}{\tau_d} = \left[\frac{\tau G_L}{\tau_L G_d}\right]^m \qquad \text{I-39}$$

for the useful exposure. If τ_i is of the order of the lowest response time, τ_d, then the minimum exposure time is given as follows,

$$\tau_{min} = \tau_L\ m^{1/m}\left(\frac{G_d}{G_L}\right) \qquad \text{I-40}$$

The dynamic gain is given by $\int_0^{\tau_i} B.dt/(L\tau)$. Performing the integration we obtain,

$$\text{Dynamic Gain} = B_m\left(\frac{\tau_d}{m}\right)\left(\frac{G_o}{\tau_L C\omega}\right)^m . L^{mn-1} . \tau^{m-1} \qquad \text{I-41}$$

In dynamic operation, the minimum exposure might be desired to be lower. If CdSe is used as the photoconductor, faster response is obtained. CdSe photoconductors are about three orders of magnitude faster than CdS

photoconductors and are about as fast as the best photographic film.

If the performance of a typical sintered CdS cell is compared with the theoretical values obtained on the basis of data belonging to it, we see that there are differences between the two treatments.

For a typical CdS cell(the 7163), $L\tau$(min) is 0.5 meter-candle-second theoretically and .2 m-c-s experimentally.

For the same cell theoretical γ value is 2.5, while experimental value is 4.3. Since high γ value produces high contrast ratio, it could be reduced by reducing either m or n. A moderate reduction in n is possible, but m can be reduced considerably by reducing the thickness of the electroluminescent layer, keeping the applied voltage constant. In the second case, photoconductive layer should also be reduced in thickness to keep the operating range same.

In Fig. I.30, the integrated dynamic characteristic for a grooved light amplifier is given.

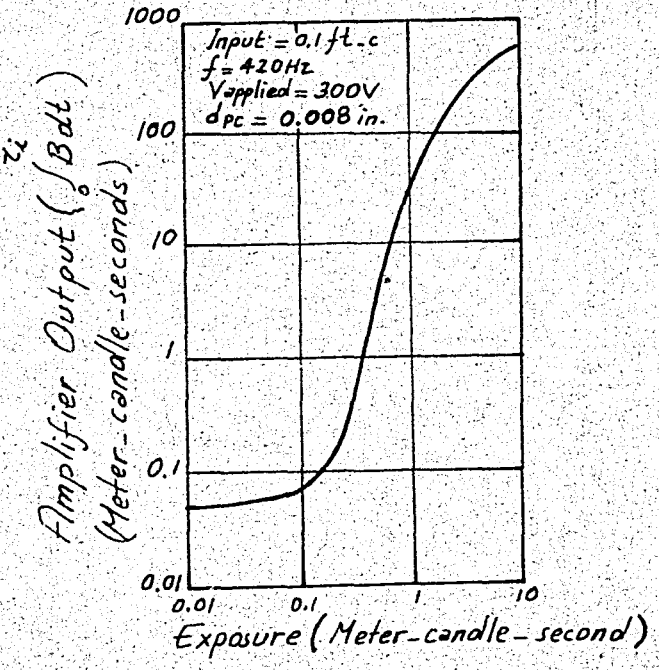

Fig. I.30 - Integrated dynamic characteristic for a grooved light-amplifier structure with a visible light input of 2870°K.

F. METHODS OF OPERATION

Improved CdS powder bonded with plastic is one of the most commonly used photoconductors in the production of panel light amplifiers. The current voltage characteristic of this material is very nonlinear. Photocurrent rises as the fourth power of the voltage over many orders of magnitude of current. However, at higher voltage levels, it rises with somewhat lower powers of voltage. Due to this nonlinearity, amplifier gain is reduced when operated with a.c. voltage. This is the conventional method of operation and is shown in Fig. I.31 with sine wave excitation.

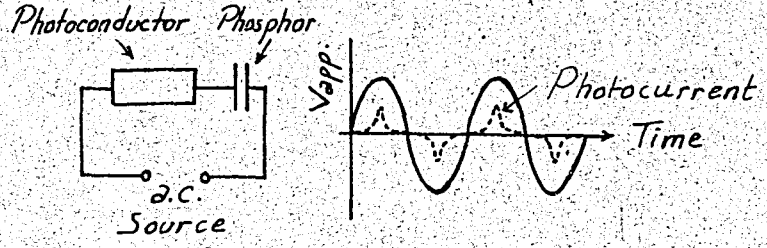

Fig. I.31 - AC operation of single element.

Because of the nonlinearity of the photoconductor, most of the photocurrent flows during a small portion of the cycle when the voltage is near its peak. With a linear photoconductor, operated under the same conditions, we would get a current of higher average value and more output light. The peak voltage which can be applied to the photoconductor is limited by breakdown. With a given peak voltage level better results are obtained by using rectangular wave shapes.

To obtain larger increase in photocurrent new methods of operation are used.

If a d.c. voltage equal to the peak a.c. voltage is applied to the photoconductor, it is found that the d.c. photocurrent is many times greater than the peak a.c. photocurrent. This is a particular property of the CdS photoconductive powder. Photosensitivity may increase 10 times, at the low-light levels.

The electroluminescent phosphor requires a.c. voltage for operation. It is inoperative with d.c. voltage. Due to these facts, simple conventional method of operation for the amplifier does not give satisfactory results.

In Fig. I.32, the restified a.c. operation of a single element is shown. Two equally illuminated photoconductors are employed. In series with each photoconductor is a diode so that a half-wave rectified voltage of opposite polarity and phase is applied to the two photoconductors. In operation during a positive half cycle, the phosphor element is charged positive by the current pulse through photoconductor A. During the next half cycle, it is charged negative by the current pulse through the other photoconductor. In this manner an a.c. voltage is developed across the phosphor. The peak photocurrent obtained with pulsed d.c. voltage is almost as great as with steady d.c. Rectified a.c. operation increases a.c. voltage across the phosphor element, for a given incident light flux.

Another method, which improves the operation of a panel light amplifier further, is shown in Fig. I.33. Here d.c. bias voltages of opposite polarity are in series with the two photoconductive elements. Since the bias voltage is set equal to the peak value of the appied a.c. voltage, pulsating d.c.

voltages, which are opposite in phase and polarity, are developed across the photoconductors. Since the voltage pulses are wider between half-value points compared to the rectified a.c. operation, wider photocurrent pulses are obtained by this method.

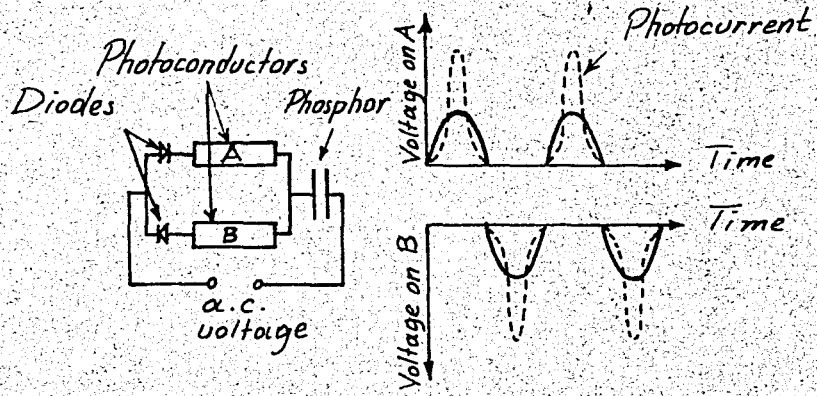

Fig. I.32 - Rectified a.c. operation of a single element

Biased a.c. operation increases the average value of the a.c. current through the phosphor, thus, producing more output light. Although the voltage applied to one photoconductor rises before the voltage on the other one falls to zero, the current flow can be neglected when the instantaneous voltage is low for most input levels because of the nonlinear property of the photoconductors.

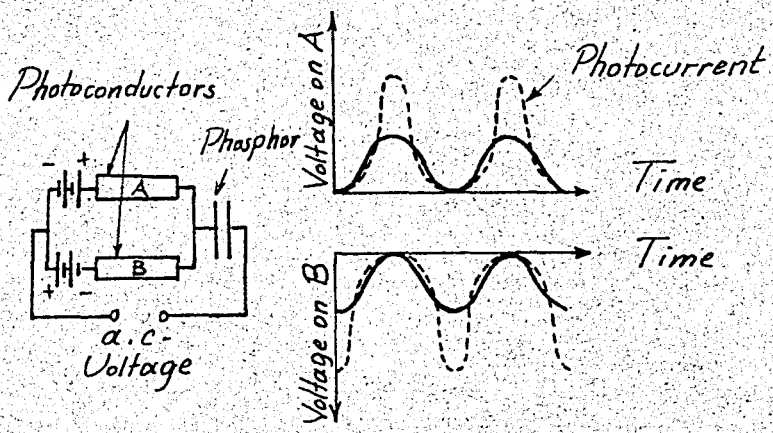

Fig. I.33 - Biased a.c. operation of single element.

To apply the rectified a.c. or biased a.c. methods of operation to the light amplifier a modification of the electrode system is necessary. In Fig. I.34 the cross-section of a light amplifier operated with biased a.c. is shown. The conducting lines on the grooved photoconductor are seperated into two sets, and each set is connected to one of the bias supplies. Incident light produces conductivity on the surfaces of the grooves at the illuminated areas. The portions of the photoconductor and phosphor area corresponding to the single element of the previous figure are shown by the heavy lines.

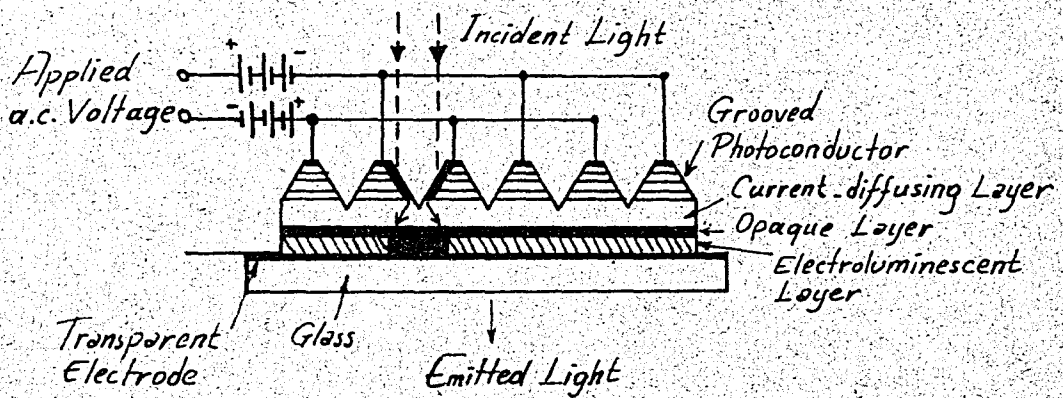

Fig. I.34 - Biased a.c. operation of light amplifier.

It is of interest to compare the three types of operation by observing the input-output characteristics belonging to them. In figure I.35, the input-output characteristics of a grooved type CdS-ZnS light amplifier, for different methods of operation are given. These are obtained by flooding the amplifier with a high light level and then allowing it to decay until an output level of 0.0012 foot-lambert is obtained and taking the readings 10 seconds after the excitation with yellow electroluminescent light source of 420 Hz frequency. The curves have a gamma value of about three.

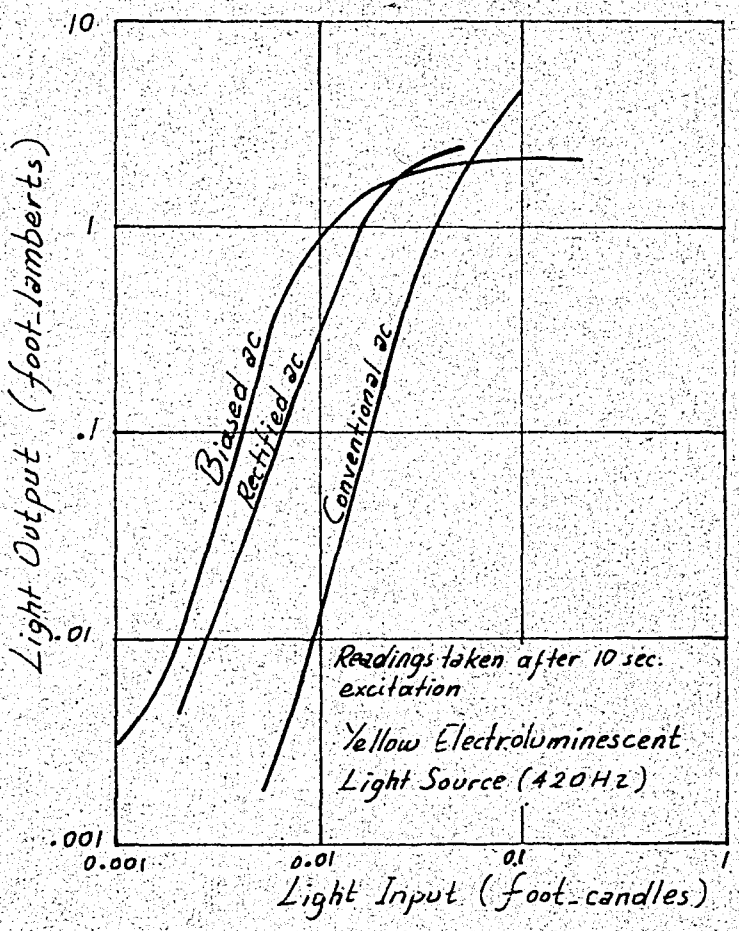

Fig. I.35 - Input-output characteristics for different methods of operation.

As seen in Fig. I.35, at low input levels, rectified a.c. operation gives 20 times as much output light as the conventional a.c. operation. This figure becomes 50 in case of biased a.c. operation. With biased a.c. operation threshold value of input is lowered to a value which is about five times less than the value with conventional a.c. operation.

In all three cases the characteristics go to saturation at high input levels. Rectified a.c. operation provides saturation at lower input levels compared to conventional a.c. operation while biased a.c. characteristic

becomes flat. Saturations for rectified and biased a.c. operations are due to the leakage of charge through the photoconductive elements during the half cycle when they are assumed to be nonconducting. Clipping action of the biased a.c. operation protects the phosphor layer from breakdown, because it limits the voltage applied to the phosphor.

The curves shift to the left or right for longer or shorter excitations respectively.

G. BUILD-UP CHARACTERISTICS

To have an idea about the build-up properties of an amplifier we shall refer to Figures I.36 and I.37. Figure I.36 shows DC photocurrent vs time for a grooved type photoconductor. These curves are obtained first flooding the photoconductor with a high light level and allowing the photocurrent to decrease to approximately 4 μA and then switching on the input light source. Each curve is obtained for a certain input light level. All of them rise as the square of time after a small input value. Their build-up times vary almost inversely with the input light level.

In case of higher applied voltages the photoconductive layer can have a sensitivity of 40 A/lumen for a yellow electroluminescent input peaked at 550 mμ. The photoconductive layer is approximately 15 mils thick and can stand more than 500 V, so a power flow of more than 10^4 watt/lumens can be expected.

The build-up property of the photoconductor effects the amplifier operation considerably as shown in Fig. I.37. These curves are obtained by using biased a.c. operation. To obtain them, the amplifier is pre-excited and

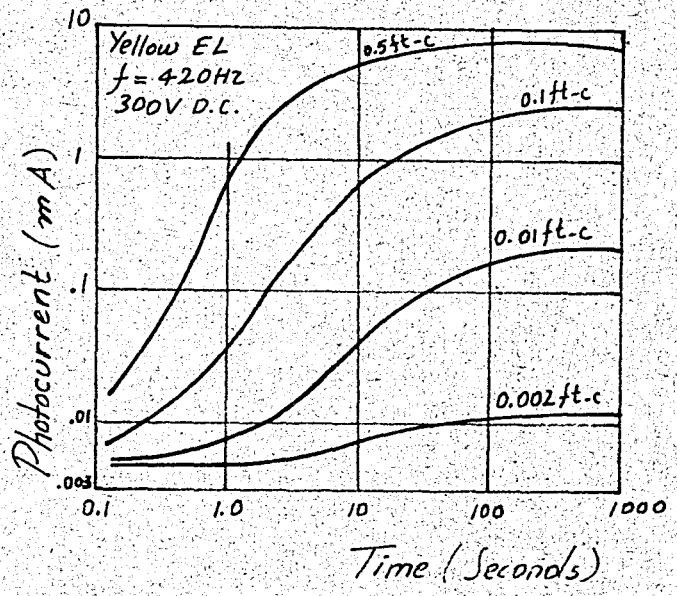

Fig. I.36 - DC photocurrent vs time for different input light levels.

allowed to decay to an output level of 0.0012 foot-lamberts and then the variation of output brightness with time is recorded. An input source of yellow electroluminescent light which has a spectral distribution identical to the amplifier output is used. The photoconductor is peaked at 750 mμ wavelength and the electroluminescent layer at 550 mμ. If we use an input peaked at 750 mμ, an energy gain of 800 is obtained.

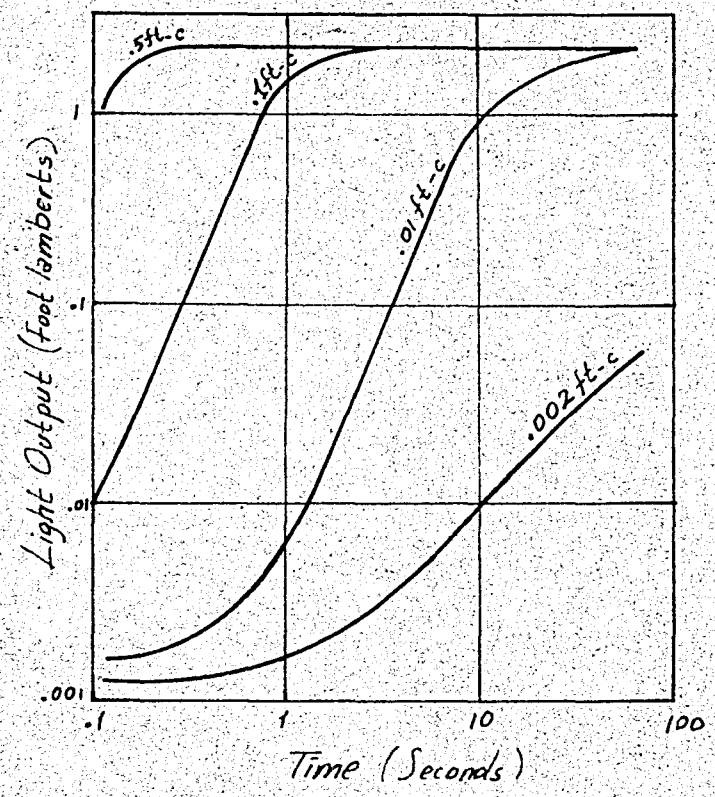

Fig. I.37 - Amplifier output vs time for different input light levels using biased a.c.

H. DECAY PROPERTIES

In Figures I.38 and I.39 decay curves of the amplifier, whose build-up characteristics were discussed before, are given. Fig. I.38, was obtained with conventional a.c. operation, while Fig. I.39 with biased a.c. operation. We see that specified amplifier has a decay time of the order of seconds. Both of the figures are obtained after an excitation time of one seconds. In Fig. I.38, the decay curve for the highest light input shows a faster rate of decay compared to some lower input curves. This is due to a temperature rise in the photoconductor which is caused by the power dissipated by the high photocurrents.

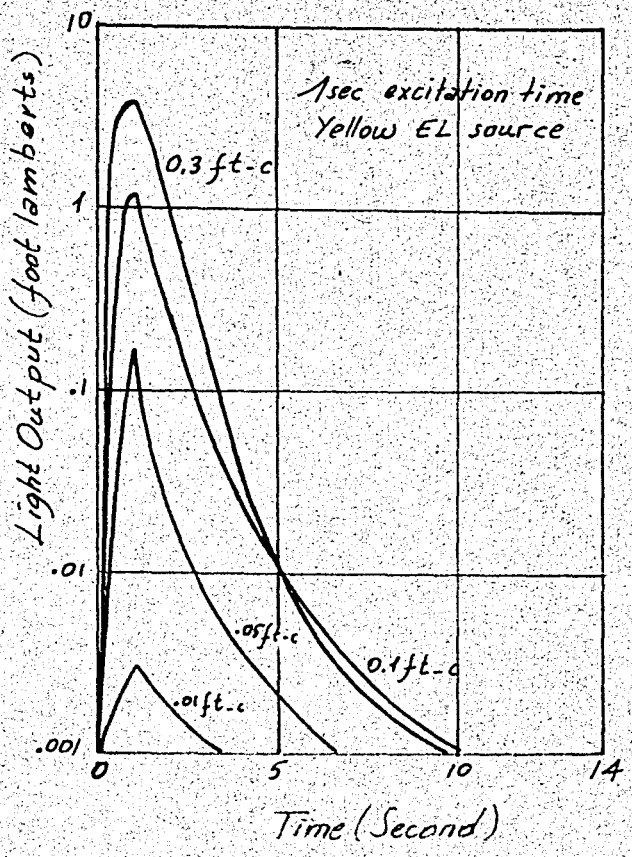

Fig. I.38 - Decay curves for a.c. operation.

In case of biased a.c. operation, an exponential decay is observed. Decay of the output can be represented by $B_2 = Ke^{-0.3t}$ where t is time. According to this relation output falls to 1/e of its initial value in approximately three seconds.

Long decay time is desirable in some X-ray applications. In viewing stationary X-ray images, patients are exposed to X-rays for shorter time. Due to the persistance of the image, it can be studied with the X-rays off. If the photograph of the image is desired, higher light output and longer persistance of the figure are advantageous.

In both cases higher decay rates are obtained at higher input light levels.

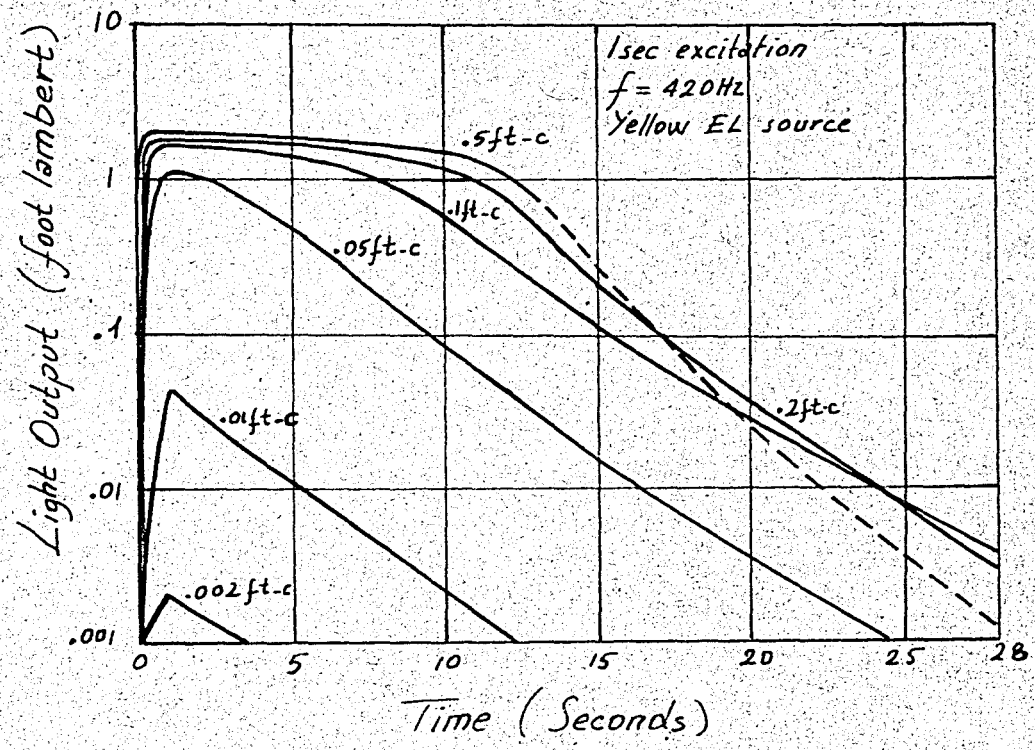

Fig. I.39 - Decay Curves for biased a.c. operation.

Time integrated input-output characteristics of the amplifier can be obtained from the decay curves. Fig. I.40 shows the characteristic obtained from Fig. I.39. This has a gamma of about 2. The maximum integrated gain

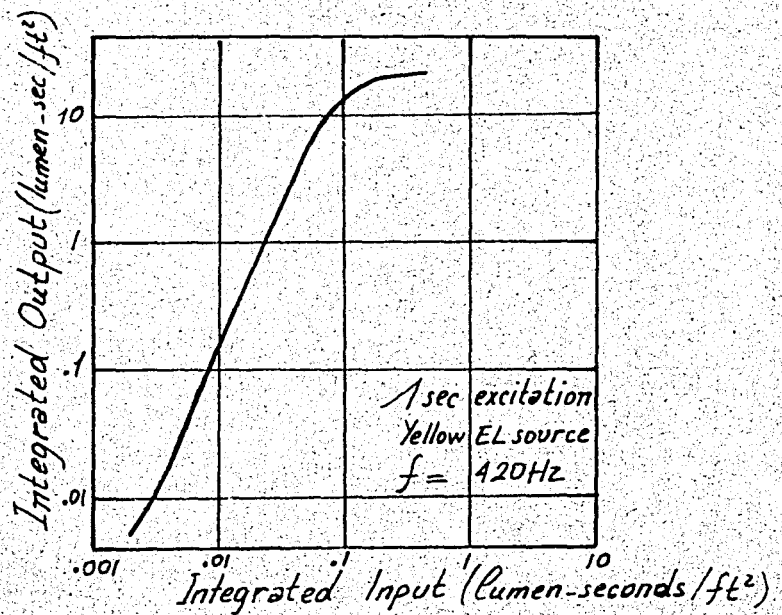

Fig. I.40 - Input-output characteristic for time integrated light.

is about 100 times with yellow electroluminescent input. This could be increased to 200 with spectral match.

I. ERASURE

In some applications a new image can be desired to form immediately after the previous one. This can be accomplished by a special erasing mechanism. After an image is built-up, the entire amplifier is flooded with radiation for one second or less and then polarity of d.c. supplies is reversed. In this way, conductivity of the photoconductor is suddenly reduced and the output of the panel is cut-off. Reverse conductivity depends upon the current flow in the initial direction so, flooding of the panel is preferable.

In Fig. I.41, an amplifier for X-ray applications with erasing means is illustrated.

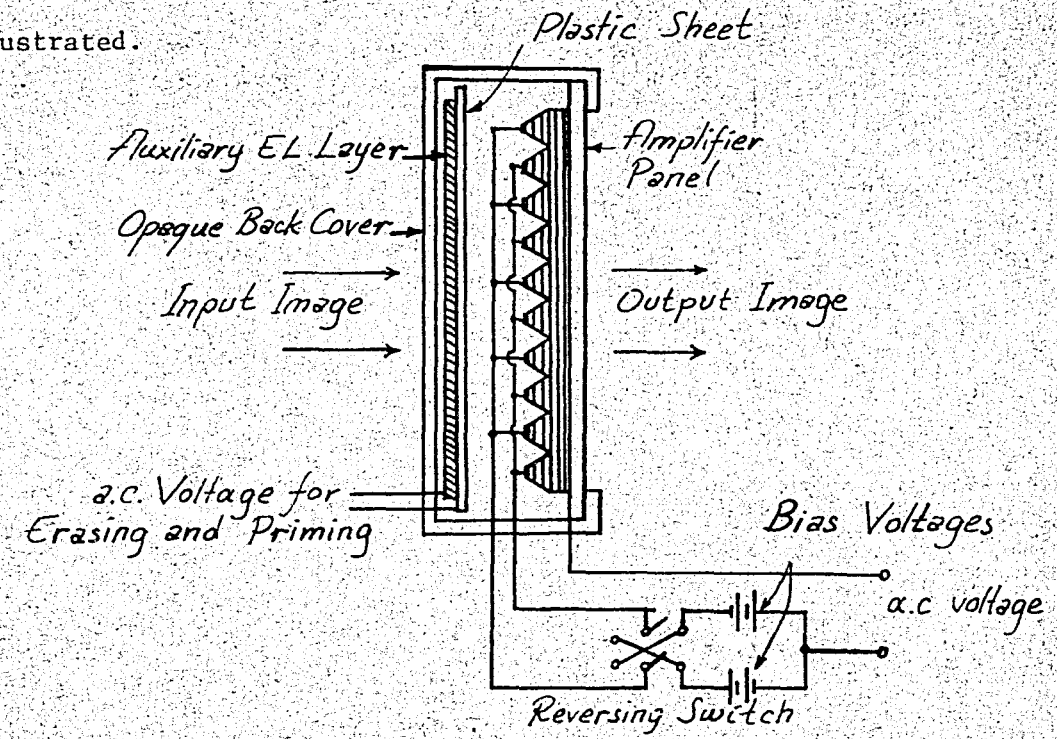

Fig. I.41 - An amplifier with erasing means.

To accomplish erasing, an auxiliary electroluminescent layer and a reversing switch is added to the amplifier. Auxiliary phosphor layer, which is used to flood the photoconductor, is about 1-mil thick. It is supported by a five-mil Mylar sheet. An aluminum layer of 40 percent light transmission covers the surface of the Mylar sheet which is in contact with the auxiliary phosphor layer and it constitutes one electrode of the phosphor.

The auxiliary phosphor layer is also used in priming. Before exciting the amplifier with X-rays, the threshold level of the photocurrent, required to produce a light output, is attained by means of the auxiliary phosphor layer. In this way, X-ray exposure on the amplifier is reduced to a minimum in building up an image.

J. APPLICATIONS

CdS-ZnS light amplifiers, we discussed so far, can operate with X-ray and infrared inputs as well as visible light. They are operative, however, in near infrared region. New photoconductive materials are required for operation further in the infrared region. These amplifiers have sluggish response to moving pictures, so they cannot be applied to television and medical diagnosis of moving objects. However, they can be applied to stationary X-ray images in medicine. High energy X-rays ($\sim$ in the MeV range) are needed in the X-ray therapy of cancer. Scattered radiation is high and may be dangerous to the person who makes beam control and alignment where the patient is located. For this reason, photographing or closed-circuit television system will be required for inspection. Using a light amplifier,

however, a short exposure can be made and the persistent figure can be inspected after the X-rays are cut off. In these applications, people can work in lit rooms. Contrast of the X-ray image can be increased and details can be percepted in a better manner. In viewing parts of the body, the patient can be exposed to lower X-ray dosages, because the image can be intensified to obtain an output of proper brightness. Similarly, the light amplifier can be used in the visualization of isotope distribution and electron microscope pictures. Panel light amplifiers give better X-ray images (100 times brighter) compared to normal fluoroscopic screens. In Fig. I.42, we can observe the difference between a light amplifier and a Patterson CB-2 screen. The amplifier can be also operated with a fluoroscope screen close to the input side of it, so that the visible image formed on the screen will be amplified by the amplifier.

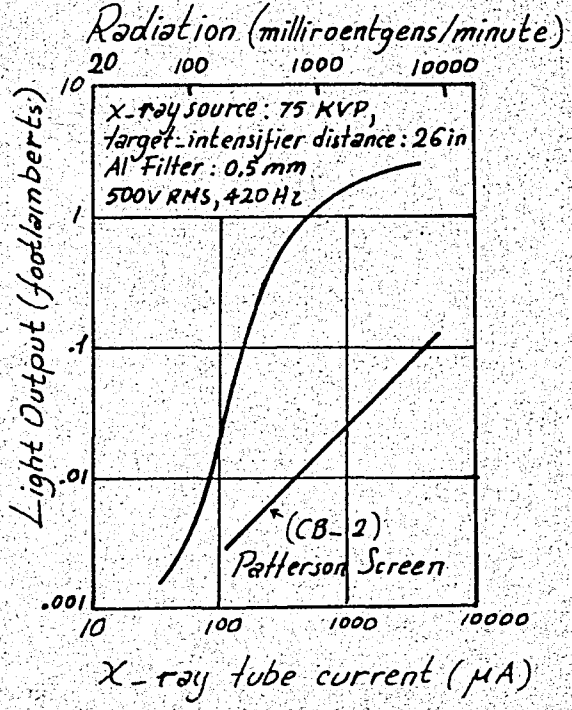

Fig. I.42 - Static characteristic for X-ray input.

The long persistence and the high light gains of the amplifier are useful in slow tv and radar applications. In the case of slow tv a single frame is desired to be scanned in a period of a minute, using low frequency video information. For viewing, the picture should be stored for a frame period or longer. In this case, a long-persistent phosphor cathode-ray tube can be used conveniently and its output can be amplified by a light amplifier of high gain and long decay, so that lit surroundings will not avoid viewing. The same convenience can be obtained in using the conventional P-7 radar screen when observing the decaying target traces. Successive input pulses at short intervals cause an increase in the output of the amplifier as it does in that of the P-7 screen.

Another application of the amplifier is to air traffic control. The position of the moving target is represented by a light point on the panel. Due to the long persistence, the path of the flying object is seen as a line of slowly decaying intensity on the panel. In this way, the position, the direction and the speed of the object can be seen.

Color pictures can be displayed by a three color strip system used, instead of a single electroluminescent. If the strip system is made by two different semiconductors, which respond to different wavelengths, two pictures of different radiation characteristics can be displayed by the same device. In the X-ray field, the object can be observed simultaneously with soft and hard radiation. When a system of red and green strips is used X-ray images can be viewed as stereo-pictures. The green strips are viewed through a green filter and one-half picture is observed. The other half-picture is observed by means of a red filter.

The performance of single element radiation converters can be improved by using ferroelectric materials. They control the brightness of the electroluminescent layer. An amplification of 50,000 is reported for these amplifiers. They are used for amplification ("lumistors", "optrons"), for storage and display and for logic networks.

Since the light amplifiers are sensitive to near -IR radiation they can be used to sense and amplify near-IR radiation from light emitting diodes.

II. FAST-RESPONSE SOLID-STATE LIGHT AMPLIFIERS

A. INTRODUCTION

The slow speed of response of solid-state light amplifiers using CdS, made them unusable as moving-picture image converters. Fast-response intensifiers can be obtained by using CdSe photoconductive layers. CdSe has a fast time-response, and its sensitivity is almost comparable to that of CdS. It is sensitive to visible light, infra-red and X-rays. By means of fast-response converters using CdSe, moving X-ray images or motion-pictures can be converted to negative or positive images of shorter persistence.

B. PROPERTIES OF THE SINTERED CdSe CELLS

The behaviour of CdSe cells at high fields ($\sim$ 800 V/mm) is our main interest. To illustrate this behaviour the standard gap of 0.5 mm. by 5 mm. is tested.

In Fig. II.1, a plot of photocurrent as a function of applied d.c. voltage for various incident illumination levels is given. To reduce heating at high voltages and currents, the time for readings were kept to a minimum.

In Fig. II.2, photocurrent is plotted as a function of light for various d.c. fields. It is seen that photocurrent is approximately proportional to voltage and rises less than linearly with input illumination. As we have seen before, photocurrent in powder photoconductors varies as the third or fourth power of the voltage and its variation with light is superlinear.

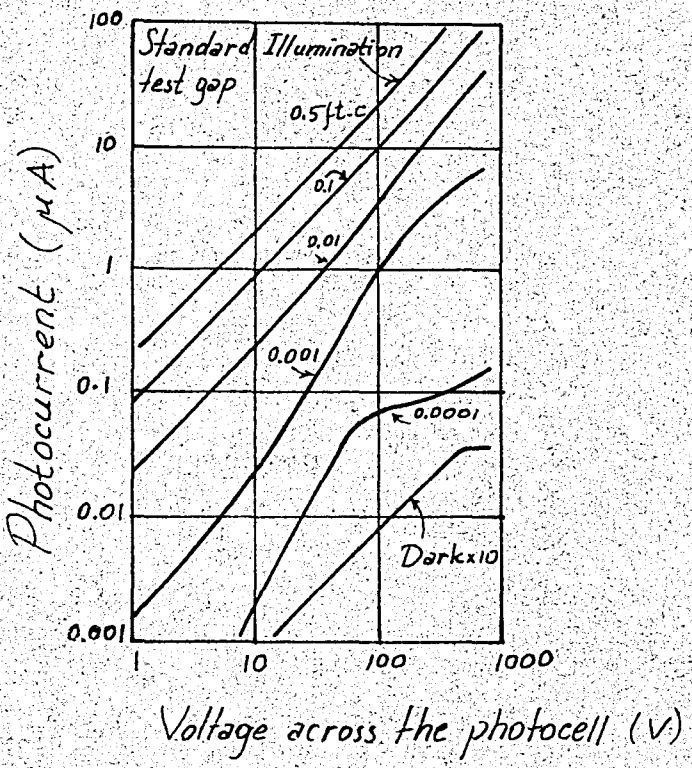

Fig. II.1 - Photocurrent versus voltage for sintered CdSe Cell.

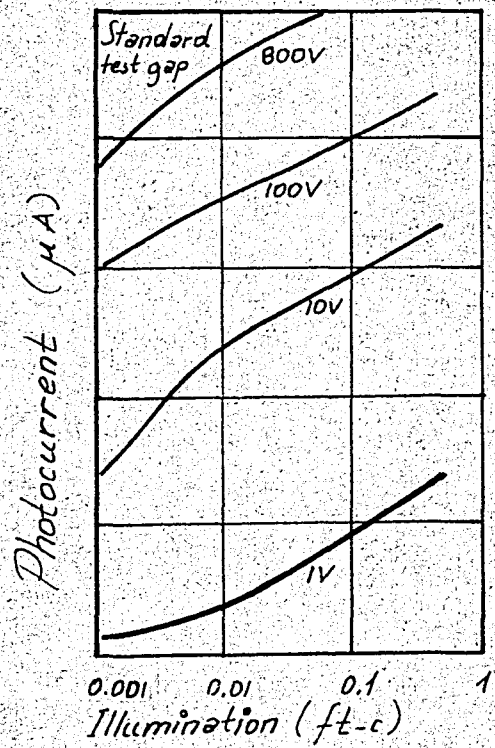

Fig. II.2 - Photocurrent vs illumination for CdSe Cell.

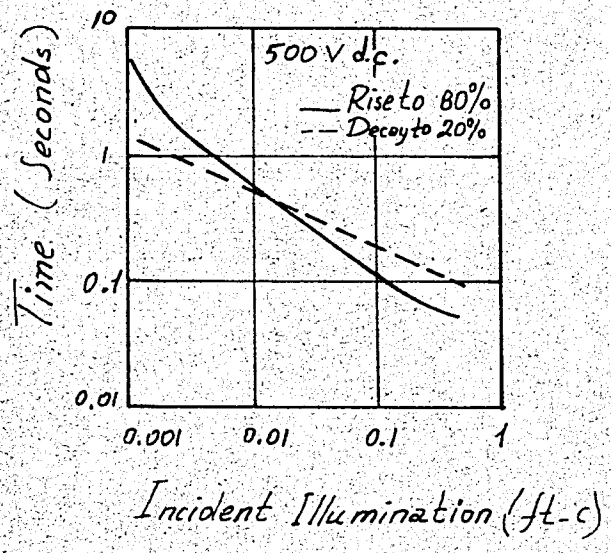

Fig. II.3 - Rise time and decay time for sintered CdSe Cell, d.c. applied voltage.

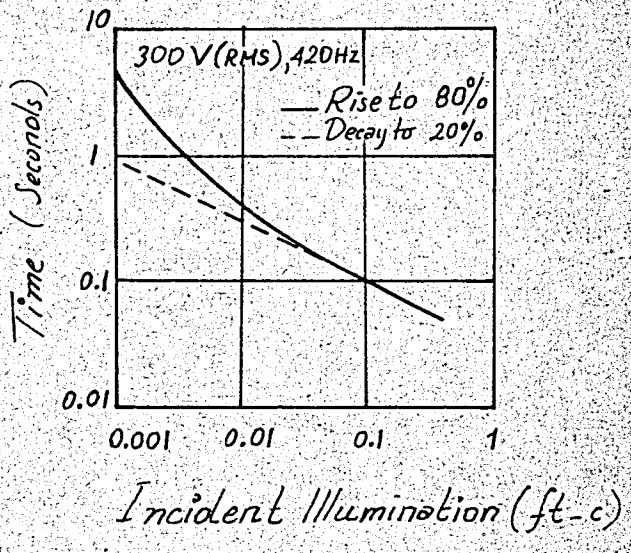

Fig. II.4 - Rise and decay times for sintered CdSe cell, a.c. applied voltage.

As we see in Figures II.3 and II.4, decay and rise characteristics of the cell for d.c. and a.c. operations are almost the same. These characteristics are different when the CdSe cell is used in series with an electroluminescent cell, because the voltage across the photoconductor changes with light input and the output versus voltage characteristics of the electroluminescent layer is non-linear. We see that, photoconductor alone has rise and decay times of 50 to 100 milliseconds for high light levels.

C. PROPERTIES OF A SINTERED CdSe CELL IN SERIES WITH AN ELECTROLUMINESCENT ELEMENT

If a CdSe cell is operated in series with an electroluminescent element, the maximum gain is reduced as the operating frequency is increased, due to the decrease of the impedance of the electroluminescent layer at higher frequencies. As the frequency is increased the rise time increases and the decay time decreases.

For high input illumination levels rise and decay times get shorter, but the gain may become very low after a certain value. This should be considered in operation. Very short time response can be obtained in the expense of the gain.

If a capacitance is added in parallel with the electroluminescent layer, the decay time decreases and the rise time increases. It decreases the sensitivity of the elemental amplifier. We see that this improves some characteristics of an amplifier while having undesirable effects on some other characteristics.

D. A FAST-RESPONSE EL-PC IMAGE CONVERTER USING CONTROL GRID

a. Introduction:

We have discussed the properties of CdSe photoconductors and have seen that due to their fast-response, they are used for the intensification of the images of moving objects.

An EL-PC image intensifier consisting of a sandwich of photoconductive

CdSe layer and an electroluminescent ZnS layer can amplify visible light, infra-red, or X-ray images. If a control grid is added to such an amplifier it can operate as either a positive or negative image intensifier, depending on the amplitude and phase of its two power supply voltages applied to the grid. The control grid is used also in adjusting the time-response characteristics of the amplifier.

It has useful applications in photography, medical diagnosis and radar systems.

b. Design of the Panel:

The cross-section of a fast-response panel is shown in Fig. II.5. It consists of three main layers, namely the photoconductive layer, the electroluminescent layer and the transparent dielectric layer.

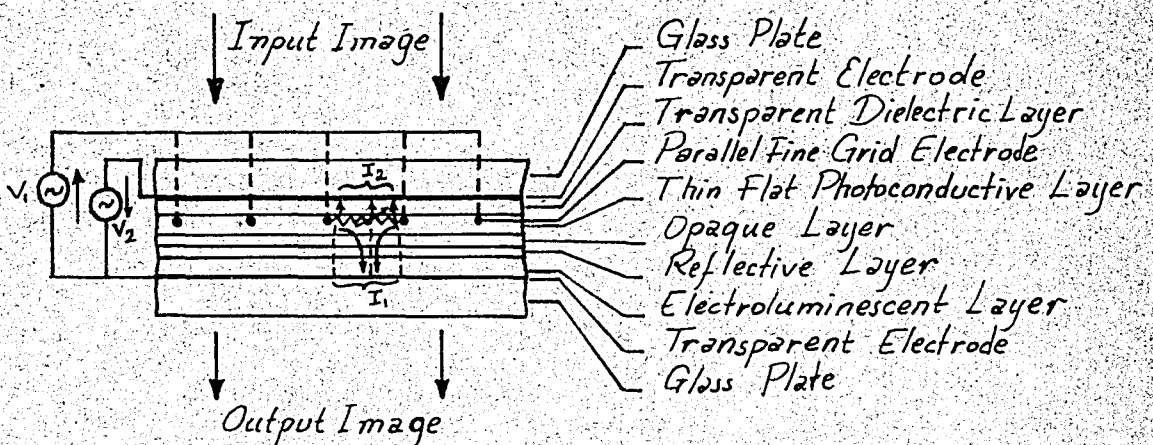

Fig. II.5 - Cross-section of a fast-response panel.

The photoconductive layer is made of CdSe powder bonded with epoxy resin. It is about 80 μ thick. A parallel, fine-grid electrode is incorporated within this layer. The electrode is formed from tungsten wire of 10 μ diameter and

0.6 mm. pitch.

The electroluminescent layer is about 50 μ thick. It is produced by bonding ZnS electroluminescent powder with epoxy resin on a transparent SnO_2 electrode on a glass plate.

The transparent dielectric layer is formed on a transparent SnO_2 electrode which is formed on a glass plate. The dielectric layer is a polyester film of 30 μ thickness.

An opaque layer of 5 to 10 μ thick is added to the amplifier to avoid optical feedback. A $BaTiO_3$ insulating layer of 50 μ thick serves to reflect light which is fed back by the EL layer.

c. Operation of the Panel:

The operation of the converter is basically dependent upon the lateral photoconductivity of the PC layer and upon the action of the parallel fine-grid electrode. Fig. II.6, represents the operation of the amplifier schematically.

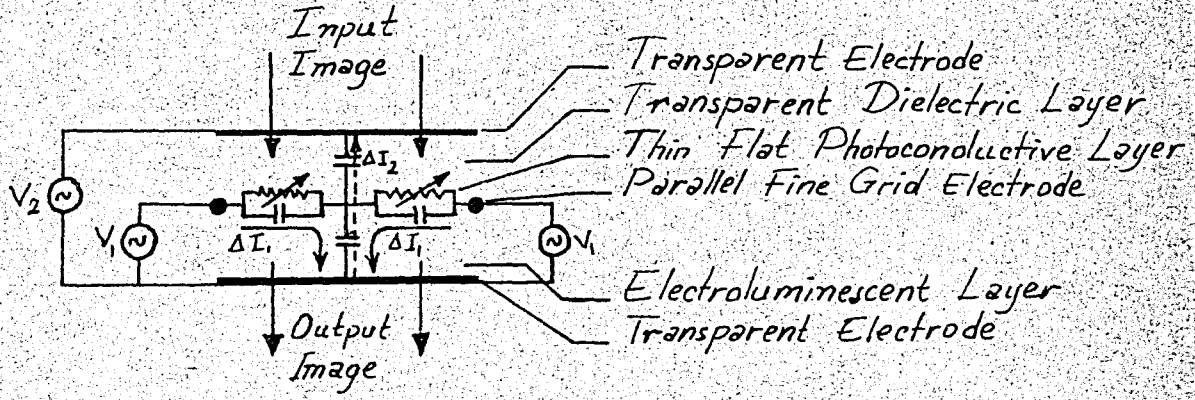

Fig. II.6 - Schematic representation of operation of the amplifier.

The input of the amplifier, which can be visible light, infra-red or X-rays, controls the conductivity and the current through the electroluminescent

layer which in turn controls the light output.

The two a.c. driving potentials V_1 and V_2 are of the same frequency but they differ in phase. The light output of the amplifier is nonlinear and proportional to the amplitude of the vector current $I_3 = I_1 \pm I_2$. I_1 is the lateral photocurrent and is an incremental function of V_1 and the input light intensity, and I_2 is the capacitive current and is an incremental function of V_2. If the amplitudes and the phase relationships of V_1 and V_2 are changed, the amplitude of I_3 is also changed. Therefore, the output light intensity becomes an incremental, decremental or V-shaped function of the input light intensity. In Fig. II.7 the output light intensity is plotted as a function of input light intensity. The curves are obtained for 1KHz operating frequency. Driving potential values can change from 0 to about 1500 volts.

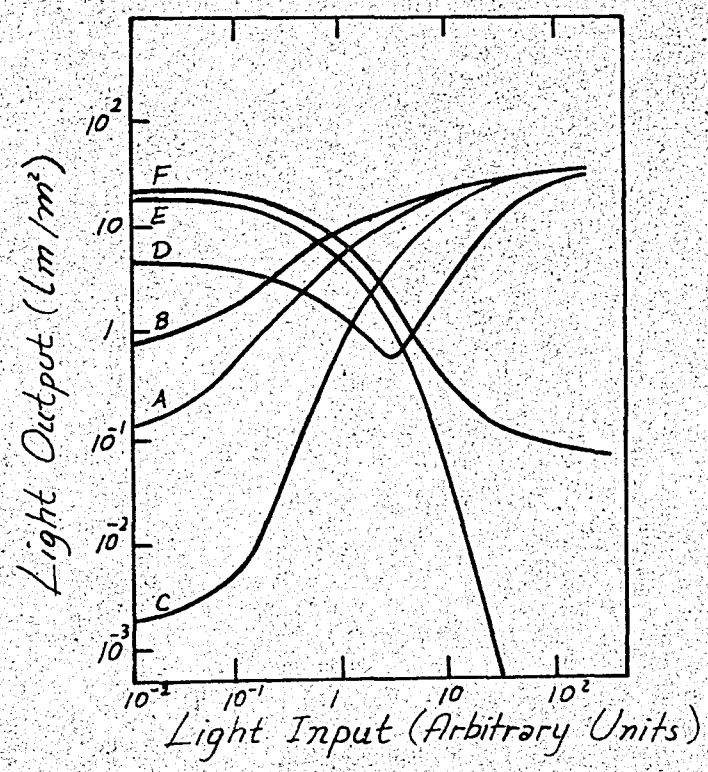

Fig. II.7 - Operating characteristics of the Image-converter Panel.

Positive Image Characteristics: Curves A, B and C are positive image characteristics for standard, low and high gamma respectively.

Curve A is for $V_2 = 0$. The photoconductive and electroluminescent layers are effectively in series across V_1. In this case $I_1 = I_3$, which increases with input light intensity, excites the electroluminescent layer.

Curve B is obtained for V_2 in phase with V_1. I_1 and I_2 are nearly in phase and the total current through the electroluminescent layer (I_3) increases. Part of I_3 is not under the control of the incident light intensity, therefore gamma and brightness range decrease.

Curve C is obtained for V_2 slightly more than and 180 degrees out of phase with V_1. In this case, lateral dark current I_1 is opposite in phase to I_2 and the dark value of I_3 is reduced considerably. When the input light is applied, I_1 changes from lateral capacitive dark current to lateral resistive photoconductive current and its amplitude increases. Due to this increase in I_1, I_3 is also increased. Therefore, a high gamma and large brightness range is obtained.

Mixed Image Characteristic: This is curve D in Fig. II.7. Curve D is for a much larger V_2, which is 180 degrees out of phase with V_1. For low input light intensities, I_2 is very high and opposite in phase compared to I_1. If the light input is increased, increasing I_1 tends to compensate the excess I_2. In this case I_3 decreases in amplitude. We obtain a negative reproduction of the input image. As the input light is increased a point is reached where I_1 exceeds I_2. Increasing the input intensity further will cause I_1 to exceed I_2 even more. Therefore, in this region an intensified positive reproduction

of the input image will be produced, I_3 being large. Curve D is a V-shaped input output characteristic. A negative, mixed or positive reproduction of the image will be produced in accordance with the input light intensity level.

Negative Image Characteristics: Curves E and F are the negative image characteristics which have negative gamma values.

Curve E is obtained for $V_1 = 0$ and V_2 very high so that the EL layer is effectively in parallel with the PC layer, and in series with the transparent dielectric layer. The current through the EL layer is constituted by I_2. As the input intensity is increased lateral photoconductivity of the PC layer increases and acts as an electrostatic shield. I_2 is bypassed to the parallel grid electrode. Since I_3 ($= I_2$) decreases with increasing input light intensity, light output also decreases with the increasing input intensity.

Curve F is obtained for V_2 very much larger than, and in phase with V_1. For low input light levels, vertical capacitive current constitutes the main portion of I_3. As the light intensity increases, I_1 increases and adds to I_2 decreasing the rate of decrease of I_3. In this case we have a lower gamma value and brightness range compared to the previous case.

These performance characteristics can be also obtained by dc. control of lateral photoconductivity and continuous phase control.

The size of the experimental panel was 20 cm x 20 cm. and the measured image resolution was greater than 800 lines using static input images. Greater resolution can be obtained for moving pictures.

d. Time-response Characteristics of the Amplifier:

Time response characteristics of the converter are shown in Figures II.8 (a) and (b). For the positive mode of operation τ_R and τ_D are of the order

of 10^{-2} sec for relatively high input light levels. In case of the negative mode of operation τ_R decreases quickly with input light levels, while τ_D decreases gradually and at high input values they are a few milliseconds.

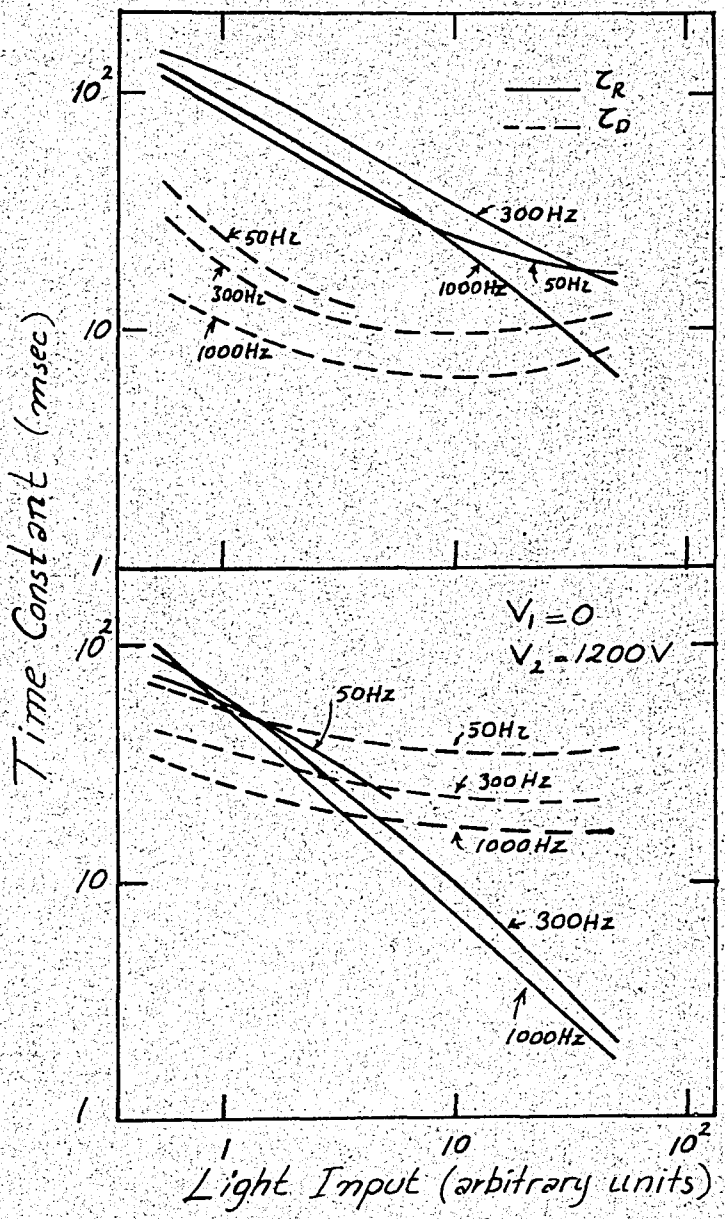

Fig. II.8 - Time constant vs Light input.

a) Positive Mode V_1 and V_2 are 180^o out of phase

b) Negative Mode

Fig. II.9 gives time constants for two light levels under several operating conditions. In all cases, a frequency of 1 kHz is used V_1 and V_2 being 180 degrees out of phase. Regions I, II, III and IV are for positive characteristics, positive characteristics of high gamma and contrast ratio, V-shaped characteristic and negative characteristics. The panel used in this experiment was 10 cm. x 10 cm. in size.

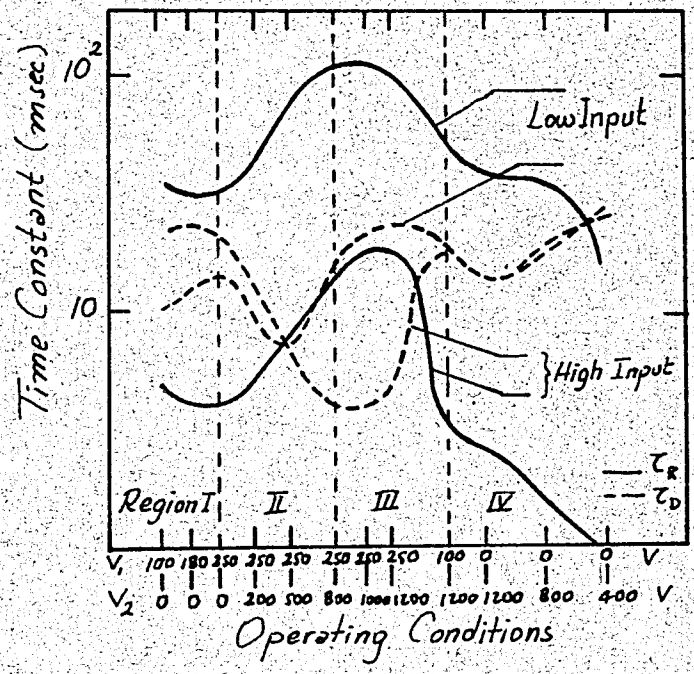

Fig. II.9 - τ_R and τ_D under various operating conditions of the image converter panel.

As seen in Fig. II.9, τ_R and τ_D are of the order of 10^{-3} to 10^{-2} seconds for both positive and negative modes of operations. This is a good enough range to convert a moving input image to a positive or negative image without persistance of the output. τ_R and τ_D can be varied at will by adjusting the applied potential.

e. Applications:

Motion Picture Film Editing Device: Fast-response characteristics of CdSe photoconductor makes the use of this converter as a motion-picture film editing device possible. The film editing device using this panel can convert a negative motion-picture film to a positive image. In Fig. II.10, the control of the gamma of the converted image is shown. The control is achieved by holding V_2 constant and changing V_1 in steps. The response time can be controlled as in the IV.th region of Fig. II.9.

This method of film editing is less expensive and simpler compared to the conventional methods.

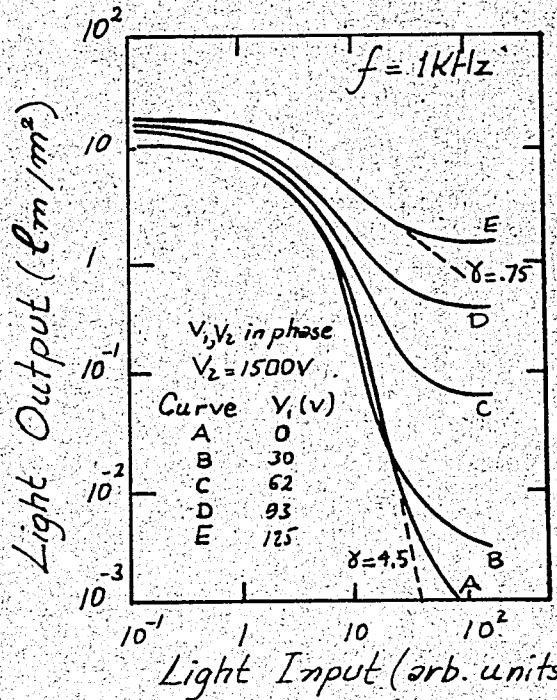

Fig. II.10 - Input light level vs output light intensity for negative mode showing various values of gamma.

Image Converting Fluoroscopic Screen: We have seen before that image intensifiers using CdS photoconductive layer can be used in X-ray applications. However, for moving objects CdSe photoconductive layer is used.

In Fig. II.11, the time constants of the converter output are shown as as a function of X-ray input levels for positive and negative modes of operations. The rise and decay times are of the order of 10^{-2} sec to 10^{-1} sec. These values are good enough for moving X-ray images. In this case also can be controlled as for the visible input.

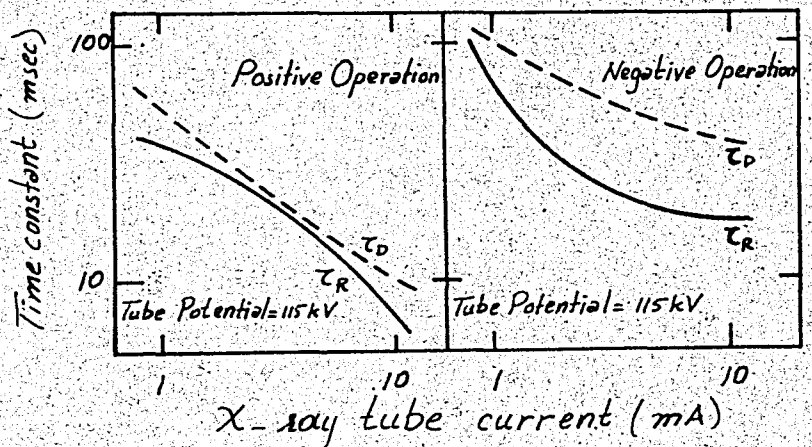

Fig. II.11 - Time Constants vs X-ray input intensity.

This type of converter gives a brighter output compared to the conventional fluoroscopic screen. The polarity of the image and the gamma values are controllable. This can be used in medical and industrial applications conveniently, because low input levels can give bright enough output images.

III. PHOSPHOR - PHOTOEMITTER INTENSIFIERS

A. INTRODUCTION

An image intensifier based on the photoemission principle mainly consists of a photocathode and a phosphor screen. If a low intensity image is focused on the photoemissive surface, electrons are emitted out of it. They are accelerated by the applied field and focused on the phosphor screen which produces the output image. To obtain considerable gain in light intensity the accelerating field should be chosen properly.

If the distance between the photoemitter and the phosphor screen is short, electron-optical focusing means can be omitted and cascaded stages can be built which give fairly good quality output images.

The noise level of such a device is the limiting factor for the smallest light signal which can be intensified.

These devices are used to intensify visible images as well as to transform invisible part of the spectrum (infrared, ultraviolet, X-rays) into visible radiation.

B. CASCADE IMAGE INTENSIFIERS

To obtain high gain intensifiers, single stages can be cascaded. To illustrate the behaviour of such intensifiers we shall take a four-stage cascade intensifier, and study its characteristics.

a. Construction of the Tube:

In Fig. III.1, the diagram of a four-stage intensifier and the cross-

section of a target is shown.

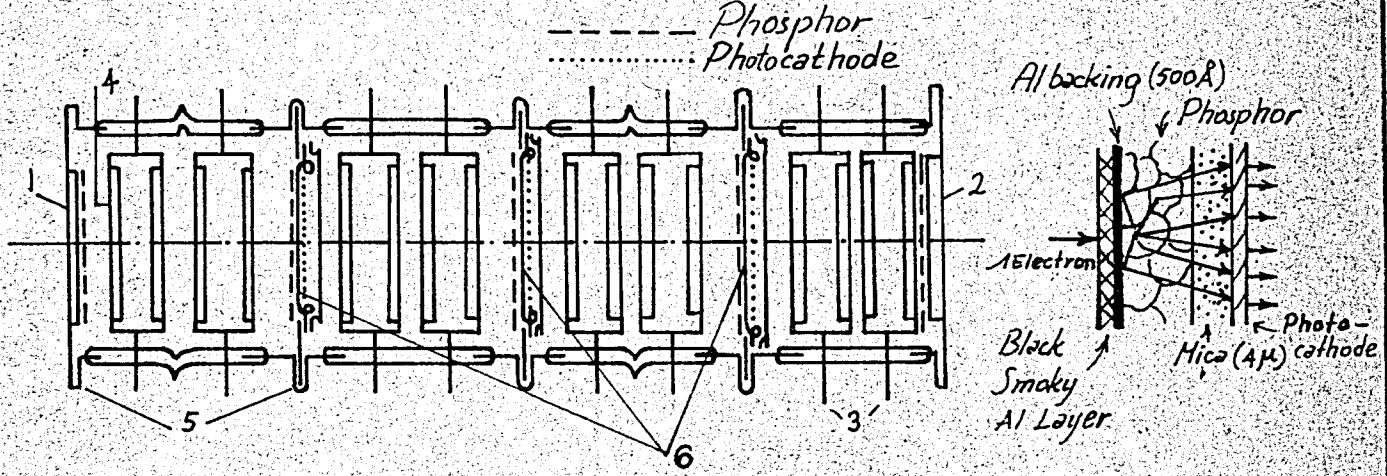

Fig. III.1-a - A four stage Intensifier. b - The Cross-section of the Target.

The envelope of the tube has four similar sections. Each section is an assembly of two rings (3) with two flanges (5) which are held together by 3 in. diameter glass cylinders. Each body section has two focusing rings (4). The phosphor-photocathode targets (6) are mounted to the flanges. The overall length of the tube is 12 in. while it has a diameter of 3.75 in.

The targets and the glass face plates (1, 2) are mounted to their positions by argon arc welding around the periphery.

For convenience in processing, the first and the third targets are not fixed while the one at the center is fixed. Before photoactivation the rotating targets are turned 180° around so that their photosurfaces face into the tube. In this way, paired activation is possible. After seal-off they are turned to their operating positions.

The most common phosphor material used is ZnS (Ag). Each phosphor screen (of the order of 10μ thick) has an aluminium backing (500 Å thick) to avoid the light feedback. Organic films are used for supporting purposes. Multialkali

photocathodes are used in the tube because they have high quantum efficiency and wide spectral response. In Figures III.2 and 3 spectral sensitivities of a Sb-Na-K-Cs (S.20) photocathode, a Sb-K-Na (S.11) photocathode, a Ag-O-Cs (S.1) photocathode and the spectral output of a ZnS (Ag)(p.11) phosphor are shown.

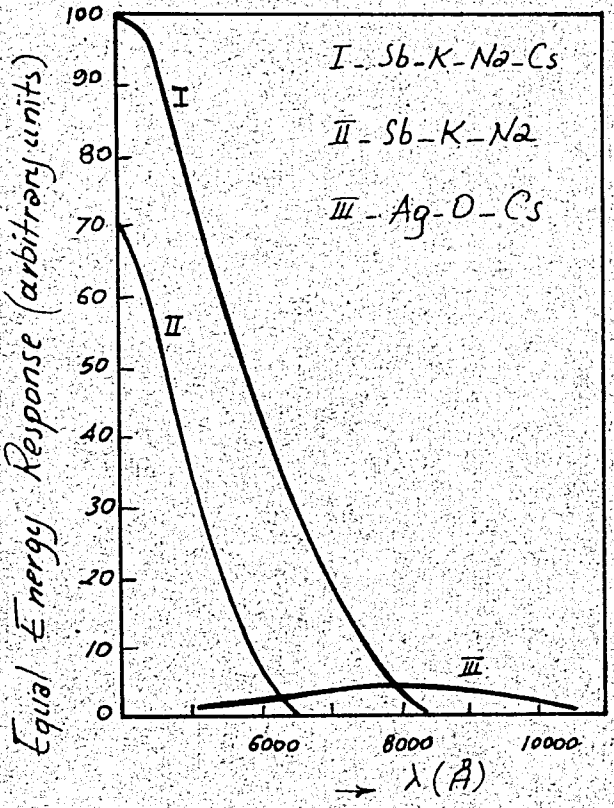

Fig. III.2 - Spectral Response of Several Photocathodes.

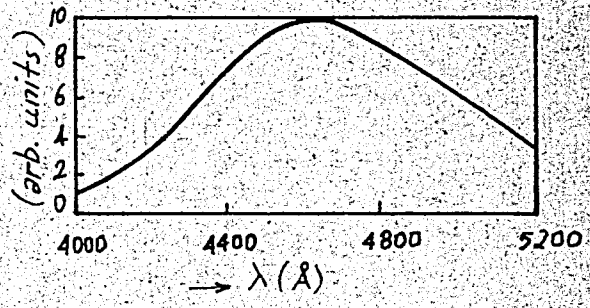

Fig. III.3 - Spectral Output of P.11 Phosphor.

To obtain high gain, spectral match between the photocathode and the phosphor is necessary.

If an overall light gain of 10^6 is desired, each stage should have a light gain of 30. If we consider this in terms of electron gain, each

sandwich should have an electron gain of 30 and the contributions of the input cathode and the output phosphor are added to this.

In Fig. III.4, electron gain of a P.11 phosphor-photocathode sandwich layers is plotted as a function of the applied potential, for a 150 μA/lm cathode sensitivity. This cathode has a quantum efficiency of about 20% for a P.11 phosphor combined with it.

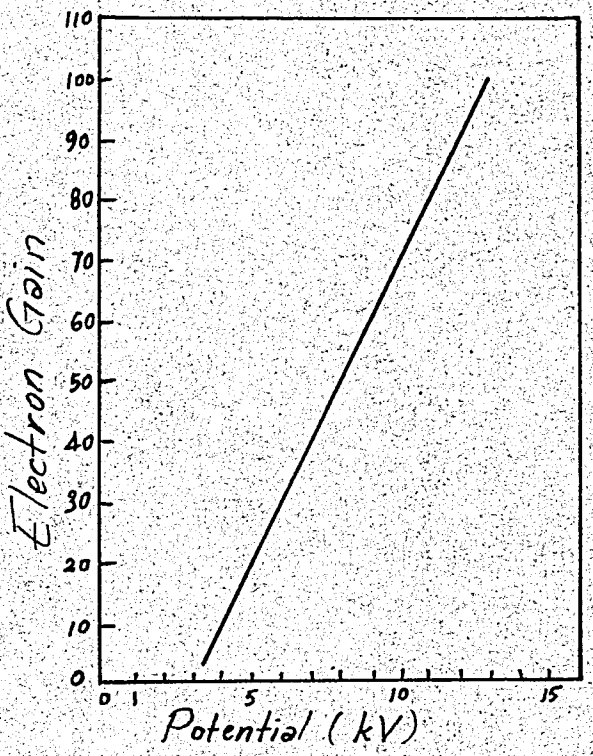

Fig. III.4 - Electron gain as a function of potential for a ZnS(Ag) phosphor - photocathode sandwich.

In Fig. III.5, the electron gain of a P.11 phosphor is plotted as a function of the current density for two different beam energies and with a 150 μA/lm cathode. At lower intensities electron gain is reduced. This is due the migration of holes from luminescent to killer centers.

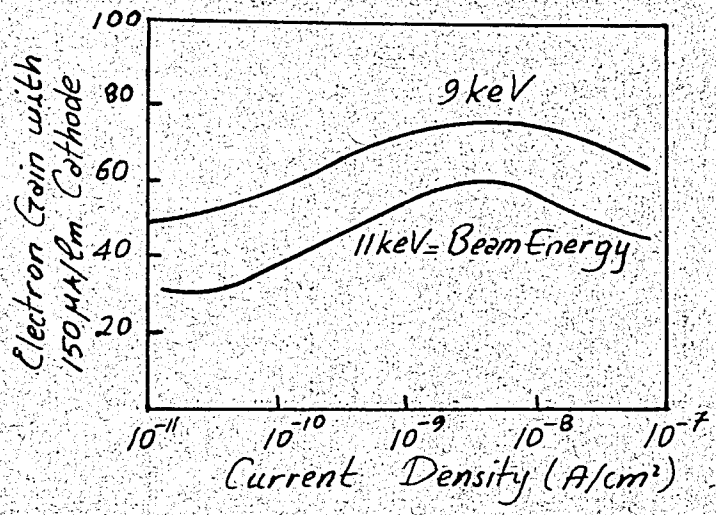

Fig. III.5 - Electron gain of phosphor as a function of the incident current density.

Average cathode sensitivities of at least 100μA/lm and stage potentials of 7 kV or more are required to obtain a light gain of 10^6.

b. Operating Characteristics of Cascade Intensifiers:

i) Focusing:

Focusing is achieved both magnetically and electrically. Axial magnetic field of 300 - 450 G is provided by a solenoid. The input cathode is earthed and potentials are applied to each stage and to the intermediate focus electrodes. In Fig. III.6, focusing arrangement for a two-stage tube is shown.

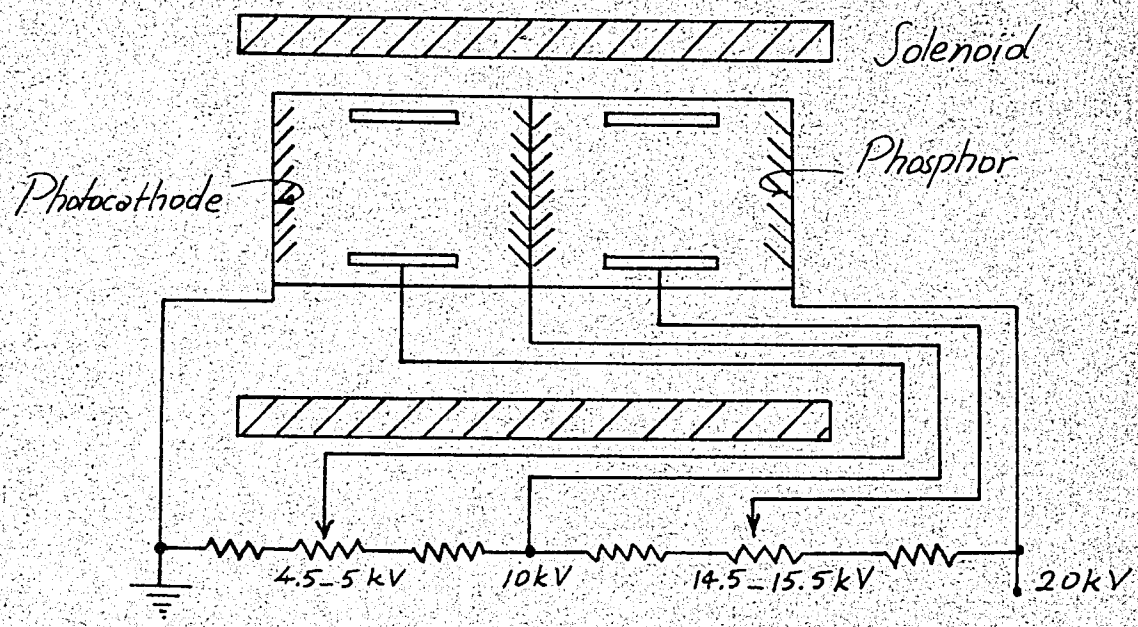

Fig. III.6 - Arrangement for focusing.

ii) Gain:

The gain of a single stage intensifier can be expressed in terms of the applied voltage, the photosurface sensitivity and the efficiency of the phosphor screen. Suppose B_i is the incident radiation (in lumens) upon the photocathode, a is the photosurface sensitivity (in A/lm), b is the efficiency of the phosphor screen (in lm/W) and V is the accelerating voltage (in V). The quantity "B_i a" gives the photocurrent and "B_i a V" the power arriving at the phosphor screen. The light output is given by,

$$B_o = b\ B_i\ a\ V \qquad \text{III-1}$$

The gain of the intensifier is the ratio of the output radiation to the input radiation. So the gain is given by,

$$G = \frac{B_o}{B_i} = abV \qquad \text{III-2}$$

For a = 50 μA/lm, b = 30 lm/W and V = 20 kV; G = 30 is obtained. This agrees with our previous discussion.

In Fig. III.7, gain characteristics of a single tube are given as a function of the overall tube potential, for various input light levels. Forms of the gain characteristics are affected by efficiency variations with incident current densities as shown in Fig. III.5. Tube gains should be measured within the range of 10^{-6} to 10^{-5} lm/ft^2. incident levels to obtain good results.

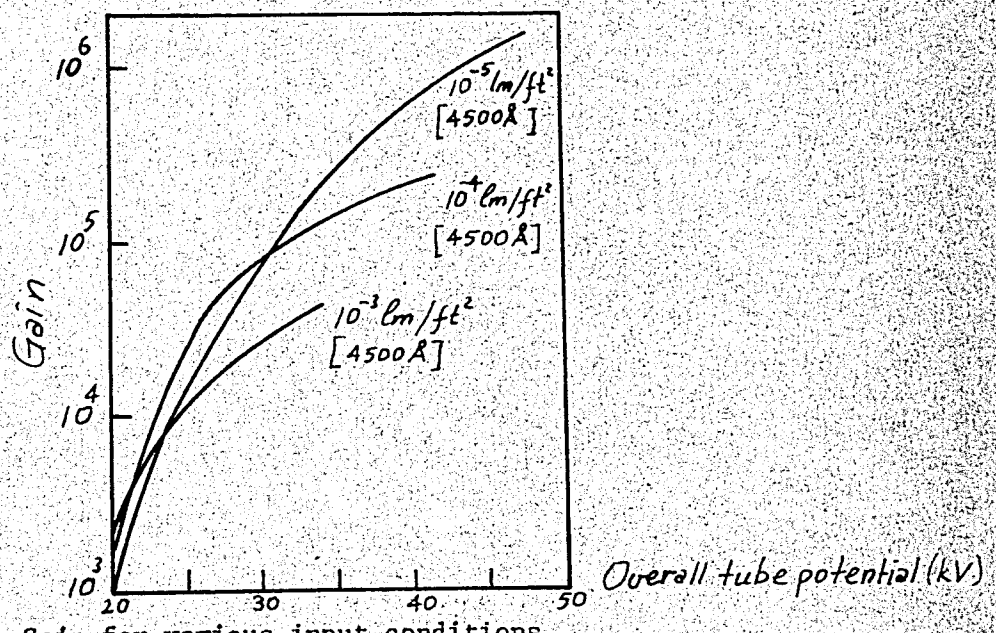

Fig. III.7 - Gain for various input conditions.

iii) Resolution:

Resolution of intensifiers are affected by the applied potentials and magnetic fields. If any one of them is reduced resolution decreases.

Resolution deteriorates as the distance from the tube center increases. This occurs because of the non-uniformities in the electrostatic field especially in the focus rings near the photocathode. Signal induced noise

also affects the resolution. It reduces image contrast causing resolution losses.

iv) Output Scintillations:

In Fig. III.8, pulse-height distribution curves for weak emission and dark emission are given. Each curve has two regions, first one belonging to the emission from the first cathode and the second region showing the effect of electron bunches released from the photocathode as a result of positive ion bombardment.

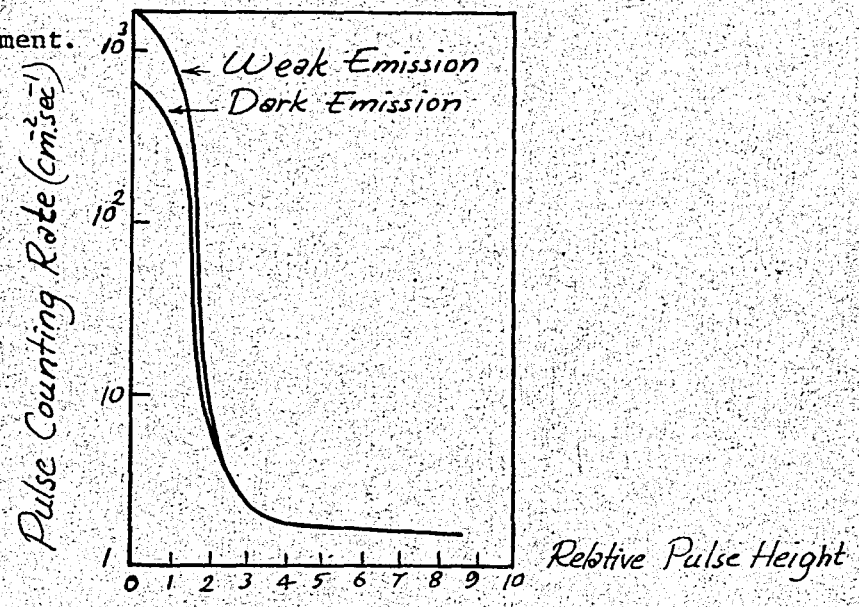

Fig. III.8 - Characteristic pulse-height distribution curves.

The output image decays completely in several seconds after the removal of the continuous input image (more than 1 second duration). For output brightnesses of 1 and 10 ft. lamberts the decay time to 10% of the initial brightness is 50 msec and 200 msec respectively. Decay time depends on the excitation time. Ion scintillation have a rise time of 100 sec.

Cascade image intensifiers have long life. Operational time is 200 h for the best tubes. During this time gain, first cathode sensitivity, and

dark current are stable.

Temperature influences the operation of a cascade image intensifier. Single electron emission reduces as the cathode is cooled to the temperatures below 20°C. On the other hand, multiple electron emission is almost independent of temperature. It is interesting to note that cooling increases the light gain which is due to the characteristics of the P.11 phosphors. Spectral distribution curve of P.11 phosphor shifts upward upon cooling.

c. Discussion:

Cascade image intensifiers have robust structure, long operational life and good gain and resolution characteristics suitable for many applications. By cooling dark emission can be reduced and gain can be increased.

Best results are obtained by using trialkali S.20 photocathodes and P.11 phosphor screens.

d. Applications:

Phosphor-photoemitter image intensifiers are used in various fields. Some applications are mentioned below.

Medical Fluoroscopy: In taking X-ray pictures for diagnosis, low X-ray doses are desirable. An X-ray image can be amplified by means of an image intensifier. In this case low dose rates are used in taking the pictures.

Nuclear Research: It is possible to measure the velocity of a high-energy nuclear particle travelling through a transparent medium by means of

the Cerenkov radiation emitted from it. For this purpose, Cerenkov rings produced from a gaseous radiator should be observed. In these observations phosphor-photoemitter light amplifiers are used in intensifying the radiation.

Field-ion Microscopy: The field-ion microscope is used in metallurgy, because it shows the atomic arrangement of a sharply pointed material by an ion image. The image obtained by the field-ion microscope can be intensified by means of an amplifier.

X-ray Microscopy: A phosphor-photoemitter light amplifier can be used to intensify the picture obtained by an X-ray microscope.

Astronomical Research: They can be used in astronomical research to obtain better photographs. They are used in photographing the faint stars, nebulae and galaxies.

C

C. INTENSIFIER ORTHICON

An intensifier orthicon is constructed by modifying the image section of a conventional orthicon. This modification is accomplished by the addition of phosphor-photoemitter screens between the photocathode and the glass target of the tube. Here we shall explain the operation of a two-stage intensifier orthicon which employs two phosphor-photoemitter screens, can also be operated in the following manner.

The image to be amplified is focused on the photocathode. Electrons emitted out of the cathode are focused by the electrostatic lens onto the first intensifier screen. If a voltage of 10 kV is applied between the photocathode and the first intensifier screen, 10 - 20 secondary electrons are emitted per incident primary electron. Secondary electrons are focused onto the second intensifier screen. Secondary electrons emitted out of the

second intensifier screen are focused on the thin glass target which is scanned by an electron beam. Modulated return beam signal is fed to an electron multiplier and a video signal is obtained out of the intensifier. This signal can be amplified further by a video amplifier and then fed into the control electrode of a cathode ray tube. If the scanning beam of the intensifier is synchronized with that of the cathode ray tube a bright output image is obtained.

The intensifier orthicon has not as good resolution as the normal orthicon tube having the same target capacity. At high light levels their signal-to-noise ratios are nearly the same.

In the system described above an Orthicon or Vidicon can be used instead of the special tube described. In this case, the gain in light intensity can be controlled electrically and no optical feedback is present. This is the advantage of this method over the others.

IV. TRANSMITTED SECONDARY ELECTRON MULTIPLICATION (TSEM) LIGHT AMPLIFIERS

A. DESCRIPTION

TSEM Image intensifiers are based upon photoemission and secondary emission principles. A transmitted secondary electron multiplication tube employs basically photocathode, thin film dynodes, a fluorescent screen and focusing means. The incident image of low intensity is focused on the photoemissive surface. Electrons emitted from the photosurface are accelerated and focused on the first dynode. Secondary electrons from the first dynode are further accelerated and focused on the second dynode where further multiplication takes place. This process is repeated down to the tube and electrons from the last dynode are accelerated and focused on the fluorescent screen where they are converted into a visible image. Focusing is achieved by superimposed uniform electric and magnetic fields. The magnetic field is provided by a long solenoid surrounding the tube. The electric field is obtained by applying voltage between the photosurface and the fluorescent screen. The potentials of the dynodes and of the intermediate accelerating electrodes are obtained from an externally applied voltage divider. The first step of focusing is accomplished by the adjustment of the relative potentials of the dynodes. The intermediate electrode is maintained at a potential of half the inter-dynode voltage. An optimum condition is reached by trial and error as the magnetic field strength is varied and the voltage divider is not touched after that. For further focusing, the current flowing through the solenoid is controlled at any voltage.

In Fig. IV.1, a five-dynode TSEM image intensifier is shown schematically.

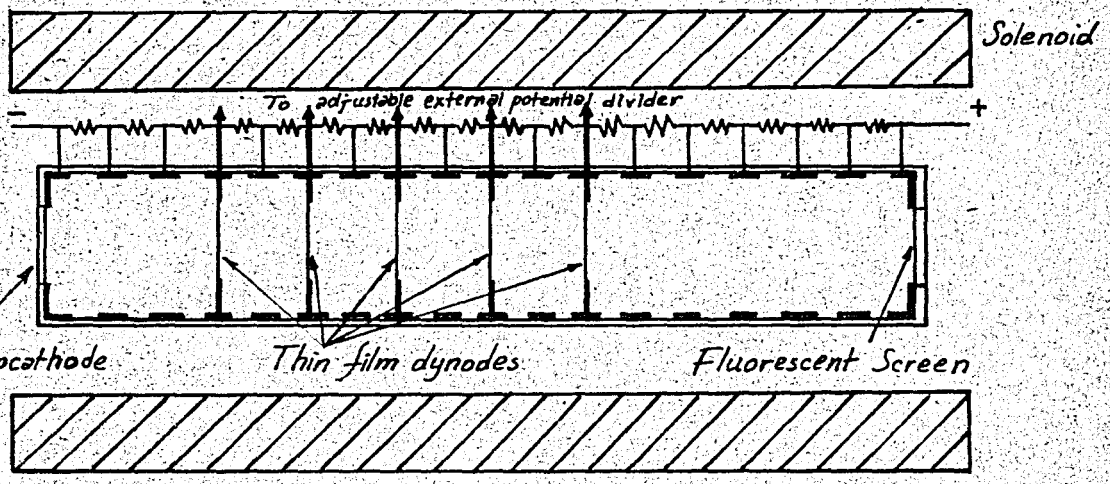

Fig. IV.1 - Diagram of five-dynode image intensifier.

Photocathodes are usually made of multi-alkalies. Most commonly used screens are made of silver-activated ZnS material. Each dynode consists of a layer of potassium chloride (25μ) backed by a layer of Al (500 Å). The aliminium layer is deposited on an edge supported aliminium oxide film of 1000 Å thick. The diameter of a dynode is about 19 mm. However, smaller and greater diameters have been reported. The dynode spacing is about 1 inch. The length of the tube is arbitrary but reported one is $10\frac{1}{4}$ inches.

B. PERFORMANCE OF THE TSEM LIGHT AMPLIFIERS

a. Current and Light Gains:

The current gain of a dynode, $\bar{m}$, is defined as the mean number of transmitted electrons per incident electron. Variation of $\bar{m}$ as a function of incident electron energy is shown in Fig. IV.2.

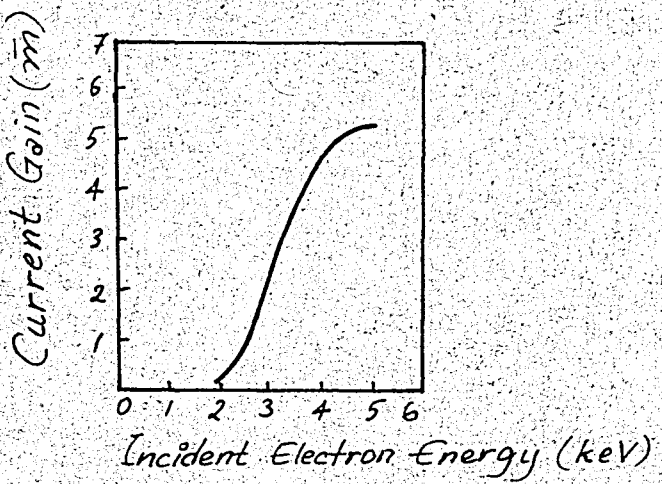

Fig. IV.2 - $\bar{m}$ as a function of incident electron energy.

In Fig. IV.3, the overall current gain, $\bar{M}$, of a tube with several dynodes at equal potential differences is given as a function of voltage applied between the photocathode and the phosphor.

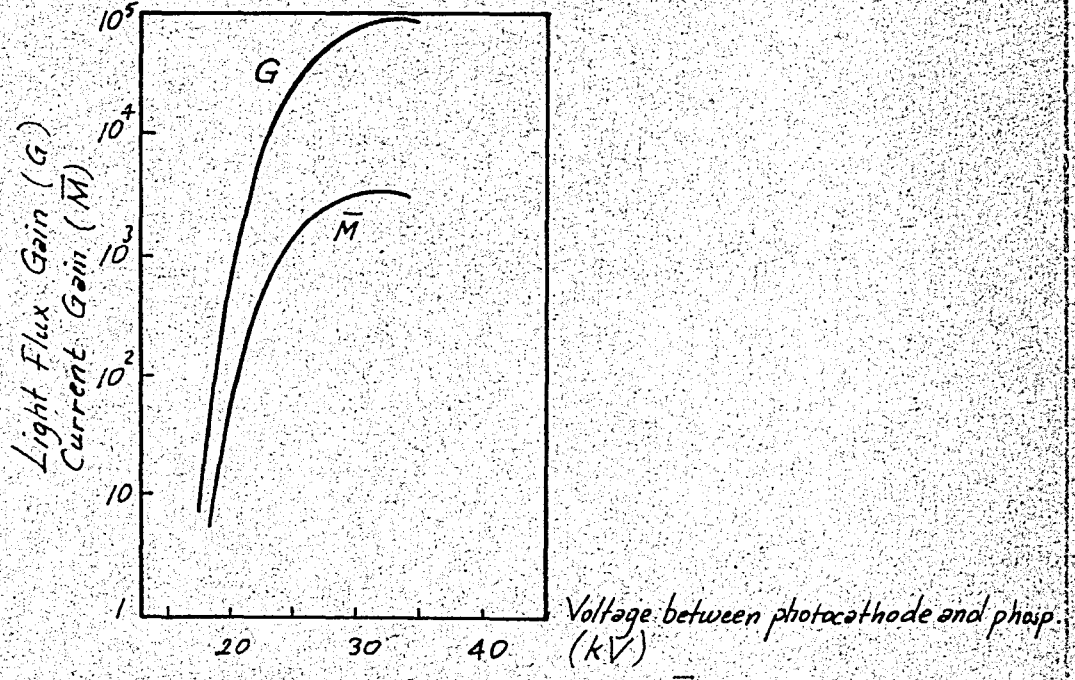

Fig. IV.3 - Variation with overall voltage of G and $\bar{M}$ for a 5-dynode tube.

The overall current gain rises steeply with the applied voltage.

The light flux gain of an intensifier is the ratio of the output flux to the input flux. It is given by,

$$G = g\bar{M} \qquad \text{IV-1}$$

where g is the light gain that would be obtained if the voltage between the last dynode and the phosphor screen were applied between the photocathode and the phosphor screen, the dynodes being removed. The value of g depends upon the photocathode sensitivity, the energy conversion efficiency of the phosphor screen, applied voltage and also the spectral quality of incident light. If the incident light and the emitted light have the same spectral quality the spectral response of the device does not effect G. In Fig. IV.3, G is plotted as a function of overall voltage under the above condition. If we compare the two curves, we see that the overall current gain $\bar{M}$ reaches its maximum value at a lower voltage compared to the light flux gain, G, of the tube, because g is a continuously increasing function of voltage.

Another interesting quantity is the number of photons produced at the anode for a single electron emitted out of the cathode. This is denoted by N, and is given as follows;

$$N = \frac{G}{\varepsilon_c} \quad \text{photon/electron} \qquad \text{IV-2}$$

where, G is the overall photon gain of the tube and ε_c is the efficiency of the photocathode.

To have an idea about the order of magnitude of N, we could take a TSEM tube (P.829), by English Electric Valve Co.) as an example. Its

trialkali S.20 type cathode has an efficiency of 0.18 (photoelectrons/photon), at the peak of the spectral sensitivity. It has five dynodes, each one having an average secondary electron multiplication factor of 5-6, depending on the operating potential. For an overall potential of 34 kV, G is measured to be 2×10^4. Using these values, N has a value of about 10^5.

b. Output Scintillations:

The electrons emitted from the photocathode of an TSEM intensifier give rise to electron pulses at its phosphor screen. For a 5-dynode tube mean pulse energy is about 40 MeV. In case of proper focusing these pulses are concentrated within an area of about 30 μ in diameter. The light output of the intensifier consists of scintillations of varying intensity. Intensity variation is due to the statistical fluctuation of the electron multiplication at each dynode and to the emission of electron groups from a single point.

To investigate the intensity distributions of scintillations, the output of the phosphor screen is fed to a photomultiplier whose output pulses are fed after shaping to a pulse-height discriminator and a pulse counter.

The noise pulses play an important role in the performance of a TSEM tube. These are of two kinds, one being the dark noise and the other one being the signal induced noise. In both of these forms of noise, single electron pulses and multiple electron pulses exist.

Light transmitted through the photocathode can be reflected back from the first dynode onto the photosurface. This causes the emission of more electrons creating signal-induced noise.

If the photocathode or other photosensitive areas are bombarded with ions, multiple electron pulses are created. Ions are created by the bombardment of the first dynode with electrons. They can be prevented from reaching the photosurface by adding a mesh in front of the first dynode and holding it at a 100 V positive potential with respect to the dynode. This mesh repels the ions but it reduces the efficiency and spoils the picture quality so, it is not used in the intensifer tubes.

In Fig. IV.4, integral pulse-height distributions for dark noise and for signal with dark noise and signal-induced noise are shown.

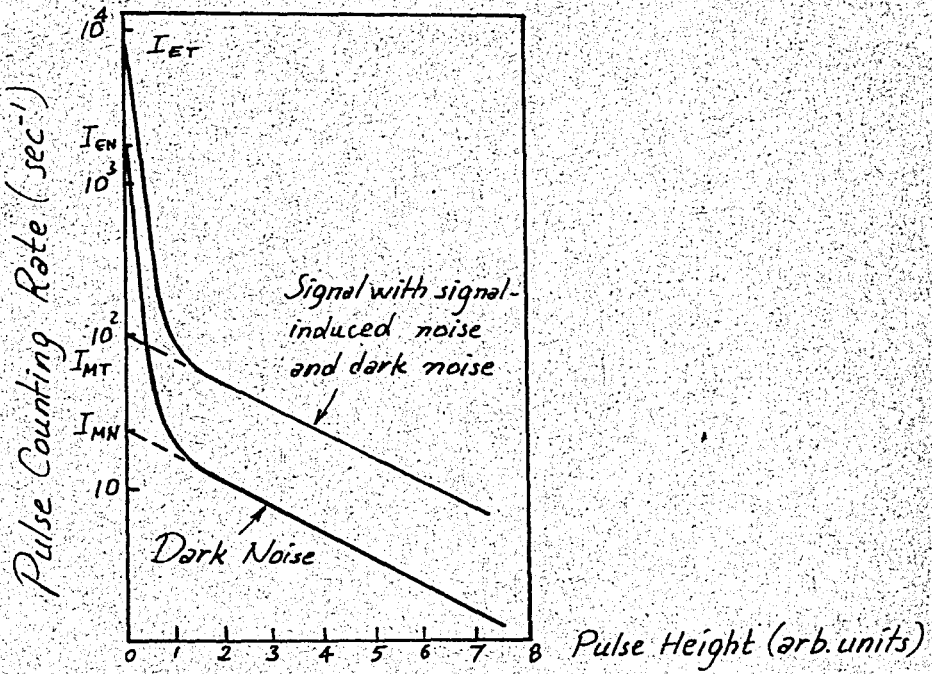

Fig. IV.4 - Integral pulse height distributions.

For both curves of Fig. IV.4, there are two linear regions. The region of low pulse heights belongs to the single-electron event, whereas the other one represents the multiple electron events. The values for total number of electrons and total number of multiple events are obtained

approximately by extrapolating the linear regions to the zero pulse height. The ratio of electrons to multiple-electron events are given by,

$$R = \frac{I_{ET} - I_{EN}}{I_{MT} - I_{MN}} \qquad \text{IV-3}$$

which has a value between 1/100 and 1/200.

The ratio of the slopes of the two parts gives the average number of electrons in one multiple-electron event. The mean value is about 18.

In Fig. IV.5, the distribution for photoemission is shown. This is obtained by subtracting the counting rates obtained in the dark from those obtained when the intensifier is weakly illuminated with visible light.

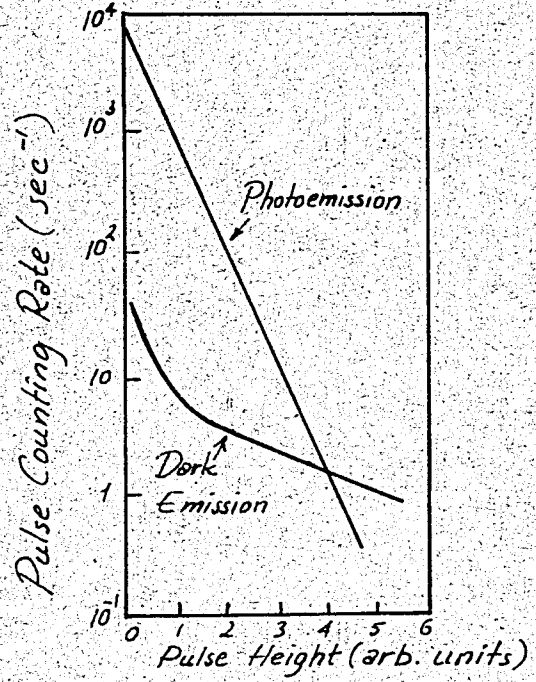

Fig. IV.5 - Integral pulse height distributions for photoemission for a 5-dynode tube.

The photoemission curve is exponential. It is obtained for single electron emission. To obtain the total number of scintillations this curve is extrapolated to zero pulse-height.

At room temperature, the photocathode of an intensifier has low dark emission, which produces a low dark current. Dark emission can be reduced by decreasing the strength of the electric field. If the length of the first image-section is doubled, the strength of the electric field is halved, so it is possible to reduce the dark emission. Further reduction can be achieved by avoiding photosensitive materials at the tube surface. The rate of scintillations due to dark emission depends upon the image tube. Values as low as 10 scintillations cm^{-2}-sec^{-1} are reported. In Fig. IV.6, integral pulse-height distributions for dark emission from a five-dynode tube are shown.

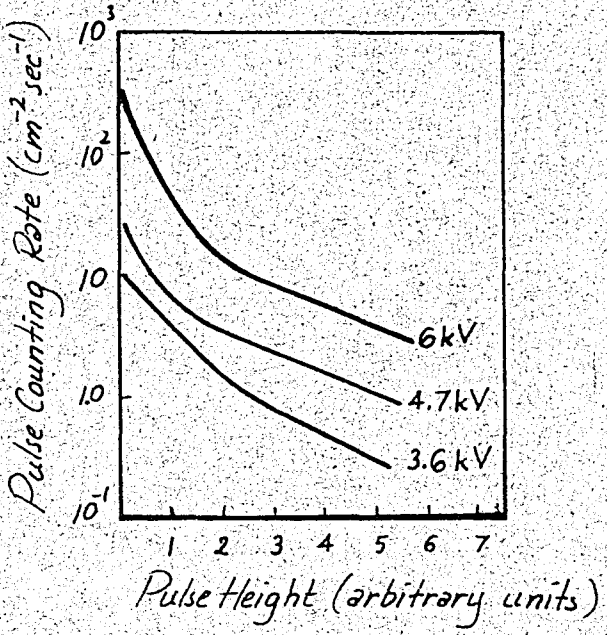

Fig. IV.6 - IPHD for dark emission.

The curves are obtained for various values of the voltage between the cathode and the first dynode. It is observed that the number of large pulses remains the same up to the values of photocurrent ten times the dark current. This is due to the insignificance of the ionization in the first

stage. If the voltage between the photocathode and the first dynode is kept constant, emission cannot be usually increased by increasing the potential of the accelerating electrodes. Sometimes this causes a reduction in emission.

c. Pulse Efficiency:

When a tube is illuminated, the output counting rate extrapolated to the zero bias is given by the following formula;

$$N_o = N_i \left[1 - P(o)\right] \qquad \text{IV-4}$$

where N_i is the photoelectrons incident on the first dynode per second, and P(o) is the probability of not producing an output pulse from the last dynode of an electron incident on the first dynode. P(o) shows the proportion of the electrons incident upon the first dynode which does not contribute to the output image. It lowers the quantum efficiency of the tube. If it decreases, the efficiency will increase. As indicated by Eq. IV-4, P(o) can be determined experimentally by measuring N_o and N_i.

In Fig. IV. 7, N_o is plotted as a function of the voltage between the photocathode and the first dynode for a constant light source and keeping the other dynode potentials at constant values for maximum current gain.

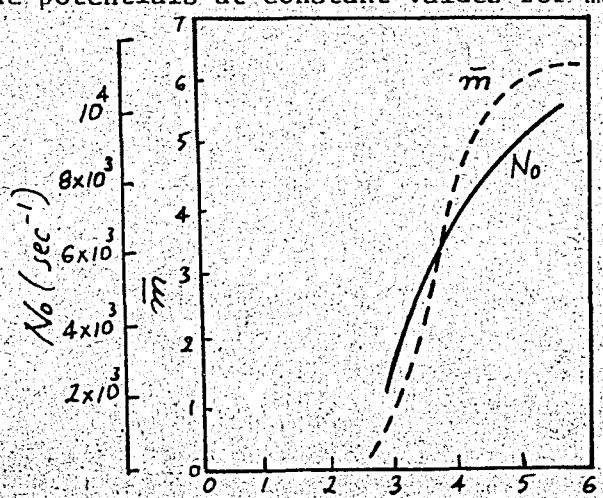

Fig. IV.7 - N_o as a function of V.

Due to the current multiplication in the tube P(o) is contributed mainly by the first dynode. This can be understood by studying P(o) more closely. P(o) can be expressed as follows,

$$P(o) = p(o) + p(1)\,P'(o) + p(2)\left[P'(o)\right]^2 \quad \ldots\ldots\ldots \quad IV\text{-}5$$

where p(m) = the probability that an electron incident on the first dynode will produce m electrons at the second one; P'(o) = the probability that an electron incident on the second dynode will produce no output pulse from the last dynode.

Case I: If $\bar{m}$ is very small, p(o) approaches unity and p(1), p(2)... are very small. If P'(o) is also small;

$$1 - P(o) \approx 1 - p(o)$$

Case II: If $\bar{m}$ is near its maximum value; $p(o) \ll 1$ and p(1), p(2) are also below unity and P(o) is of the same order as P'(o). So in this case also we get

$$1 - P(o) \approx 1 - p(o)$$

In both cases we see that P(o) is mainly influenced by the characteristic of the first dynode. If the voltage between the first dynode and the photocathode is decreased to decrease dark emission or light gain, the quantum efficiency is reduced.

d. Single Electron Detection Efficiency:

The single electron detection efficiency of an intensifier tube can be

determined by means of the effect of a single electron emitted from the photocathode upon the photographic film, on which the photograph of the anode is recorded.

The efficiency is related to the "noise" of the film. The recording film has a number of background grains b, in the limiting spot size, at any time. The noise of the background is given by $\pm\sqrt{b}$ (= 11 for IIa-0 film). A significant signal should produce a developable number of grains above the background level. This number can be represented as $K\sqrt{b}$. The number of the photons to develop $K\sqrt{b}$ grains is given by $SK\sqrt{b}$, where S is the required number of photons to develop one grain. The relation between the number of photons to develop $K\sqrt{b}$ grains and the gain of the tube is given by,

$$SK\sqrt{b} = \frac{G}{\varepsilon_c} f \qquad \text{IV-6}$$

where f is the fraction of photons collected by the lens. For various values of G we obtain different K values. The efficiency of single electron detection can be determined as a function of K, if the single electron constitutes as meaningful signal.

For a set of representative values;

$S = 150$

$\varepsilon_c = 0.10$

$f = 10^{-2}$

$G = 1.65 \times 10^4$ K

K depends on the assumed size of the electron burst that reaches the anode. The diameter of the spot produced on the film by the photons leaving the anode for one initial cathode electron can be about 40μ for unity

magnification. If a known number of electrons produced by a weak light source are emitted from the cathode and short-exposure photographs of the anode are taken, the fraction of the electrons which can be considered as a function of K can be determined by scanning the film. Experiments show that a maximum efficiency of %50 is obtained for $K > 20$.

e. Resolution:

The resolution of a transmitted secondary electron multiplication type image intensifier is determined mainly by the energy of the secondary electrons emitted from the dynodes. The inhomogeneity of this energy limits the resolution of the tube. The resolution is given by,

$$R = \frac{kV}{l\bar{v}} \qquad \text{IV-7}$$

where V is the voltage applied across the tube, l is the interdynode distance, $\bar{v}$ is the mean initial energy of the transmitted electrons. The factor k depends on the angular distribution and the energy distribution of electrons from the dynodes, the relative lengths of the inter-dynode and phosphor stages, and the detectable modulation in the output image.

In Fig. IV.8, the variation of resolution as a function of the voltage between the photocathode and the phosphor screen is shown. The five-dynode tube has a resolution which shows a slow change with the overall voltage. According to the shapes of the curves we conclude that $\bar{v}$ and k cannot be independent of V. If k is constant $\bar{v}$ increases by 15% between 20 kV and 36 kV values of the overall potential.

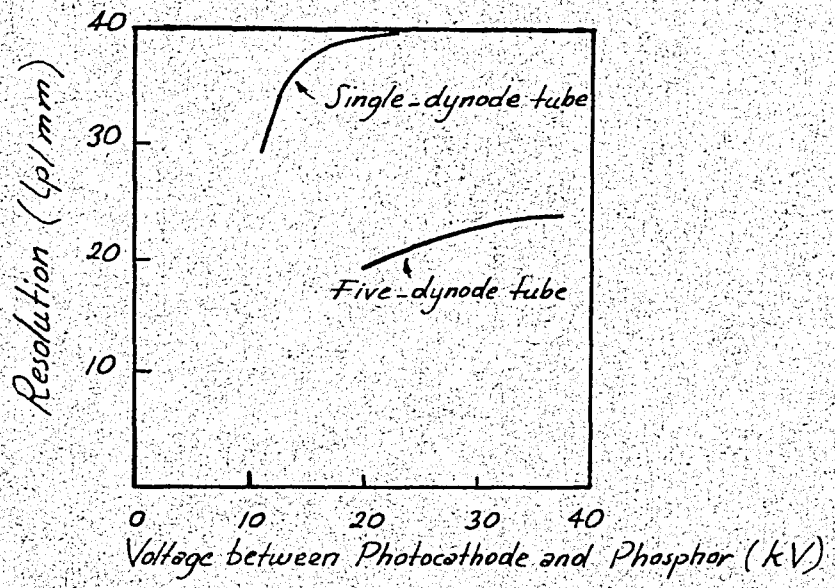

Fig. IV.8 - Resolution as a function of overall potential.

Near maximum light gains, the five-dynode tube has a limiting resolution of 23-24 lp/mm. Dynode spacing, l, influences the resolution. If it is decreased better resolution is obtained. For a 2 cm. dynode spacing a resolution of 30 lp/mm. is obtained at 29 kV overall voltage. This is an improved result compared to the present 4 cm. inter-dynode spacing amplifiers.

In TSEM image intensifiers, the field of view can be increased by modifying the image section of the tube. This could be accomplished by using larger photocathodes and demagnification techniques. Demagnification is provided by a field system consisting of parallel magnetic and electric field. For a 2:1 demagnification ratio, a resolution of 30 lp/mm. is obtained at the center of the phosphor while it was 16 lp/mm at the center of the

photocathode. If the demagnification ratio is increased, say to a value of 2.1:1, resolution becomes worse. So, with unity magnification, uniform magnetic field and regulated power supplies, the best resolution is obtained.

f. Operational Life:

Electron bombardment decreases the secondary emission coefficient of potassium chloride. This is a drawback in the use of the KCl dynodes. To test this effect, single-dynode tubes with reversible photocathodes (caesium excluded from the working part) were constructed. By illuminating these tubes by a constant light source, phosphor and photocathode currents were measured at various moments. In this way the current gain and the photocathode sensitivity can be determined. In Fig. IV.9, these are plotted as a function of the charge density input and output of the dynode.

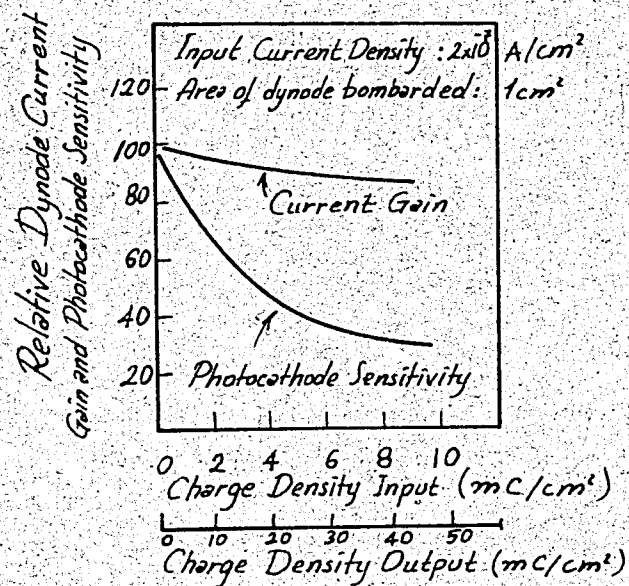

Fig. IV.9 - Relative variation of current gain and photocathode sensitivity as a function of charge into and out of the dynode.

As we see in the figure, photocathode sensitivity shows a more rapid fall compared to the current gain. The reason for the rapid fall in the sensitivity is the attack of the released chlorine to the photocathode. In case of ceasiated surfaces, this sensitivity drops almost as slowly as the current gain.

In case of five-dynode tubes, the gain and the sensitivity fall at equal rates. The rate is twice as much as the one for single dynode structures.

So far we have discussed conventional secondary electron multiplication intensifiers. It is possible to improve some properties of them as required by the application. However, while improving one characteristic others may be weakened.

C. SECONDARY ELECTRON IMAGE INTENSIFIERS WITH HIGH GAIN DYNODE

In TSEM image intensifiers dynodes of high yield are desired. The total gain of such an intensifier is proportional to the n.th power of the mean dynode yield. So, the higher the dynode yield the greater will be the gain of the tube for a certain overall voltage. To obtain good resolution the number of stages should be reduced as much as possible for a given gain. This could be accomplished by using high yield dynodes.

In the detection of weak images, good contrast performance is desired. By using high-yield dynodes, the ratio of secondary electrons to the penetrating primaries can be increased. Since the penetrating primaries are not focused from stage to stage and create the background, an increase in the secondary electron yield will imporve the contrast performance of the tube.

If internal electric fields exist in a dynode its emission increases. This is not observed significantly in the standard films which consist of a layer of alkali halide of 500 Å thick (Usually KCl is evaporated on to a conductive backing of Al of 200-300 Å thick, which is supported by a metal mesh or aluminium oxide film of the same thickness.)

Image intensifiers based on the field-enhanced transmission type emission can be constructed by using low-density dynodes and control grids. In Fig. IV.10, the cross-section of such a tube is shown.

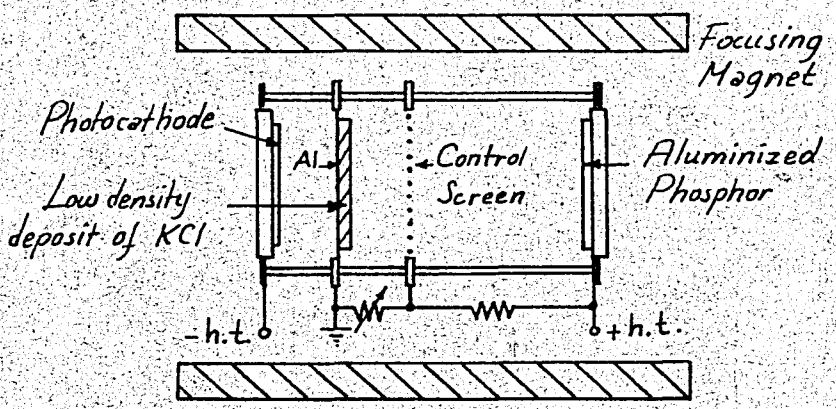

Fig. IV.10 - Field-enhanced transmission type image intensifier.

The exit surface of the low density dynode becomes positive with respect to the aluminium backing as the secondary electrons are emitted. Due to the high density of positive charges at this surface an internal field which tends to increase the drift velocity of the secondary electrons towards the surface is created. The maximum potential the exit surface can have with respect to the Al backing is equal to the potential of the control screen with respect to the Al backing. The internal field is given by V_c/d, where V_c is the screen potential and d is the thickness of the layer.

After a certain value of the screen potential, localized emission centers form in low density dynodes, which cause instabilities. This takes place for a screen voltage of more than 500 V for a 10μ layer, which means a field strength of about 5×10^5 V/cm.

The time required to charge the exit surface to the screen potential till a constant value of secondary emission is reached can be given by,

$$t = \frac{DV_c \, 10^{-13}}{d(\bar{\delta} - 1)J_p} \qquad \text{IV-8}$$

where $\bar{\delta}$ is the average yield during t (in seconds), J_p is the beam current density (in A/cm^2), d is the dynode thickness (in cm), V_c is the screen potential (in V) and D is the dielectric constant of the low density deposit (~ 1).

For a current density of 10^{-12} A/cm^2 the saturation is reached in many hours. This time can be reduced by flooding the dynode with high current densities.

With this mechanism we observe the effect of secondary emission with field enhancement as well as the emission without enhancement and internal multiplication phenomenon.

In Fig. IV.11, we have the electron gain characteristic of a tube using caesium autimonide photosurface and a blue P.11 type phosphor, having 1 in^2 useful area.

At δ = 100 localized discharges start. With such tubes a photon gain of 1000 to 2000 and a stable electron gain of 50 is obtained. A resolution value of 24 lp/mm is reported. As we have pointed out before, the contrast

degradation of this tube is less, compared to the conventional tubes of equal gain.

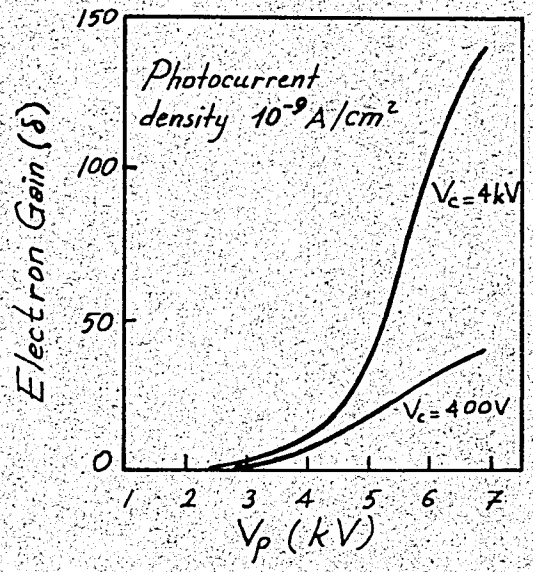

Fig. IV.11 - Electron Gain vs primary voltage.

D. CHANNELLED SECONDARY EMISSION IMAGE INTENSIFIER

This type of intensifier is obtained by modifying the dynode structure of a non-imaging photomultiplier. In Fig. IV.12, diagram of such an intensifier is illustrated.

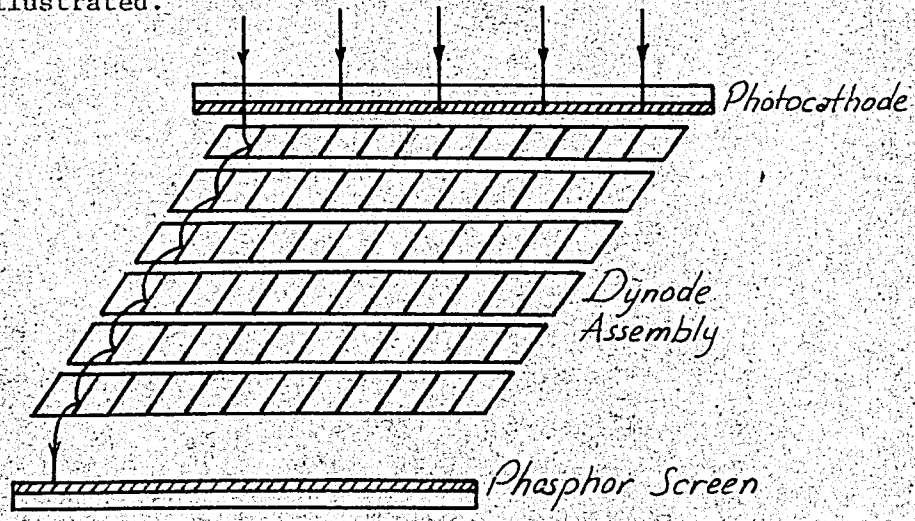

Fig. IV.12 - Diagram of the Channelled Intensifier.

The dynode consists of channels each of which confines the electrons from an element of the photocathode. Each cell of the dynode is a short cylinder whose inside walls are coated with a secondary electron emitter and its ends are sliced at 55^{o}.

Electrons emitted from the photocathode produce secondary electrons in the first dynode striking the cell walls. These secondaries go into the second dynode and produce more secondary electrons. The deflection of electrons to the cell walls are accomplished by the asymmetrical fields resulting from the cell structure.

The length of a cylinder should not be too short to cause an electron to miss one dynode and to stray into the next channel or it should not be too long to cause the secondaries fall back in itself due to the weakened field of the next dynode. The angle between the axis and the end planes of a cylinder must not be too obtuse avoiding strong deflection or it must not be too acute to cause the penetration of the field due to one dynode too far into the next one.

Experiments show that 65% of the secondary electrons produced in one dynode can be drawn to the next one.

With these intensifiers best results were obtained by using MgO as the secondary emitter. No magnetic focusing means are needed, because this is accomplished inherently.

Channelled intensifiers have limited resolution, but this can be improved by constructing smaller channels. They give high brightness gain with small total applied voltages compared to the conventional intensifiers using secondary emission principle. Their production is difficult but

operation is simple.

These intensifiers are used in X-ray fluoroscopy or in scintillation chamber works because large area tubes can be manufactured.

E. APPLICATIONS

Transmitted secondary electron multiplication tubes are used in various fields. Below are listed some applications of them.

Astronomical Uses: High gain TSE tubes are used in astronomy in obtaining astronomical spectra. TSE tube used for this purpose should have a low dark background, a S.20 photocathode, high gain and high resolution.

Observation of Čerenkov Ring Images: TSE intensifiers can be used for the observation of Čerenkov ring images as well as phosphor-photoemitter intensifiers. They are used in medical fluoroscopy, field-ion microscopy, X-ray microscopy in the same manner as the phosphor-photoemitter intensifiers are used.

F. COMPARISON OF TSEM AND PHOSPHOR - PHOTOEMITTER LIGHT AMPLIFIERS

Comparing a TSEM amplifier and a phosphor-photoemitter amplifier of the same overall light gain (10^5) we shall try to arrive at some conclusions about their differences. We shall take a 5-stage TSEM intensifier and a 3-stage cascade image intensifier and compare their gain, time response, dark emission, resolution and contrast characteristics.

The gain of the dynodes differ from each other in the two tubes. For the TSEM tube peak current gain of a dynode occurs at 5 kV primary accelerating

potential and it is 5 or 7. The overall electron gain is 3000-18000 and the overall light gain is 10^5, taking into consideration the input photoemitter and the output phosphor.

In case of phosphor-photoemitter light amplifiers dynode gains vary from 50 to 100 for a 15 kV primary voltage. In this case an overall electron gain of 2500 to 10000 is obtained. Considering the effects of the input photocathode and the output phosphor an overall light gain of 10^5 is again obtained.

From the overall light gain point of view both types give the same result.

In Fig. IV.13, light gains of the two types of amplifiers are plotted as a function of the overall potential.

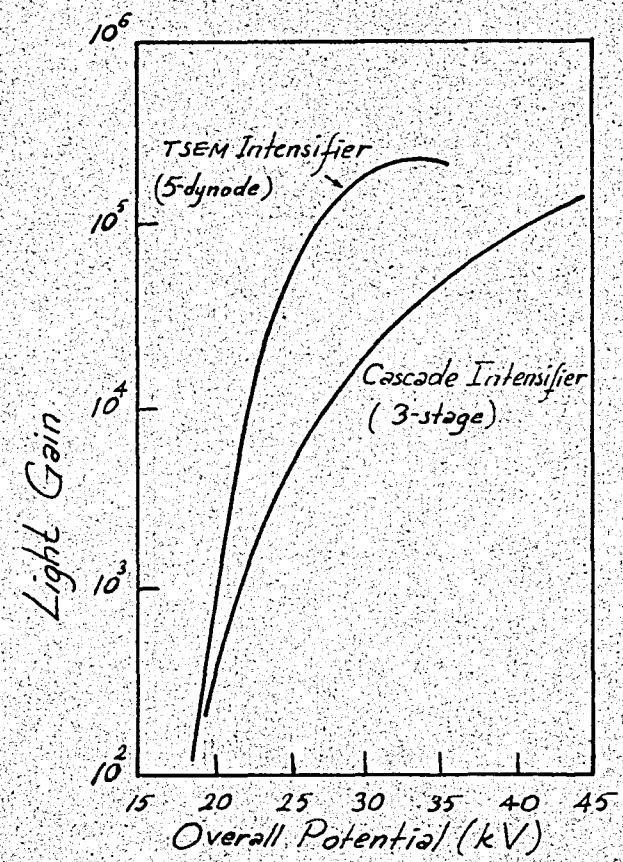

Fig. IV.13 - Light-gain as a function of overall potential.

If we compare the two tubes from the point of view of time response we see that the cascade amplifier shows a greater decay time at a given output light level. In both cases, time response can be improved by using faster decay phosphors, but in this case the gain is decreased due to the low efficiency of the fast-decay phosphors.

The time response of the TSEM tube is determined by the decay time of the phosphor. This is of the order of 1 msec for the P.11 output phosphors. The delay between the excitation by a primary electron and the emission of secondary electrons is of the order of 10^{-10} sec. This time and the transit time of the electrons, being very small compared to the phosphor decay time, can be neglected.

In case of the cascade amplifiers the number of phosphor layers is greater, so the decay time of each screen effects the time response of the amplifier.

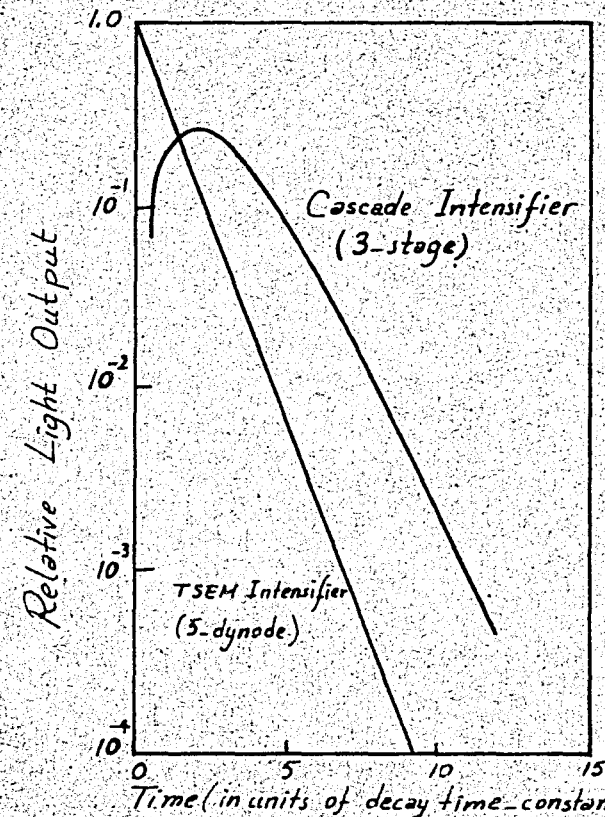

Fig. IV.14 - Relative Light output as a function of time.

In Fig. IV.14, time response characteristics of a single exponential decay phosphor and three identical ones being in series are given.

TSEM tubes having an interstage potential of 5 kV have the dark emission value of 100 scintillations $cm^{-2}sec^{-1}$ at room temperature. For these tubes dark emission values of the order of 10 scintillations $cm^{-2}sec^{-1}$ can be obtained. In case of cascade intensifiers minimum dark emission value obtained is 30 scintillations $cm^{-2}sec^{-1}$. This higher value is due to higher overall stage potentials.

From the resolution point of view both kinds of tubes give the same results. For similar operating conditions the order of resolution is about 30-35 lp/mm.

Cascade image intensifiers have better contrast performance compared to TSEM tubes. Loss of contrast is due to the penetrating primaries.

G. CONCLUSION

In view of the above comparison we can conclude that TSEM tubes show better performance from the time response, dark emission and resolution points of view. If we consider contrast performance, cascade intensifier tubes give better results.

V. LIGHT AMPLIFICATION BY THE ELECTRON BOMBARDMENT-INDUCED CONDUCTIVITY PRINCIPLE (EBIC)

A. INTRODUCTION

If a thin film of insulator placed between two electrodes is bombarded with high energy electrons (of the order of tens of keV), a secondary current flows. This current (I) is much greater than the primary current of the bombarding electrons (I_o). The ratio I/I_o is the gain of the target.

This principle can be utilized in light amplification. If one of the surfaces of the insulator is scanned by an electron beam of constant energy, while the other surface is bombarded with electrons emitted from a photocathode, a secondary current is produced in accordance with the incident image focused upon the photosurface. Since this induced current is read by the scanning beam a video signal can be obtained. By amplifying and feeding this to a display unity a brighter image is obtained.

B. EXPERIMENTAL SET-UP

To observe the phenomenon of EBIC an experiment is set up as shown in Fig. V.1. The target used is a layer of insulator sandwiched between the two Alelectrodes. It is placed in a vacuum system. If the target is not bombarded a negligible current flows through the insulator due to the polarizing voltage V. If it is bombarded with the electrons of energy eV_o a great secondary current (I) flows under the influence of the applied field. If the current of the bombarding beam is I_o, the gain of the target

is given by I/I_o.

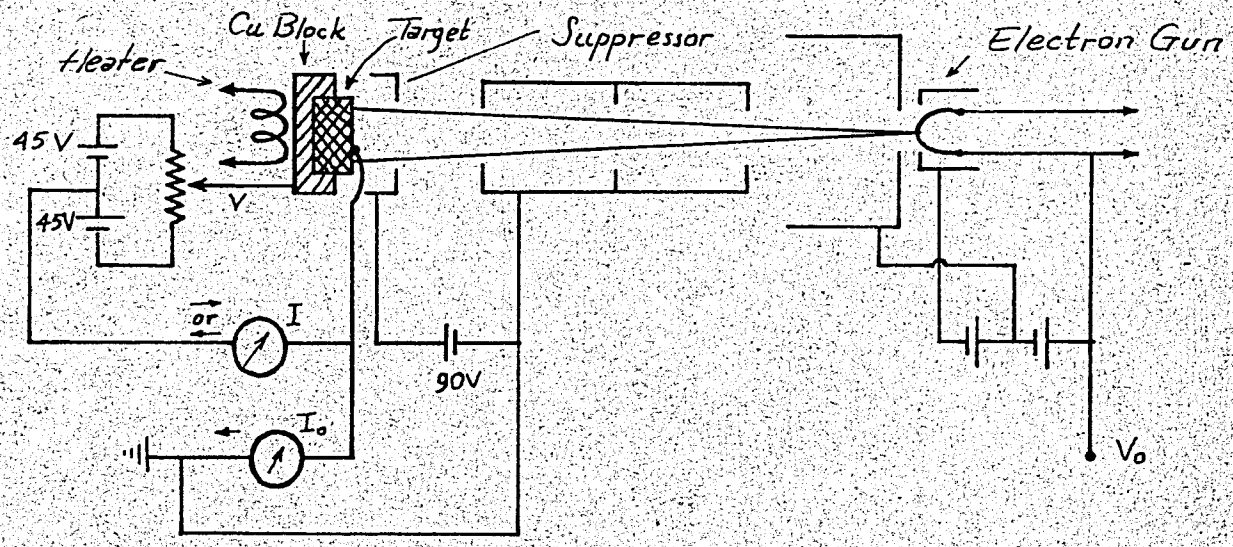

Fig. V.1 - Experimental Set-up to show EBIC.

C. EBICON TUBE FOR IMAGE INTENSIFICATION

Ebicon tube is based upon the electron bombardment induced conductivity principle. In these tubes conductivity is induced by means of the bombarding electrons. In Videcon tubes it was achieved by the incident photons.

In Fig. V.2, an Ebicon tube and the structure of its target are shown schematically. The tube has two sections one being the electron - imaging section and the other one being the scanning section. Between these two sections is placed a dielectric target. It is produced by depositing a dielectric layer on a thin film of Al on aliminium oxide. Aliminium film is thin enough to be penetrated by the high-energy electrons. It serves as a support and asignal electrode. The main function of the target is to provide preamplification before the signal is fed to a video amplifier.

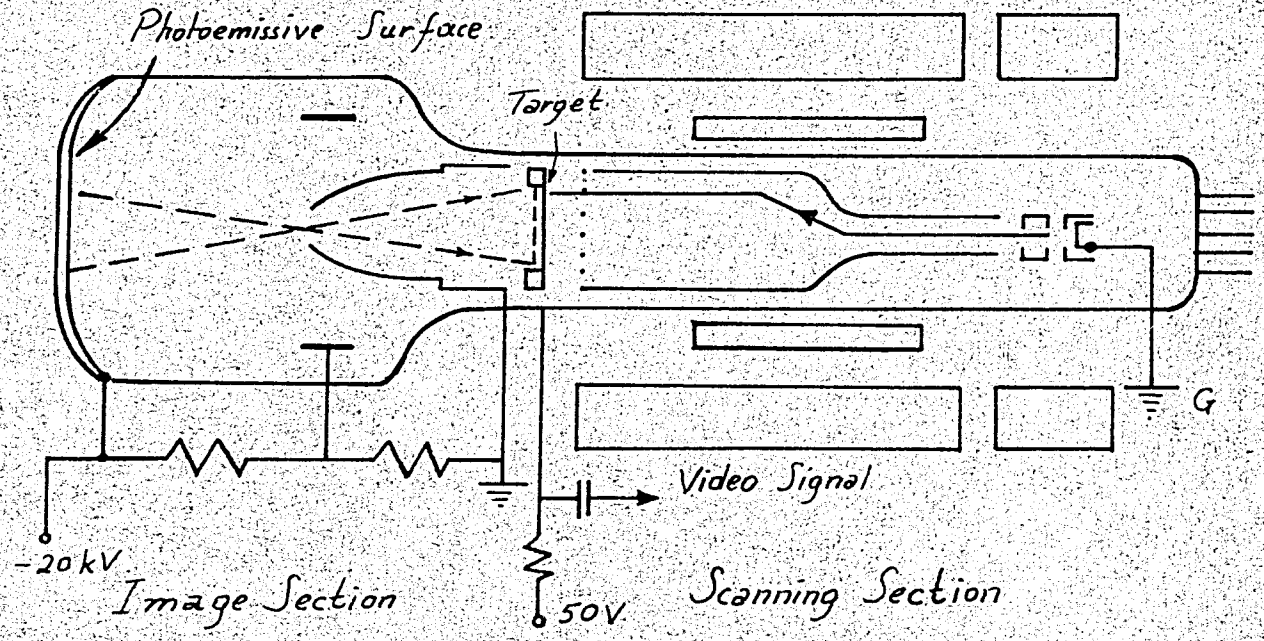

(a)

Fig. V.2 - Ebicon Tube and Target

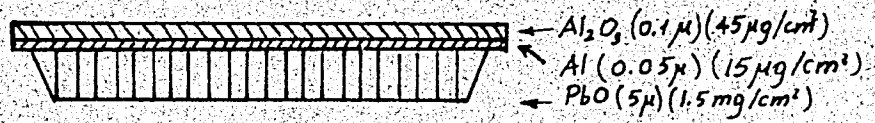

(b)

The target is scanned by a low-velocity electron beam (~1 keV) which is created by an electron gun. This beam charges the surface of the target to cathode or ground potential. If an image is focused onto the photoemissive surface, electrons emitted out of it are accelerated and focused upon the target. These high-energy electrons (~ tens of keV) induce conductivity in the target and charge target points positively for one frame period. If a positively charged point is scanned by the low-energy beam it will be charged back to the ground potential and the charging current will flow through the

resistor and the video signal will be derived from it. This current is equal to the bombarding current multiplied by the gain of the target. The video signal could be derived from the return beam as well. It is amplified further by a video amplifier and fed to a display unit.

Ebicon tubes can have useful target gains of more than 500. They are simple and their external circuitry is not complex. They are used in light amplification, the range of the amplified light depending on the sensitivity of the photoemissive surface.

Ebicon tubes which are sensitive to ultra-violet radiation are called Uvicons. They are used in rocket and satellite experiments to map the sky with broad-band television photometers. Here we shall discuss some characteristics of the Uvicon tubes their photosurfaces and targets.

BaF_2, CsI and Cs_2Te are three materials which can be used in producing ultra-violet sensitive photosurfaces. Their spectral responses are plotted in Fig. V.3.

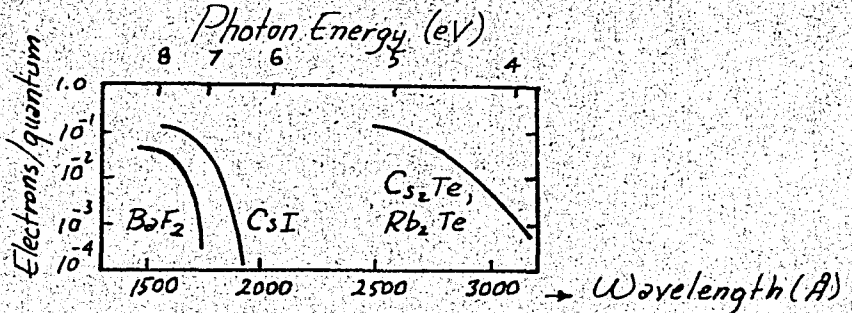

Fig. V.3 - Spectral Response of some Photosurfaces in the Ultra-violet.

Using these three materials it is possible to obtain ultra-violet sensitive photosurfaces at 1500 Å, 2000 Å and 3000 Å long wave-length cut-offs. By placing filters in front of these photocathodes short wavelength cut-off

can be controlled. To obtain a short wavelength cut-off at 1100 Å a LiF window can be used.

The materials described above are insulators and emit electrons from the side upon which the radiation is incident. Since an optically transmitting and electrically conducting photosurface is required for Uvicons a film of 100 Å thick palladium can be deposited inside surface of the LiF window. Photocathode materials are evaporated on the palladium.

As target material As_2S_3 is commonly used. Before installation the target should be tested. The time constants of the targets can be measured. The rise time of the signal to (1 - 1/e) of its final value is 0.1 - 0.2 seconds while it decays to 1/e of its initial value in 0.03 - 0.2 sec. These values depend on the target which is used.

In Fig. V.4, the target gain of an Uvicon tube using As_2S_3 as the target material is plotted as a function of target voltage. The higher target

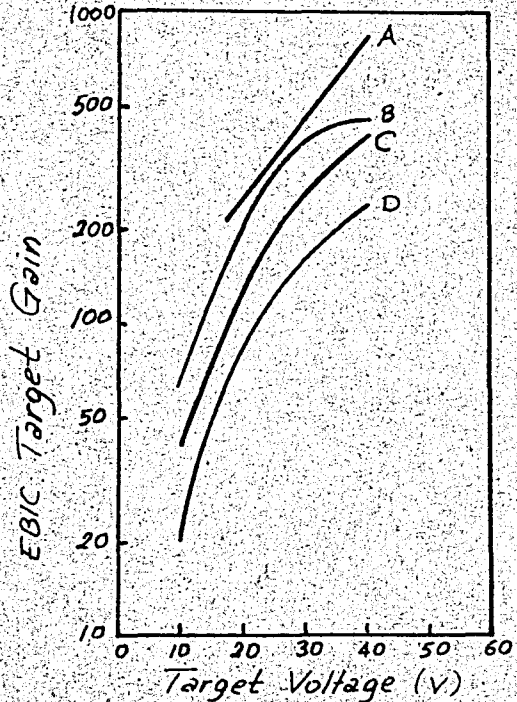

Target Input Current Densities:

A: 6.3×10^{-12} A/cm²

B: 2.3×10^{-11} A/cm²

C: 1.3×10^{-10} A/cm²

D: 1.3×10^{-10} A/cm²

A, B, C 15kV Accelerating Voltage

D 10kV Accelerating Voltage

Fig. V.4 - Target Gain vs Target Voltage.

gains are obtained for lower bombarding current densities.

It is of interest to plot the transfer characteristics of an As_2S_3 target. These are shown in Fig. V.5. We see that gamma values of less than unity are obtained for this material.

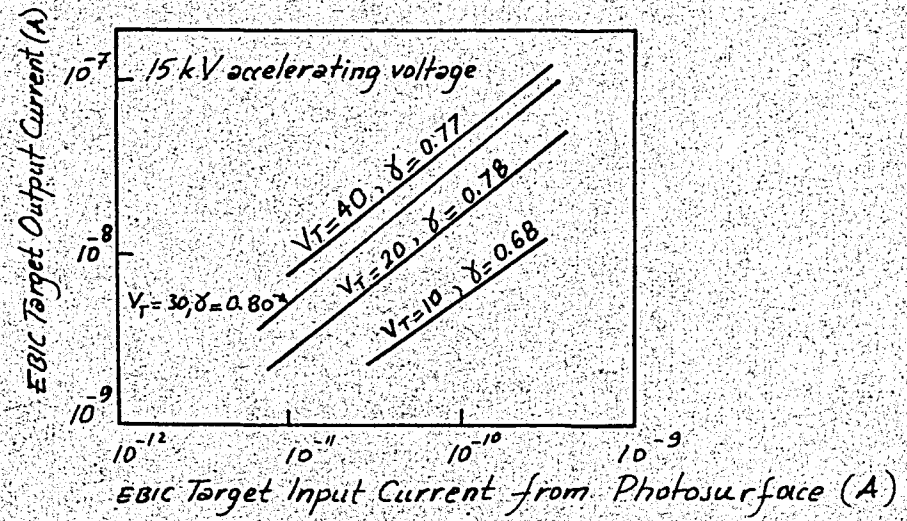

Fig. V.5 – Transfer characteristics measured on an Uvicon Tube with As_2S_3 target.

The resolution has a value of 8.3 lp/mm at the photocathode surface.

D. DISCUSSION

Electron induced bombardment conductivity and photoconductivity have some common features. In both phenomena charge carriers should be excited and transported to the electrodes efficiently. The sensitivity of the EBIC tube depends on the field strength in the 1μ thick region near the signal plate.

The lag of the bombardment induced conductivity process is of the order of the lag of the photoconductive process. Resolving power of the EBIC tube is good as could be expected from such a thick EBIC target.

IV. COMPARISON OF PHOTOCONDUCTOR-ELECTROLUMINESCENT PHOSPHOR AMPLIFIER WITH PHOTOELECTRIC IMAGE TUBES

Both types of the amplifiers have some advantages and disadvantages over each other. For this reason, each of them can give promising results in different application fields.

Solid-state image intensifiers have a photoconductor efficiency of nearly unity. In case of photoelectric tubes photocathode efficiency is 10%. If we compare the power gain provided by the tube potential and the photoconductor we see that this is of the order of 10^4 in case of tubes and 10^6 for the photoconductor. The efficiency of the phosphor is 20% whereas the corresponding efficiency of the electroluminescent layer is about 1%. In spite of these differences in the corresponding parts of the devices overall gains of the same order can be obtained from them.

Solid-state light amplifier does not have any limitations in size as in the case of image tubes. Since it is a flat device 1:1 pictures can be shown by it. This characteristic is valuable in X-ray fluoroscopy. It needs a simple power supply and no focusing means, its gamma can be controlled easily by varying the applied voltage or frequency. Since it has a high stopping power for X-rays due to its thick photoconductor, it is promising in radiology. For the observation of non-moving objects CdS photoconductor is used. If faster response is desired CdSe photoconductors can be satisfactorily used.

In solid-state amplifiers, noise limitations are more severe compared to the photoemissive devices. For this reason amplifier tubes are preferred for astronomical purposes.

VII. REFERENCES

1. Batey, P.H., and Slark, N.A., "Performance of the Transmission Secondary Electron Image Intensifier". In "Advances in Electronics and Electron Physics", ed. by J.D. Mc Gee, D. Mc Mullan, E. Kahan, Vol. 22A, p. 63. Academic Press, London and New York, (1966).

2. Broerse, P.H., "Electron Bombardment Induced Conductivity in Lead Monoxide". In "Advances in Electronics and Electron Physics", ed. by J.D. Mc Gee, D. McMullan, E. Kahan, Vol. 22A, p.305. Academic Press, London and New York, (1966).

3. Charman, W.N., "The Influence of Temperature on the Performance of a Cascade Image Intensifier". In "Advances in Electronics and Electron Physics", ed. by J.D. Mc Gee, D. McMullan, E. Kahan, Vol.22A, p.101. Academic Press, London and New York, (1966).

4. Davis, G.P., "Experiences with Magnetically Focused Cascade Image Intensifiers". In "Advances in Electronics and Electron Physics", ed. by J.D. McGee, W.L. Wilcock and L. Mandel, Vol.16, p. 119. Academic Press, New York and London, (1962).

5. Diemer, G., Klasens, H.A., van Santen, I.G., "Solid-state Image Intensifiers". Philips Research Reports, Vol. 10, p.410 (1955)

6. Emberson, D.L., "A Comparison of Some Properties of Image Intensifiers of the Transmitted Secondary Emission Multiplication Type and of the Cascade Type". In "Advances in Electronics and Electron Physics", ed. by J.D. Mc Gee, D. McMullan, E. Kahan, Vol. 22a, p. 129, Academic Press, London, and New York, (1966).

7. Emberson, D.L., Todkill, A., Wilcock, W.L., "Further Work on Image Intensifiers with Transmitted Secondary Electron Multiplication". In "Advances in Electronics and Electron Physics", ed. by J.D. Mc Gee, W.L. Wilcock and L. Mandel, Vol. 16, p. 127. Academic Press, London and New York, (1962).

8. Flinn, E.A., "Progress Report on a Channelled Image Intensifier". In "Advances in Electronics and Electron Physics", Ed. by J.D. Mc Gee, W.L. Wilcock and L. Mandel, Vol. 16, p. 155. Academic Press, New York and London, (1962).

9. Garlick, G.F.J., "Recent Developments in Solid State Image Amplifiers". In "Advances in Electronics and Electron Physics", ed. by J.D. Mc Gee, W.L. Wilcock, L. Mandel, Vol.16, p.607. Academic Press, New York and London, (1962).

10. Goetze, G.W., "Transmission Secondary Emission from Low Density Deposits of Insulators". In "Advances in Electronics and Electronic Physics", ed. by J.D. Mc Gee, W.L. Wilcock, L. Mandel, Vol.16, p.145. Academic Press, New York and London, (1962).

11. Hadley, C.P., Christensen, R.W., "Solid-state Image Intensifier Under Dynamic Operation". RCA Review, p.670, Dec. 1959.

12. Iredale, P., Hinder, G.W., Parham, A.G., Ryden, D.I., "The Observation of Cerenkov Ring Images with an Image Intensifier System of High Gain". In "Advances in Electronics and Electron Physics", ed. by J.D. Mc Gee, D. Mc Mullan, E. Kahan, Vol.22B, p.801, Academic Press, London and New York, (1966).

13. Kazan, B., "An Improved High-gain Panel Light Amplifier"., Proc. of the IRE, Vol.45, p.1358, (Oct. 1957).

14. Kazan, B., "Solid-state Panel Amplifies X-rays", Electronics, p.84, (September 12, 1958).

15. Kazan, B., and Nicoll, F.H., "An Electroluminescent Light-Amplifying Picture Panel". Proc. IRE, Vol.43, p.1888, (Dec. 1955).

16. Kohashi, T., Miyaji, K., "EL-PC Image Intensifier Uses Control Grid". In "Optoelectronic Devices and Circuits", Compilation by S. Weber, McGraw-Hill, New York, (1964).

17. Kohashi, T., Nakamura, H., Maeda, H., Miyaji, K., "A Fast-response Solid-state Image Converter". In "Advances in Electronics and Electron Physics", ed. by J.D. Mc Gee, D. Mc Mullan, E. Kahan, Vol.22B, p.683. Academic Press, London, and New York, (1966).

18. Mc Gee, J.D., Airey, R.W., Aslam, M., "High Quality Phosphor Screens for Cascade Image Intensifiers". In "Advances in Electronic and Electron Physics", ed. by J.D. Mc Gee, D. McMullan, E. Kahan, Vol.22A p.571. Academic Press, London and New York, (1966).

19. Mc Gee, J.D., Airey, R.W., Aslam, M., Powell, J.R., and Catchpole, C.F., "A Cascade Image Intensifier". In "Advances in Electronics and Electron Physics", ed. by J.D. Mc Gee, D. McMullan, E. Kahan, Vol.22A, p. 113, Academic Press, London, and New York, (1966).

20. Millman, J., Halkias, C.C., "Electronic Devices and Circuits" Mc Graw-Hill, New York, 1967.

21. Nicoll, F.H., "Properties of a Single-Element Light Amplifier Using Sintered CdSe Photoconductive Material". RCA Review, Vol.20, No.4, p.658, (December 1959).

22. Nicoll, F.H., and Kazan, B., "Large Area High-Current Photoconductive Cells Using Cadmium Sulfide Powder". Jour. of the Opt. Soc. of America, Vol.45, p.647 (August 1955).

23. Randall, R.P., "Operating Characteristics of a Four-stage Cascade Image Intensifier". In "Advances in Electronics and Electron Physics", ed. by J.D. Mc Gee, D. McMullan, E. Kahan, Vol.22A, p.87, Academic Press, London and New York, (1966).

24. Reynolds, G.T., "The Distribution of Single Electron Pulse Sizes from Multidynode Electron Multipliers, and Single Electron Detection". In "Advances in Electronics and Electron Physics", ed. by J.D. Mc Gee, D. McMullan, E. Kahan, Vol.22A, p.71, Academic Press, London and New York (1966).

25. Reynolds, G.T., "Sensitivity of Image Itensifier-Film Systems for Observing Weak Light Sources". In "Advances in Electronics and Electron Physics", ed. by J.D. Mc Gee, D. McMulland, E. Kahan, Vol. 22A, p.381. Academic Press, London, and New York (1966).

26. Schneeberger, R.J., Skorinko, G., Doughty, D.D. and Feibelman, W.A., "Electron Bombardment Induced Conductivity Including its Application to Ultra-violet Imaging in the Schuman Region". In "Advances in Electronics and Electron Physics" ed. by J.D. Mc Gee, W.L. Wilcock, L. Mandel, Vol.16, p.235. Academic Press, New York and London, (1962).

27. Slark, N.A., Woolgar, A.J., 'A Transmission Secondary Emission Image Intensifier". In "Advances in Electronics and Electron Physics", ed. by J.D. Mc Gee, W.L. Wilcock, L. Mandel, Vol.16, p. 141, Academic Press, New York, and London, (1962).

28. Stewart, R.D., "A Solid-state Image Converter". IEEE Transactions on Electron Devices, Vol. ED-15, No.4, (April, 1968).

29. Stürmer, W., "Some Applications of Solid-state Image Converters (SSIC)". In "Advances in Electronics and Electron Physics", ed. by J.D. Mc Gee, W.L. Wilcock, L. Mandel, Vol.16, p. 613. Academic Press, New York and London, (1962).

30. van der Ziel, A., "Solid-state Physical Electronics", Prentice-Hall, Inc., Englewood Cliffs, N.J., (1958 and 1968).

31. Weimer, P.K., "Image Intensifier Camera Tubes". In "Advances in Electronics and Electron Physics" ed. by L. Marton, Vol.13, p.419-123, Academic Press, New York and London, (1960).

32. Whitmell, D.S., Southon, M.J., "Image Intensification in Field-ion Microscopy". In "Advances in Electronics and Electron Physics", ed. by J.D. Mc Gee, D. McMullan, E. Kahan, Vol.22B, p.903, Academic Press, London, and New York, (1966).

33. Wilcock, W.L., Baum, W.A., "Astronomical Tests of an Imaging Photomultiplier". In "Advances in Electronics and Electron Physics", ed. by J.D. Mc Gee, W.L. Wilcock, L. Mandel, Vol.16, p.383, Academic Press, New York and London (1962).

34. Zavoiskii, E.K., Butslov, M.M., Smolkin, G.E., "Maximum Amplification Factor and Noise of Photomultipliers". Soviet Physics - Doklady, Vol.I, p. 743, (1956).